Performance Analysis of Emerging Solutions to RF Spectrum Scarcity Problem in Wireless Communications

by

Muneer Usman
B.Sc., GIK Institute of Engineering Sciences and Technology, Pakistan, 2002

A Thesis Submitted in Partial Fulfillment of the
Requirements for the Degree of

MASTERS OF APPLIED SCIENCE

in the Department of Electrical and Computer Engineering

Performance Analysis of Emerging Solutions to RF Spectrum Scarcity Problem in Wireless Communications

by

Muneer Usman
B.Sc., GIK Institute of Engineering Sciences and Technology, Pakistan, 2002

Supervisory Committee

Dr. Hong-Chuan Yang, Supervisor
(Department of Electrical and Computer Engineering)

Dr. Michael McGuire, Departmental Member
(Department of Electrical and Computer Engineering)

Supervisory Committee

Dr. Hong-Chuan Yang, Supervisor
(Department of Electrical and Computer Engineering)

Dr. Michael McGuire, Departmental Member
(Department of Electrical and Computer Engineering)

ABSTRACT

Wireless communication is facing an increasingly severe spectrum scarcity problem. Hybrid free space optical (FSO)/ millimetre wavelength (MMW) radio frequency (RF) systems and cognitive radios are two candidate solutions. Hybrid FSO/RF can achieve high data rate transmission for wireless back haul. Cognitive radio transceivers can opportunistically access the underutilized spectrum resource of existing systems for new wireless services. In this work we carry out accurate performance analysis on these two transmission techniques.

In particular, we present and analyze a switching based transmission scheme for a hybrid FSO/RF system. Specifically, either the FSO or RF link will be active at a certain time instance, with the FSO link enjoying a higher priority. We consider both a single threshold case and a dual threshold case for FSO link operation. Analytical expressions are obtained for the outage probability, average bit error rate and ergodic capacity for the resulting system.

We also investigate the delay performance of secondary cognitive transmission with interweave implementation. We first derive the exact statistics of the extended delivery time, that includes both transmission time and waiting time, for a fixed-size secondary packet. Both work-preserving strategy (i.e. interrupted packets will resume transmission from where interrupted) and non-work-preserving strategy (i.e. interrupted packets will be retransmitted) are considered with various sensing schemes. Finally, we consider a M/G/1 queue set-up at the secondary user and derive the closed-form expressions for the expected delay with Poisson traffic. The analytical results will greatly facilitate the design of the secondary system for particular target application.

Contents

List of Figures

ACKNOWLEDGEMENTS

I would like to thank:

My parents for providing for my education since my childhood

Dr. Mohamed-Slim Alouini and Dr. Hong-Chuan Yang for providing me the support for my graduate studies

Dr. Michael McGuire for serving on the supervisory committee

Dr. Yang Shi for agreeing to serve on the oral examination committee

Chapter 1

Introduction

Wireless communications is one of the most useful technologies of modern times. This technology enables long-range communications, which are impossible or impractical to implement with the use of wires in certain scenarios. The birth of wireless communications dates from the late 1800s, when M.G. Marconi did the pioneering work establishing the first successful radio link between a land-based station and a tugboat [1]. Since then, wireless communication systems have been developing and evolving at a furious pace. In the early stages, wireless communication systems were primarily used by military applications. During the last few decades, with increasing civil applications of mobile services, commercial wireless communication systems have been dominating the development.

An important natural resource for wireless communication is the radio frequency (RF) spectrum. The RF spectrum extends from 3 KHz to 300 GHz frequencies and corresponds to the low frequency region of the electromagnetic (EM) spectrum, which otherwise contains infra-red rays, visible light, ultra-violet rays, X-rays, and Gamma rays at higher frequencies. The RF spectrum is divided into different frequency ranges or categories, as depicted in Fig. 1.1. The properties of the RF waves, such as range and attenuation, change with frequency, and therefore, different frequencies are suitable for different types of communication links. In a wireless communication system, the information to be transmitted is generally modulated (superimposed) on to a carrier signal having a frequency in the RF range. The modulated signal is transmitted through the wireless channel, and the original (information) signal is recovered at the receiver by demodulating the received signal.

RF spectrum is a finite and scarce, but reusable resource. With the increase in the volume of wireless services, the RF spectrum needs effective management and efficient utilization. RF spectrum scarcity is one of the most serious problems

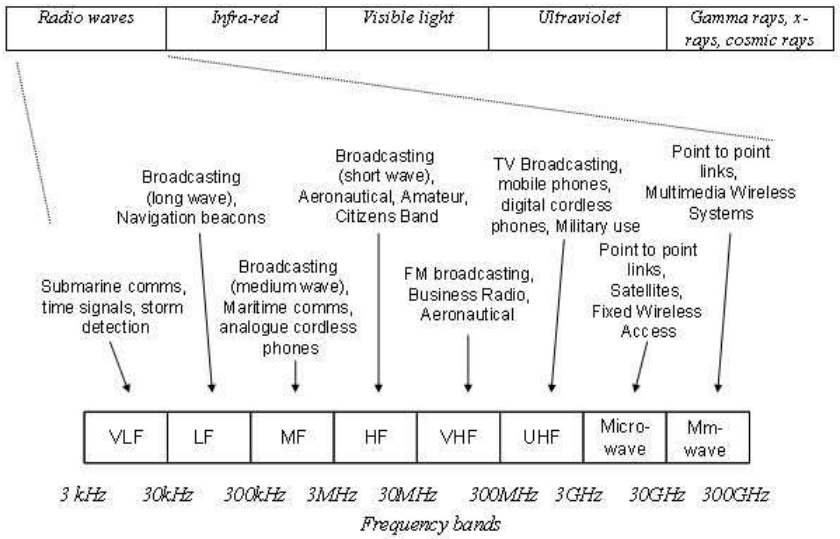

Figure 1.1: Radio frequency spectrum.

nowadays faced by the wireless communications industry. Shortage of spectrum will be a setback to innovations, competition, businesses and consumers. Hence, a lot of research effort is being carried out to address this problem. There are generally two directions to solve the spectrum shortage problem. One is the use of high-frequency spectrum. The millimetre-wavelength (MMW) RF spectrum is not currently utilized fully, and can be used for some applications, though it has some limitations. Free-space optical (FSO) communication is also a prospective technique, which can be used for short-distance line-of-sight communication. The other prospective approach is to improve the utilization efficiency of existing spectrum. Cognitive radio is a promising candidate in this direction by exploiting temporal/spatial spectrum opportunities over the existing licensed frequency bands [2–10]. In this paper we carry out accurate performance analysis of hybrid FSO/RF and cognitive radio systems.

1.1 FSO/RF Hybrid System

MMW refers to the extremely high frequency (EHF) band of the RF spectrum, with frequency ranging from 30 GHz to 300 GHz, or equivalently, a wavelength of about 1 mm to 10 mm. These frequencies face high atmospheric attenuation due to rain, water vapour, and oxygen, and thus can only be used for communication

upto a few kilometres [11, 12]. These waves can propagate only in line-of-sight, since they are blocked by buildings and walls. Though all these factors limit the communication range, but at the same time allow for frequency reuse at small distances. At these frequencies, larger modulation bandwidth is available, thus enabling communication at a much higher data rate than the lower frequency counterparts. The short wavelengths enable the use of small antennas, thus reducing the beam width, and further increasing the potential for frequency reuse. Being an unlicensed frequency band, MMW RF operation at 60 GHz frequency band has recently gained much interest.

FSO communication, also sometimes called laser communication, refers to an optical communication technology that transmits information through light travelling in free space (air or vacuum). In FSO communication the carrier frequency is selected from the optical spectrum, typically on the order of 10^{14}Hz [13]. Like MMW RF, FSO also faces high atmospheric attenuation, and thus is suitable for communication upto a few kilometres only, with high potential of frequency reuse and high level of security. Again, the antenna, which is a light source, is very small and produces a very narrow directed beam. Being in the optical range, FSO systems can achieve data rates comparable to optical fibre cables, without the hassle of actually laying out the cables.

FSO communication and MMW RF communication have thus emerged as effective solutions for high data rate wireless transmission over short distances. They can help address the continuous demand for higher data rate transmission in presence of the growing scarcity of RF spectrum. Meanwhile, the FSO channel and MMW RF channel exhibit complementary characteristics to atmospheric and weather effects. In particular, FSO link performance degrades significantly due to fog, but is not sensitive to rain [14, 15]. Contrarily, 60 GHz RF is very sensitive to rain but is quite indifferent to fog. Thus, FSO and RF transmission systems are good candidates for joint deployment to provide reliable high data rate wireless back haul.

Most previous work on hybrid FSO/RF systems focus on soft-switching between two links [16–19], in which the data is simultaneously transmitted through both links using hybrid channel codes. Specifically, [16] uses hybrid channel codes in a hybrid FSO/RF system. A rateless coded automatic repeat-request (ARQ) scheme for hybrid FSO/RF systems has been proposed in [17]. [18] proposes a bit-interleaved coded modulation scheme for such hybrid systems. The use of short-length raptor codes has been proposed by [19]. The link availability of hybrid FSO/RF was investigated in [20] from information theory perspective. On another front, [21] introduces diversity combining of parallel FSO and RF chan-

nels, while assuming both link transmit identical information simultaneously. The performance of a similar hybrid FSO/RF system with non-Gaussian noise has been analyzed in [22]. These diversity schemes typically lead to some rate loss compared to soft-switching schemes. Meanwhile, both classes of transmission schemes above require the FSO and RF links to be active continuously, even when experiencing poor quality, which will lead to wasted transmission power and generate unnecessary interference to the environment. In this thesis, we present and analyze a switching based transmission scheme for hybrid FSO/RF system, where either FSO or RF link will be active at a certain time instance, with the FSO link enjoying a higher priority. We consider both a single threshold case and a dual threshold case for FSO link operation. Analytical expressions are obtained for the outage probability, average bit error rate and ergodic capacity for the resulting system.

1.2 Cognitive Radio

A cognitive radio is an intelligent communication system/device, which effectively makes use of the underutilized RF spectrum by exploiting temporal/spatial spectrum opportunities, also referred to as spectrum holes, over the existing licensed frequency bands. It makes use of advanced radio and signal-processing technology along with novel spectrum-allocation policies to achieve its task [2]. This technology has the capability to revolutionize the way spectrum is allocated worldwide as well as provide sufficient bandwidth to support the demand for higher quality and higher data rate wireless products.

Cognitive radio is a promising solution to the RF spectrum scarcity problem. Different techniques exist for opportunistic spectrum access (OSA). In *underlay* cognitive radio implementation, the primary and secondary users simultaneously access the same spectrum, with a constraint on the interference to primary transmission caused by the secondary user (SU). It is assumed that the SU has knowledge of the interference caused by its transmitter to the primary receiver(s) [2]. With *interweave* cognitive implementation, the secondary transmission creates no interference to the primary user (PU). Specifically, the SU can access the channel only when it is not used by PU and must vacate the occupied channel when the PU appears. Spectrum handoff procedures are adapted for returning the channel to the PU and then re-accessing that channel or another channel later to complete the transmission. As such, the secondary transmission of a given amount of data may involve multiple spectrum handoffs, which results in extra transmission de-

lay. The total time required for the SU to complete a given packet transmission, also called the extended delivery time (EDT) [23], will include the waiting periods before accessing the channel and become more than the actual time needed for transmission.

There has been a continuing interest in the delay and throughput analysis for secondary systems, especially for underlay implementation. [24] analyzes the delay performance of a point-to-multipoint secondary network, which concurrently shares the spectrum with a point-to-multipoint primary network in the underlay fashion, under Nakagami-m fading. The packet transmission time for secondary packets under PU interference is investigated in [25], where multiple secondary users are simultaneously using the channel. An optimum power and rate allocation scheme to maximize the effective capacity for spectrum sharing channels under average interference constraint is proposed in [26]. [27] examines the PDF and CDF of secondary packet transmission time in underlay cognitive system. [28] investigates the M/G/1 queue performance of the secondary packets under the PU outage constraint. [29] analyzes the interference caused by multiple SUs in a "mixed interleave/underlay" implementation, where each SU starts its transmission only when the PU is off, and continues and completes its transmission even after the PU turns on.

For interweave implementation strategy, [30] discusses the average service time for the SU in a single transmission slot and the average waiting time, i.e. the time the SU has to wait for the channel to become available, assuming general primary traffic model. A probability distribution for the service time available to the SU during a fixed period of time was derived in [31]. A model of priority virtual queue is proposed in [32] to evaluate the delay performance for secondary users. [33] studies the probability of successful data transmission in a cooperative wireless communication scenario with hard delay constraints. A queuing analysis for secondary users dynamically accessing spectrum in cognitive radio systems was carried out in [34]. [23] derives bounds on the throughput and delay performance of secondary users in cognitive scenario based on the concept of EDT. [35] calculates the expected EDT of a packet for a cognitive radio network with multiple channels and users.

When the secondary transmission is interrupted by PU activities, the secondary system can adopt either non-work-preserving strategy, where interrupted packets transmission must be repeated [23], or work-preserving strategy, where the secondary transmission can continue from the point where it was interrupted, without wasting the previous transmission [35]. These can be achieved with the application of rateless codes such as Fountain code [36, 37]. Work-preserving strategy

also applies to the transmission scenario with small and individually coded sub-packets transmission. In this thesis, we investigate the delay analysis of secondary cognitive transmission with interweave implementation for both work-preserving strategy and non-work-preserving strategy with various sensing schemes. We first derive the exact statistics of the extended delivery time for a fixed-size secondary packet that includes both transmission time and waiting time. Finally, we consider a generalized M/G/1 queue set-up at the secondary user and derive the closed-form expressions for the expected delay with Poisson traffic.

1.3 Thesis Structure

The remainder of this thesis is organized as follows. In Chapter 2, a low-complexity hard-switching scheme for hybrid FSO/RF transmission is considered, which will transmit data using either the FSO link or the MMW RF link. In Chapter 3, we analyze the performance of a simple primary user, single secondary user cognitive radio system under work-preserving strategy and investigate the statistical characteristics of the resulting EDT. In Chapter 4, a similar cognitive radio system under non-work-preserving strategy is analyzed. Chapter 5 summarizes the thesis and discusses some future research directions.

Chapter 2

Practical Switching based Hybrid FSO/RF Transmission and its Performance Analysis

In this chapter, we consider a low-complexity hard-switching scheme for hybrid FSO/RF transmission, which will transmit data using either the FSO link or the MMW RF link. The FSO link will be used as long as its link quality is above a certain threshold. When the FSO link quality becomes unacceptable, the system will revert to the RF link. Using only a single link at a time will result in lower power consumption at the transmitter, and will not require the use of combining or multiplexing operation at the receiver. In fact, such implementation are widely adopted in commercially available hybrid FSO/RF products, like fSONA and MRV products [38]. To the best of our knowledge, a detailed analysis of such a hard-switching based hybrid FSO/RF system is not available in literature. In this chapter, we analyze the performance of such a low-complexity transmission scheme for hybrid FSO/RF systems. We derive closed-form analytical expressions for the outage probability, the average bit error rate (BER), and the ergodic capacity for the hybrid system under practical fading channel models. In addition to the single FSO threshold implementation, we consider the dual FSO threshold implementation, which can avoid the frequent on/off transitions of the FSO link [39]. Specifically, exact expressions have been obtained for the outage probabilities and BERs of both FSO and RF links, and capacity for the RF link. An approximate expression has been obtained for the capacity of the FSO link. These expressions are then applied to obtain analytical expressions for the same metrics for the overall system. Numerical results show that the hybrid FSO/RF scheme achieves better reliability and performance than conventional FSO only system.

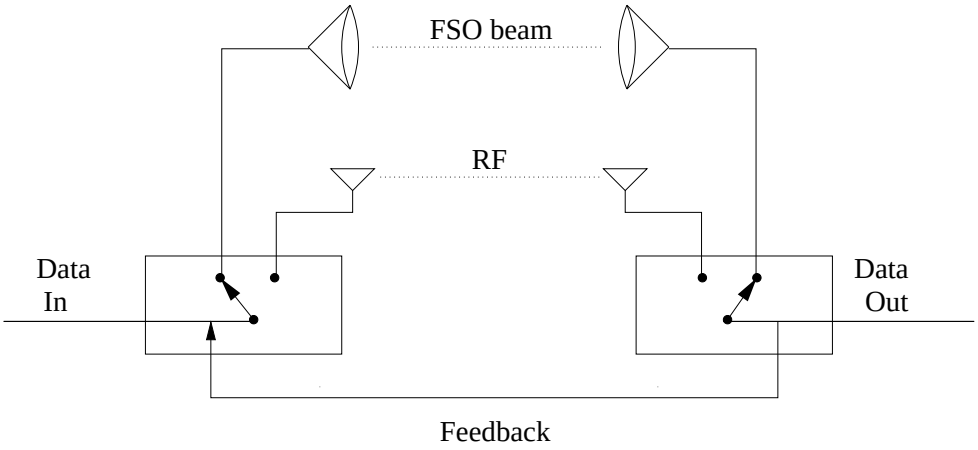

Figure 2.1: System block diagram of a hybrid RF/FSO system.

Using dual FSO threshold will not significantly degrade system performance, while having the potential to extend FSO link life time.

2.1 System and Channel Model

We consider a hybrid FSO/RF system, where the FSO link works in parallel with an RF link as shown in Fig. 2.1. To keep the receiver implementation simple, the transmission occurs only on one of the links at a time. Due to generally higher data rates available, FSO will be given a higher priority and will be used for transmission whenever its link quality is acceptable.

The FSO link adopts intensity modulation and direct detection (IM/DD), together with quadrature modulation scheme [21, 40, 41]. Specifically, the information is first modulated using a quadrature modulation scheme. The modulated electrical signal is then directly modulated on the transmitter's laser intensity. To avoid any clipping while modulating on to the laser intensity, a DC bias must be added to the modulated electrical signal to ensure that the value of the signal is non-negative. Hence, the intensity of the transmitted optical signal can be written as [21]

$$I(t) = P_T(1 + \mu x(t)) \tag{2.1}$$

where P_T is the average transmitted optical power, μ is the modulation index $(0 < \mu < 1)$ which is introduced to eliminate over-modulation induced clipping, and $x(t)$ is the quadrature modulated electrical signal. At the receiver end of the FSO sub-system, the incident optical power on the photodetector is converted into an electrical signal through direct detection. After the DC bias is filtered out, the

electrical signal is demodulated to obtain the discrete-time equivalent baseband signal, given by

$$r[k] = \alpha \cdot h \cdot g \cdot x[k] + n[k], \tag{2.2}$$

where α is a constant depending on the average transmitted optical power P_T, the receiver's optical-to-electrical conversion efficiency, and the modulation index μ [21], g represents the average gain of the FSO link, h is the turbulence-induced random fading channel gain with $E[h] = 1$, $x[k]$ represents the complex baseband information symbol over the k^{th} symbol period with average electrical symbol energy E_s, and $n[k]$ is the zero mean circularly symmetric complex Gaussian noise component with $E\{n[k]n^*[k]\} = \sigma_n^2$. Based on the above equation, the instantaneous electrical SNR at the output of the FSO receiver, denoted by γ_{FSO}, can be shown to be equal to

$$\gamma_{FSO} = \frac{\alpha^2 g^2 E_s h^2}{\sigma_n^2}. \tag{2.3}$$

For analytical tractability, we adopt log-normal fading model for turbulence induced fading [39, 42–45], which is valid particularly for light atmospheric turbulence condition, while assuming that there are no pointing errors associated with the laser beam. Specifically, the fading coefficient h has the probability density function (PDF)

$$f_h(h) = \frac{1}{\sqrt{8\pi}h\sigma_x} e^{-\frac{[\ln(h) - 2\mu_x]^2}{8\sigma_x^2}}, \tag{2.4}$$

where μ_x and σ_x represent the mean and variance of the log-amplitude fading respectively [39, 43–45]. It has been shown that the condition $E[h] = 1$ implies $\mu_x = -\sigma_x^2$ [46]. Based on Eqs. (2.3) and (2.4), the instantaneous SNR of the FSO link can be shown to have the following PDF

$$f_\gamma^{FSO}(\gamma) = \frac{1}{\sqrt{32\pi}\gamma\sigma_x} e^{-\frac{\left[\ln\left(\frac{\gamma}{\gamma_{FSO}}\right) + 8\sigma_x^2\right]^2}{32\sigma_x^2}}, \tag{2.5}$$

where $\bar{\gamma}_{FSO}$ is the average electrical SNR, which is, as shown appendix A.1, given by

$$\bar{\gamma}_{FSO} = E[\gamma_{FSO}] = \frac{\alpha^2 g^2 E_s}{\sigma_n^2} e^{4\sigma_x^2}. \tag{2.6}$$

For the RF link, we assume the Nakagami-m fading model where the received SNR has the PDF

$$f_\gamma^{RF}(\gamma) = \left(\frac{m}{\bar{\gamma}_{RF}}\right)^m \frac{\gamma^{m-1}}{\Gamma[m]} e^{-\frac{\gamma}{\bar{\gamma}_{RF}}m}, \tag{2.7}$$

where $\bar{\gamma}_{RF}$ is the average SNR, m is a parameter indicating fading severity, and $\Gamma[.]$ is the standard Gamma function.

2.2 Switched FSO/RF Transmission with Single FSO Threshold

In this scenario, the FSO link will be used if the instantaneous SNR of the FSO channel is above a threshold γ_{th}^{FSO}. If the SNR of the FSO link is below γ_{th}^{FSO}, then the system will check the RF link; if the RF link SNR is above a threshold γ_{th}^{RF}, the RF link will be used for transmission. If the SNRs of both links are below their respective thresholds, an outage will be declared. In the following, we calculate the outage probability, the average BER during the non-outage period of time, and the ergodic capacity for this implementation scenario.

2.2.1 Outage Probability

The outage probability can be calculated based on the above mode of operation as

$$P_{out}^{(1)} = P^{FSO}(\gamma_{th}^{FSO}) \times P^{RF}(\gamma_{th}^{RF}), \tag{2.8}$$

where $P^{FSO}(.)$ is the cumulative distribution function (CDF) of the FSO link SNR, given by

$$P^{FSO}(\gamma_{th}) = \int_0^{\gamma_{th}} f_\gamma^{FSO}(\gamma)d\gamma = 1 - \frac{1}{2}\text{erfc}\left(\frac{\ln\left(\frac{\gamma_{th}}{\bar{\gamma}_{FSO}}\right) + 8\sigma_x^2}{\sqrt{32}\sigma_x}\right), \tag{2.9}$$

$P^{RF}(.)$ is the CDF of the RF link SNR, given by

$$P^{RF}(\gamma_{th}) = \int_0^{\gamma_{th}} f_\gamma^{RF}(\gamma)d\gamma = \frac{\gamma\left[m, \frac{\gamma_{th}}{\bar{\gamma}_{RF}}m\right]}{\Gamma[m]}, \tag{2.10}$$

erfc (.) denotes the complementary error function, and $\gamma[.,.]$ is the lower incomplete Gamma function.

Fig. 2.2 shows the variation of the outage probability with the average SNR of the FSO link, for a fixed value of γ_{th}^{FSO} and γ_{th}^{RF}. The varying average SNR of the FSO link corresponds to a varying weather condition. The three curves correspond to FSO only, hybrid FSO/RF where RF link has an average SNR of 5 dB, and hybrid FSO/RF where RF link has an average SNR of 10 dB cases. As can be seen, using the hybrid system improves the outage performance of the system, particularly when a high quality RF link is used. Even with a low quality RF link, some improvement can be observed. The simulation results included validate our analytical results.

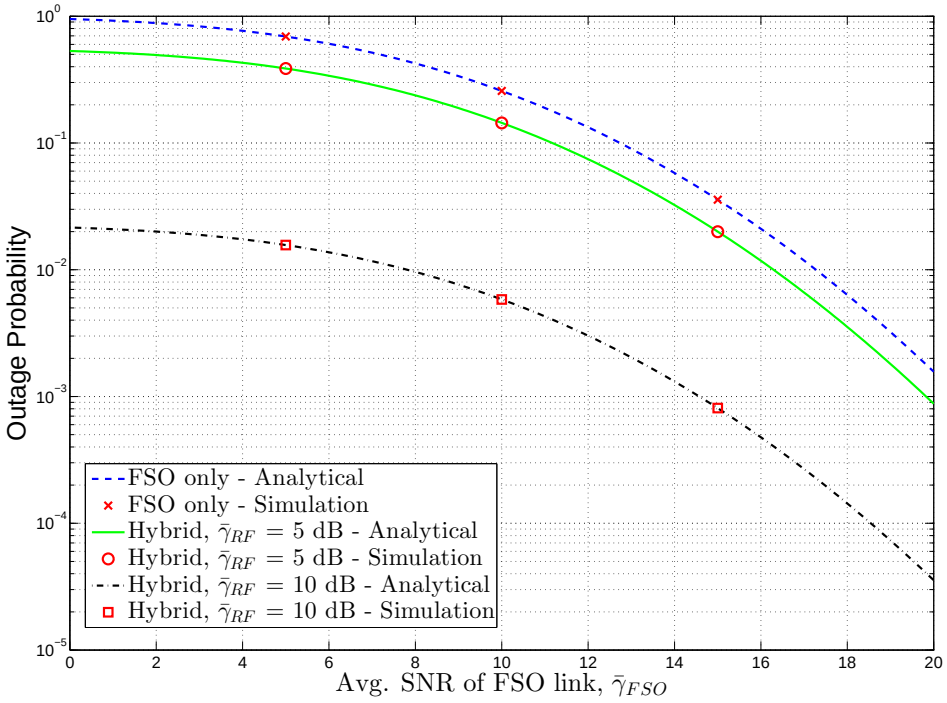

Figure 2.2: Outage probability for single FSO threshold case as a function of average SNR of the FSO link - $\gamma_{th}^{FSO} = \gamma_{th}^{RF} = 5$ dB , $m = 5$, $\sigma_x = 0.25$.

2.2.2 Average Bit Error Rate

For the purpose of the average BER calculation, we will assume that the data is modulated using M-PSK, and then transmitted through the FSO link or the RF link. We will assume that both the FSO and RF links operate at the same data rate. The generalization to different rate cases and other modulation schemes is straightforward. The BER for M-PSK with Gray coding, as a function of the instantaneous SNR is given by [47, Eq. (5.2.61)],

$$p(e|\gamma) = \frac{A}{2}\text{erfc}\,(\sqrt{\gamma}B), \tag{2.11}$$

where $A = 1$ and $B = 1$ when $M = 2$ (BPSK), and $A = \frac{2}{\log_2 M}$ and $B = \sin\frac{\pi}{M}$ when $M > 2$.

The average BER during non-outage period can be calculated, in terms of the average BER when the FSO link is active and that when the RF link is active, as

$$\overline{BER}^{(1)} = \frac{B_{FSO}(\gamma_{th}^{FSO}) + P^{FSO}(\gamma_{th}^{FSO}) \cdot B_{RF}(\gamma_{th}^{RF})}{1 - P_{out}^{(1)}}, \tag{2.12}$$

where $P_{out}^{(1)}$ was given in Eq. (2.8), P^{FSO} was given in Eq. (2.9), and $B_{FSO}(.)$ and $B_{RF}(.)$ are defined as

$$B_{FSO}(\gamma_{th}) = \int_{\gamma_{th}}^{\infty} p(e|\gamma) f_{\gamma}^{FSO}(\gamma) d\gamma \tag{2.13}$$

and

$$B_{RF}(\gamma_{th}) = \int_{\gamma_{th}}^{\infty} p(e|\gamma) f_{\gamma}^{RF}(\gamma) d\gamma, \tag{2.14}$$

respectively.

Substituting Eq. (2.11) into Eq. (2.13), and applying the series expansion of the complementary error function, we get

$$\begin{aligned} B_{FSO}(\gamma_{th}) &= \int_{\gamma_{th}}^{\infty} \frac{A}{2}\text{erfc}\,(B\sqrt{\gamma}) f_{\gamma}^{FSO}(\gamma) d\gamma \\ &= \int_{\gamma_{th}}^{\infty} \frac{A}{2}\left[1 - \frac{2}{\sqrt{\pi}}\sum_{j=0}^{\infty}\frac{(-1)^j (B\sqrt{\gamma})^{2j+1}}{j!(2j+1)}\right] \times f_{\gamma}^{FSO}(\gamma) d\gamma. \end{aligned} \tag{2.15}$$

Breaking the above into two parts, and carrying some manipulation, we arrive at

$$B_{FSO}(\gamma_{th}) = \frac{A}{4}\text{erfc}\left(\frac{\ln\left(\frac{\gamma_{th}}{\bar{\gamma}_{FSO}}\right) + 8{\sigma_x}^2}{\sqrt{32}\sigma_x}\right) - \frac{A}{\sqrt{\pi}}\sum_{j=0}^{\infty}\frac{(-1)^j B^{2j+1}}{j!(2j+1)}\int_{\gamma_{th}}^{\infty}\frac{\gamma^{j-0.5}}{\sqrt{32\pi}\sigma_x}e^{-\frac{\left[\ln\left(\frac{\gamma}{\bar{\gamma}_{FSO}}\right)+8{\sigma_x}^2\right]^2}{32{\sigma_x}^2}}d\gamma \tag{2.16}$$

Using the change of variable $y = \frac{\ln(\frac{\gamma}{\bar{\gamma}_{FSO}})+8\sigma_x^2}{\sqrt{32}\sigma_x}$, the above integral becomes

$$B_{FSO}(\gamma_{th}) = \frac{A}{4}\text{erfc}\left(\psi(\gamma_{th})\right) - \frac{A}{\sqrt{\pi}}\sum_{j=0}^{\infty}\left[\frac{(-1)^j B^{2j+1}}{j!(2j+1)} \times \int_{\psi(\gamma_{th})}^{\infty}\frac{1}{\sqrt{\pi}}e^{-y^2}e^{(j+0.5)(\ln(\bar{\gamma}_{FSO})-8\sigma_x^2+\sqrt{32}\sigma_x y)}dy\right], \tag{2.17}$$

where

$$\psi(\gamma_{th}) = \frac{\ln(\frac{\gamma_{th}}{\bar{\gamma}_{FSO}}) + 8\sigma_x^2}{\sqrt{32}\sigma_x}. \tag{2.18}$$

It can be shown, with the application of the definition of erfc (.) function, that the above expression finally simplifies to

$$B_{FSO}(\gamma_{th}) = \frac{A}{4}\text{erfc}\left(\psi(\gamma_{th})\right) - \frac{A}{2\sqrt{\pi}}\sum_{j=0}^{\infty}\left[\frac{(-1)^j B^{2j+1}}{j!(2j+1)}\bar{\gamma}_{FSO}^{(j+0.5)}e^{(8j^2-2)\sigma_x^2} \times \text{erfc}\left(\psi(\gamma_{th}) - (j+0.5)\sqrt{8}\sigma_x\right)\right]. \tag{2.19}$$

For the RF link, substituting Eqs. (2.7) and (2.11) into Eq. (2.14), we get

$$B_{RF}(\gamma_{th}) = \int_{\gamma_{th}}^{\infty}\frac{A}{2}\text{erfc}\left(\sqrt{\gamma}B\right)\left(\frac{m}{\bar{\gamma}_{RF}}\right)^m\frac{\gamma^{m-1}}{\Gamma[m]}e^{-\frac{\gamma}{\bar{\gamma}_{RF}}m}d\gamma. \tag{2.20}$$

For integer values of m, the above integral becomes [48]

$$B_{RF}(\gamma_{th}) = \left\{-\frac{A}{2}\frac{\text{erfc}\left(\sqrt{\gamma}B\right)}{\Gamma[m]}\Gamma\left[m, \frac{\gamma}{\bar{\gamma}_{RF}}m\right]\right\}\Bigg|_{\gamma_{th}}^{\infty} + \left\{\frac{AB}{2\sqrt{\pi}}\sum_{n=0}^{m-1}\frac{\Gamma\left[n+\frac{1}{2}, \gamma\cdot(B^2+\frac{m}{\bar{\gamma}_{RF}})\right]}{\Gamma(n+1)(B^2+\frac{m}{\bar{\gamma}_{RF}})^{n+\frac{1}{2}}}\left(\frac{m}{\bar{\gamma}_{RF}}\right)^n\right\}\Bigg|_{\gamma_{th}}^{\infty}, \tag{2.21}$$

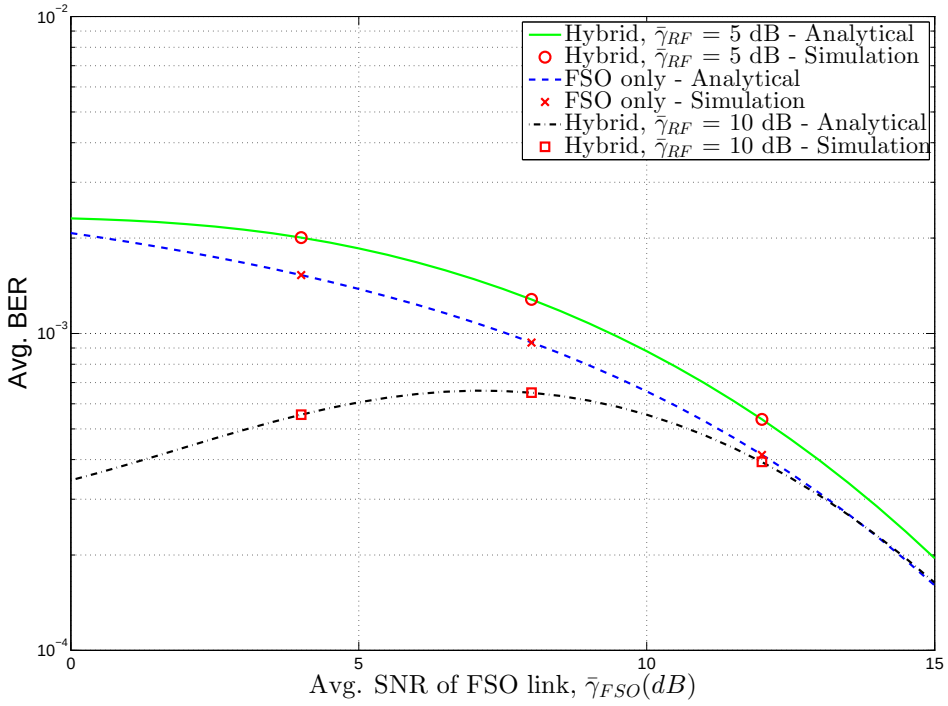

Figure 2.3: Average bit error rate for non-outage period of time for single FSO threshold case as a function of average SNR of the FSO link with BPSK - $\gamma_{th}^{FSO} = \gamma_{th}^{RF} = 5$ dB , $m = 5$, $\sigma_x = 0.25$.

which, after the substitution of the limits, simplifies to

$$B_{RF}(\gamma_{th}) = \frac{A}{2}\frac{\text{erfc}\left(\sqrt{\gamma_{th}}B\right)}{\Gamma[m]}\Gamma\left[m, \frac{\gamma_{th}}{\bar{\gamma}_{RF}}m\right] - \frac{AB}{2\sqrt{\pi}}\sum_{n=0}^{m-1}\frac{\Gamma\left[n+\frac{1}{2}, \gamma_{th}.(B^2+\frac{m}{\bar{\gamma}_{RF}})\right]}{\Gamma(n+1)(B^2+\frac{m}{\bar{\gamma}_{RF}})^{n+\frac{1}{2}}}\left(\frac{m}{\bar{\gamma}_{RF}}\right)^n. \quad (2.22)$$

Fig. 2.3 shows the variation of the average BER against the average SNR of the FSO link, for a fixed value of γ_{th}^{FSO} and γ_{th}^{RF}. As seen in the figure, when using a low quality RF link, the BER performance deteriorates slightly. This is expected because now, instead of turning the transmission off, a weak channel is being used for transmission which affects the average BER. With a high quality RF link, considerable improvement is seen, especially over low FSO SNR region. In fact, as the average SNR of the FSO link improves, the BER performance of the overall system slightly deteriorates first. This is because at a very low value of $\bar{\gamma}_{FSO}$, the high-quality RF link is being used frequently. As $\bar{\gamma}_{FSO}$ becomes larger, the weak FSO link is used more often, which increases the average BER. When

$\bar{\gamma}_{FSO}$ increases further, the FSO link becomes better and the BER performance of the system again improves. The simulation results have also been included which are found to conform to the analytical results.

2.2.3 Ergodic Capacity

The ergodic capacity of the hybrid FSO/RF system for the single FSO threshold case under consideration can be computed as

$$C^{(1)} = C_{FSO}(\gamma_{th}^{FSO}) + P^{FSO}(\gamma_{th}^{FSO}) \cdot C_{RF}(\gamma_{th}^{RF}), \tag{2.23}$$

where $C_{FSO}(\gamma_{th}^{FSO})$ and $C_{RF}(\gamma_{th}^{RF})$ are the capacities of the FSO and RF link respectively, when they are active, and are given by

$$C_{FSO}(\gamma_{th}) = \int_{\gamma_{th}}^{\infty} W_{FSO} \cdot \log_2(1+\gamma) f_{\gamma}^{FSO}(\gamma) d\gamma \tag{2.24}$$

and

$$C_{RF}(\gamma_{th}) = \int_{\gamma_{th}}^{\infty} W_{RF} \cdot \log_2(1+\gamma) f_{\gamma_{RF}}(\gamma) d\gamma, \tag{2.25}$$

respectively, W_{FSO} is the bandwidth of the FSO link, and W_{RF} is the bandwidth of the RF link.

Substituting Eq. (2.5) into Eq. (2.24), we have

$$C_{FSO}(\gamma_{th}) = \int_{\gamma_{th}}^{\infty} \frac{W_{FSO}\log_2(1+\gamma)}{\sqrt{32\pi}\gamma\sigma_x} e^{-\frac{\left[\ln\left(\frac{\gamma}{\bar{\gamma}_{FSO}}\right)+8\sigma_x^2\right]^2}{32\sigma_x^2}} d\gamma. \tag{2.26}$$

After applying the high SNR approximation $\ln(\gamma) \approx \ln(1+\gamma)$, and then using the replacement $y = \frac{\ln(\frac{\gamma}{\bar{\gamma}_{FSO}})+8\sigma_x^2}{\sqrt{32}\sigma_x}$, the above expression becomes

$$C_{FSO}(\gamma_{th}) \approx \int_{\psi(\gamma_{th})}^{\infty} \frac{W_{FSO}}{\ln(2)} \frac{\sqrt{32}\sigma_x y + \ln(\bar{\gamma}_{FSO}) - 8\sigma_x^2}{\sqrt{\pi}} e^{-y^2} dy, \tag{2.27}$$

where $\psi(\gamma_{th})$ is defined in Eq. (2.18). Carrying out integration, it can be shown that the above expression simplifies to

$$C_{FSO}(\gamma_{th}) \approx \frac{W_{FSO}}{\ln(2)} \frac{\sqrt{8}\sigma_x}{\sqrt{\pi}} e^{-[\psi(\gamma_{th})]^2} + \frac{W_{FSO}}{\ln(2)} \frac{\ln(\bar{\gamma}_{FSO}) - 8\sigma_x^2}{2} \text{erfc}\left(\psi(\gamma_{th})\right). \tag{2.28}$$

For the RF link, substituting Eq. (2.7) into Eq. (2.25), we have

$$C_{RF}(\gamma_{th}) = \int_{\gamma_{th}}^{\infty} W_{RF} \cdot \log_2(1+\gamma) \left(\frac{m}{\bar{\gamma}_{RF}}\right)^m \frac{\gamma^{m-1}}{\Gamma[m]} e^{-\frac{\gamma}{\bar{\gamma}_{RF}}m} d\gamma. \tag{2.29}$$

After using the replacement $y = 1+\gamma$, and performing binomial expansion and some manipulation, we arrive at

$$\begin{aligned} C_{RF}(\gamma_{th}) = &\left(\frac{m}{\bar{\gamma}_{RF}}\right)^m \frac{W_{RF} \cdot e^{\frac{m}{\bar{\gamma}_{RF}}}}{\ln(2)} \\ &\times \sum_{p=0}^{m-1} \left[\frac{(-1)^{m-p-1}}{\Gamma(p+1)\Gamma(m-p)} \times \int_{1+\gamma_{th}}^{\infty} y^p \ln(y) e^{-\frac{y}{\bar{\gamma}_{RF}}m} dy\right]. \end{aligned} \tag{2.30}$$

Finally, we can obtain the closed-form expression for $C_{RF}(.)$ as

$$\begin{aligned} C_{RF}(\gamma_{th}) = &\left(\frac{m}{\bar{\gamma}_{RF}}\right)^m \frac{W_{RF} \cdot e^{\frac{m}{\bar{\gamma}_{RF}}}}{\ln(2)} \\ &\times \sum_{p=0}^{m-1} \left[\frac{(-1)^{m-p-1}}{\Gamma(p+1)\Gamma(m-p)} \times M(p+1, \frac{\bar{\gamma}_{RF}}{m}, 1+\gamma_{th})\right], \end{aligned} \tag{2.31}$$

where

$$\begin{aligned} M(\alpha,\theta,\beta) = &\int_{\beta}^{\infty} y^{\alpha-1} \ln(y) e^{-\frac{y}{\theta}} dy = \theta^{\alpha}\Gamma(\alpha) \left[e^{-\frac{\beta}{\theta}} \ln(\beta) - \mathrm{Ei}\,(-\frac{\beta}{\theta})\right] \\ &+ \sum_{n=1}^{\alpha-1} \left[\frac{\Gamma(\alpha)}{\Gamma(n+1)} \left[\theta^{\alpha-n} e^{-\frac{\beta}{\theta}} \beta^n \ln(\beta) + \theta^{\alpha}\Gamma(n, \frac{\beta}{\theta})\right]\right], \end{aligned} \tag{2.32}$$

$\mathrm{Ei}\,(.)$ is the exponential integral, and $\Gamma(.,.)$ is the upper incomplete Gamma function.

Fig. 2.4 shows the variation of the ergodic capacity against the average SNR of the FSO link, for a fixed value of γ_{th}^{FSO} and γ_{th}^{RF}. It is evident that using the hybrid scheme improves the capacity of overall system, particularly at lower SNRs. In fact, when the RF link quality is high, the capacity over low $\bar{\gamma}_{FSO}$ range is slightly higher than median $\bar{\gamma}_{FSO}$ range, as the system benefits from the frequent switching to the RF link over low $\bar{\gamma}_{FSO}$ range. In order to show the variation of normalized capacity, we have assumed $W_{FSO} = W_{RF}$. Since the calculation of the capacity for the FSO link involved an approximation, the analytical results provide a lower bound on the capacity, as validated by simulation results. At high SNR values, the approximation becomes more accurate, as is evident from the graph.

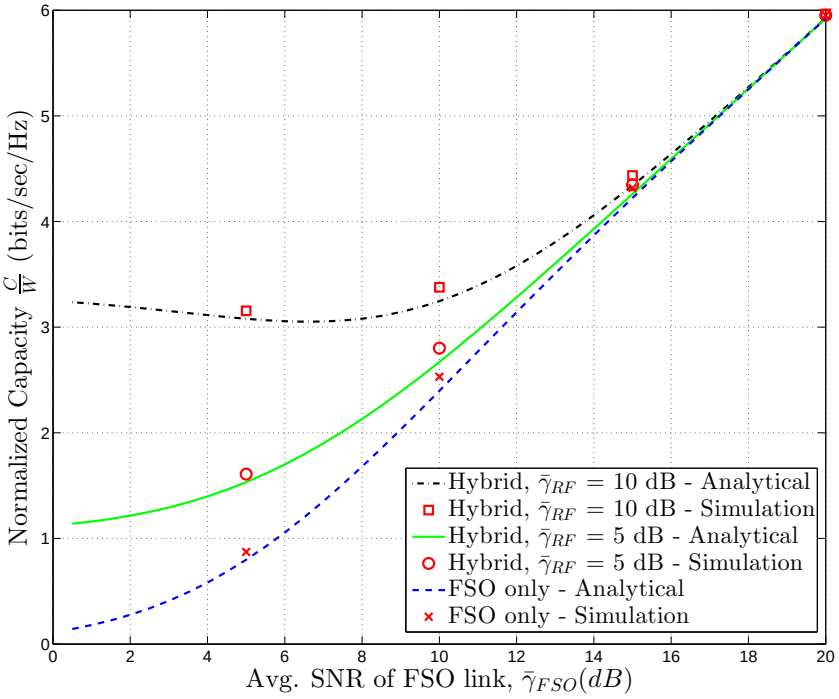

Figure 2.4: Ergodic capacity for single FSO threshold case as a function of average SNR of the FSO link - $\gamma_{th}^{FSO} = \gamma_{th}^{RF} = 5$ dB , $m = 5$, $\sigma_x = 0.25$.

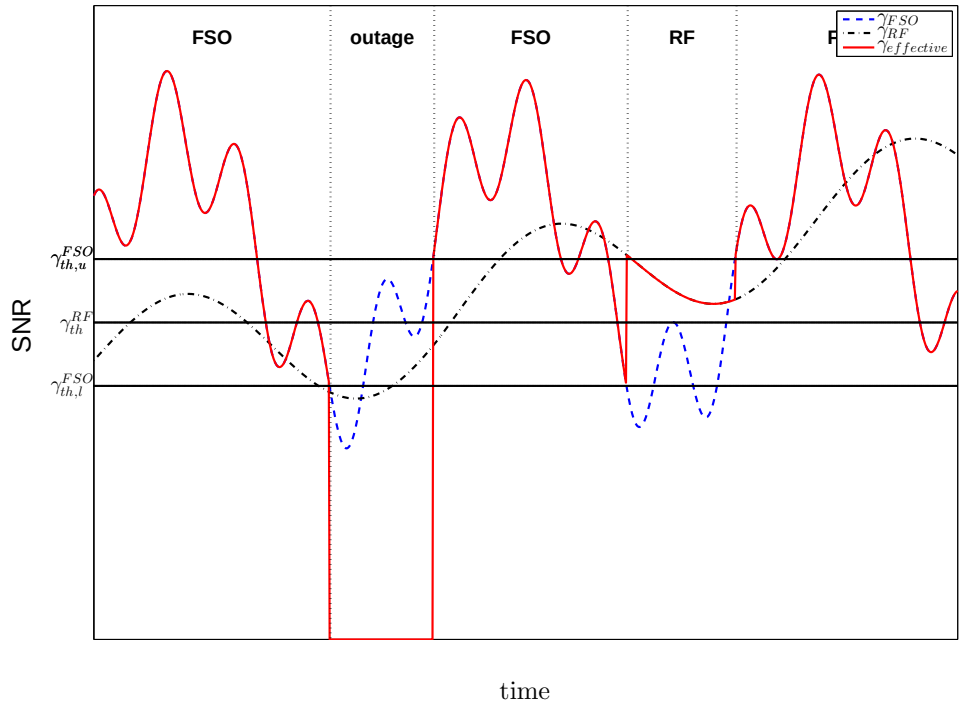

Figure 2.5: Operation with dual FSO threshold.

2.3 Switched FSO/RF Transmission with Dual FSO Threshold

A practically useful variation on the scheme considered in previous section is the use of two thresholds for the FSO link to reduce frequent on/off transitions of the FSO link [39]. This is important in order to extend the life time of the FSO communication link. In this scenario, the FSO link continues operation until the SNR of the FSO link falls below $\gamma_{th,l}^{FSO}$, in which case it will turn off. The FSO link will only turn back on when the SNR reaches above $\gamma_{th,u}^{FSO}$ where $\gamma_{th,u}^{FSO} > \gamma_{th,l}^{FSO}$. As in single threshold scenario, the RF link will be used for data transmission only if its SNR is above a threshold γ_{th}^{RF} and the FSO link is off. If both links are off, then an outage will be declared. A sample illustration of the above mode of operation is depicted in Fig. 2.5. Note that when the SNR of FSO link is between $\gamma_{th,l}^{FSO}$ and $\gamma_{th,u}^{FSO}$, either RF link or FSO link may be used, depending on the previous status of FSO link. The gap between the lower and upper thresholds will affect the frequency of on/off transitions. The larger the gap, the lower the transition frequency.

To facilitate the understanding of the following analysis, we further elucidate

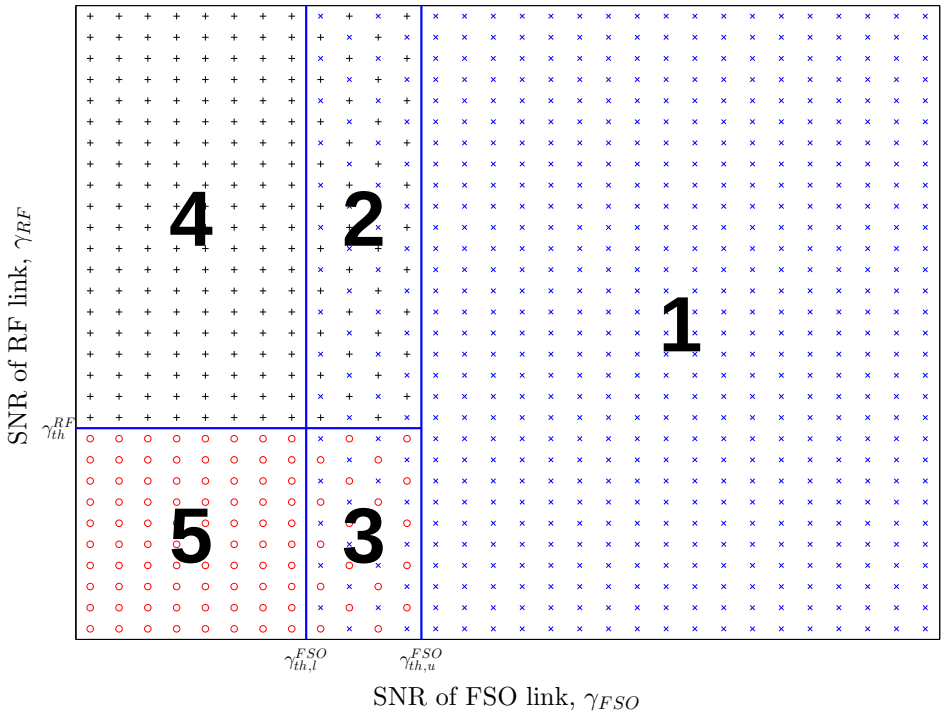

Figure 2.6: Operation regions of dual FSO threshold case.

the operation modes of hybrid FSO/RF system with dual FSO threshold using Fig. 2.6. The SNR thresholds $\gamma_{th,u}^{FSO}$, $\gamma_{th,l}^{FSO}$, and γ_{th}^{RF} divide the possible SNR values of FSO and RF link into five regions. In region 1, since the FSO link SNR is above the upper threshold, FSO will be used for transmission. In region 2, the on/off status of the FSO link depends on the last state of the FSO SNR, i.e. whether it was above $\gamma_{th,u}^{FSO}$ or below $\gamma_{th,l}^{FSO}$. Both FSO link and RF link may be used for transmission. In region 3, the chances of FSO link being on or off are same as that in region 2, but the RF link is off in this region. Thus, either FSO link is being used for transmission or an outage is declared. In region 4, FSO link is certainly off, while the RF link is on, and hence the RF link will be used for transmission. In region 5, both the links are off and an outage is declared.

2.3.1 Outage Probability

Based on the above mode of operation, outage occurs when both links are off. FSO link is off if $\gamma_{FSO} < \gamma_{th,l}^{FSO}$ or $\gamma_{th,l}^{FSO} < \gamma_{FSO} < \gamma_{th,u}^{FSO}$ but γ_{FSO} was previously less than $\gamma_{th,l}^{FSO}$. The probability that the FSO link is off, denoted by

$P_{out}^{FSO}(\gamma_{th,l}^{FSO}, \gamma_{th,u}^{FSO})$, can be calculated as

$$P_{out}^{FSO}(\gamma_{th,l}^{FSO}, \gamma_{th,u}^{FSO}) = P_{low}^{FSO} + P_{med}^{FSO} \frac{P_{low}^{FSO}}{P_{hi}^{FSO} + P_{low}^{FSO}}, \tag{2.33}$$

where P_{low}^{FSO} is the probability that the FSO link SNR is below $\gamma_{th,l}^{FSO}$, given by

$$P_{low}^{FSO} = P^{FSO}(\gamma_{th,l}^{FSO}), \tag{2.34}$$

P_{med}^{FSO} is the probability that the FSO link SNR is between $\gamma_{th,l}^{FSO}$ and $\gamma_{th,u}^{FSO}$, given by

$$P_{med}^{FSO} = P^{FSO}(\gamma_{th,u}^{FSO}) - P^{FSO}(\gamma_{th,l}^{FSO}), \tag{2.35}$$

P_{hi}^{FSO} is the probability that the FSO link SNR is above $\gamma_{th,u}^{FSO}$, given by

$$P_{hi}^{FSO} = 1 - P^{FSO}(\gamma_{th,u}^{FSO}), \tag{2.36}$$

and $P^{FSO}(.)$ was given in Eq. (2.9). Specifically, $\frac{P_{low}^{FSO}}{P_{hi}^{FSO}+P_{low}^{FSO}}$ represents the probability that the FSO link SNR was previously below $\gamma_{th,l}^{FSO}$ given the FSO link SNR was not between $\gamma_{th,l}^{FSO}$ and $\gamma_{th,u}^{FSO}$.

The outage probability of the overall hybrid system is hence given by

$$P_{out}^{(2)} = P_{out}^{FSO}(\gamma_{th,l}^{FSO}, \gamma_{th,u}^{FSO}) \times P^{RF}(\gamma_{th}^{RF}), \tag{2.37}$$

where $P^{RF}(.)$ is given by equation (2.10).

Fig. 2.7 shows the variation of the outage probability with the average SNR of the FSO link, for fixed values of γ_{th}^{RF} and $\bar{\gamma}_{RF}$. The three curves correspond to different gaps between the upper and lower FSO thresholds, i.e. $\gamma_{th,u}^{FSO} = \gamma_{th,l}^{FSO} =$ 5 dB; $\gamma_{th,u}^{FSO} = 5.5$ dB and $\gamma_{th,l}^{FSO} = 4.5$ dB; and $\gamma_{th,u}^{FSO} = 6$ dB and $\gamma_{th,l}^{FSO} = 4$ dB cases, respectively. The first curve essentially corresponds to the single threshold case. We see that the performance difference between single FSO threshold case and dual FSO threshold cases is minimal. In fact, at high values of average FSO link SNR, $\bar{\gamma}_{FSO}$, minor improvement is seen for the dual FSO threshold case, which may be attributed to the fact that with high $\bar{\gamma}_{FSO}$, most of the operation in region 2 of Fig. 2.6 is preceded by operation in region 1, which means that the FSO link will be transmitting for a greater amount of time.

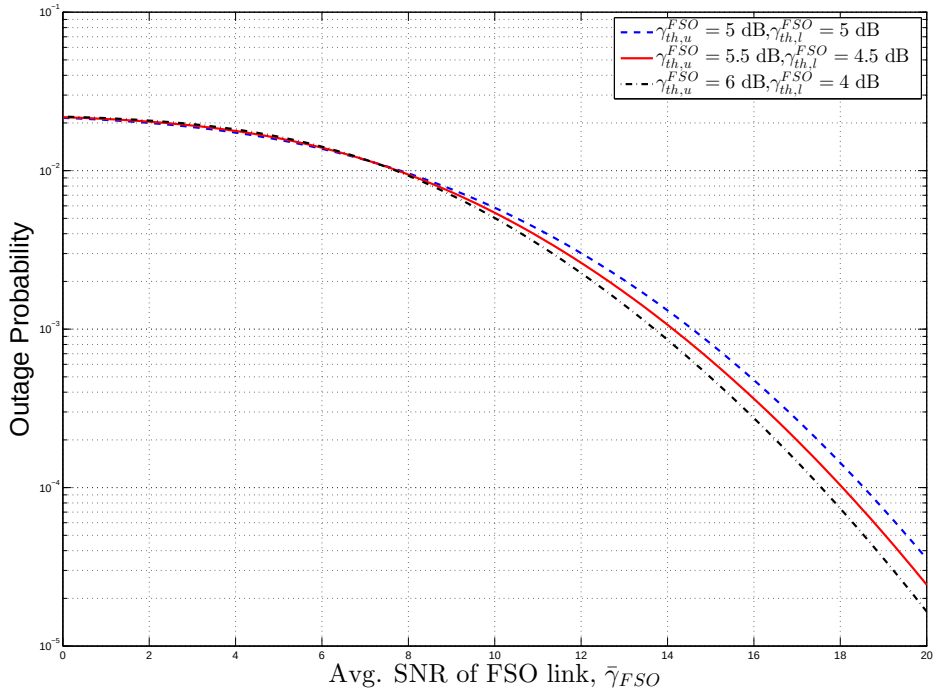

Figure 2.7: Outage probability for dual FSO threshold case as a function of average SNR of the FSO link - $\bar{\gamma}_{RF} = 8$ dB , $\gamma_{th}^{RF} = 5$ dB , $m = 5$, $\sigma_x = 0.25$.

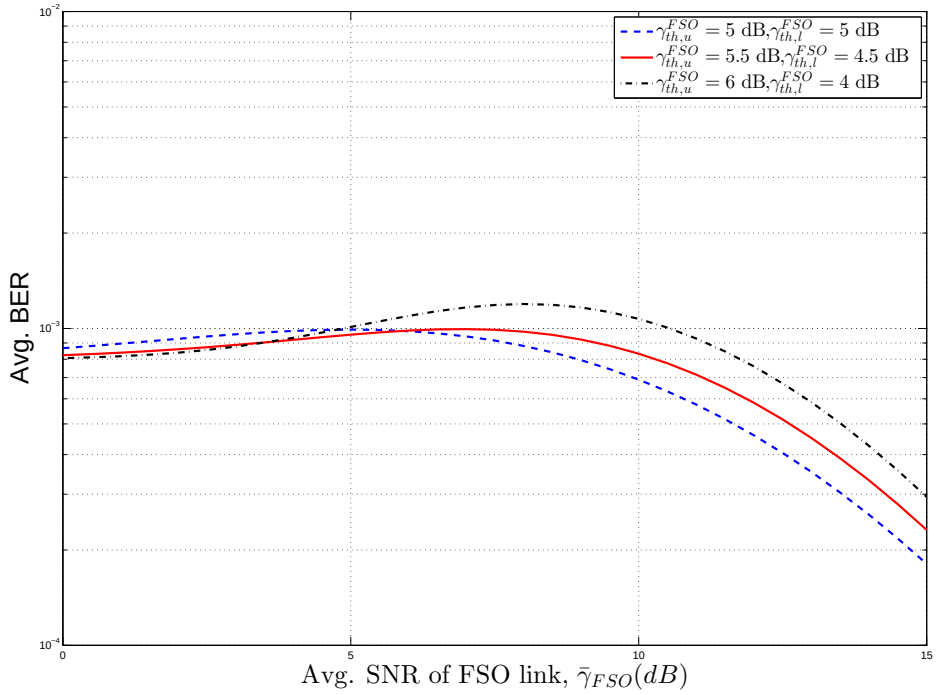

Figure 2.8: Average bit error rate for dual FSO threshold case as a function of average SNR of the FSO link - $\bar{\gamma}_{RF} = 8$ dB , $\gamma_{th}^{RF} = 5$ dB , $m = 5$, $\sigma_x = 0.25$.

2.3.2 Average Bit Error Rate

Based on the mode of operation of the hybrid system with dual FSO threshold, the average BER of the system can be calculated as

$$\overline{BER}^{(2)} = \frac{1}{1 - P_{out}^{(2)}} \times \Big[B_{FSO}(\gamma_{th,u}^{FSO}) + P_{out}^{FSO}(\gamma_{th,l}^{FSO}, \gamma_{th,u}^{FSO}) \cdot B_{RF}(\gamma_{th}^{RF}) + \big[B_{FSO}(\gamma_{th,l}^{FSO}) - B_{FSO}(\gamma_{th,u}^{FSO}) \big] \cdot \frac{P_{hi}^{FSO}}{P_{hi}^{FSO} + P_{low}^{FSO}} \Big], \quad (2.38)$$

where $B_{FSO}(.)$ and $B_{RF}(.)$ are defined in Eqs. (2.13) and (2.14) respectively. The first addition term in the bracket corresponds to the operation in region 1 of Fig. 2.6, the second term in regions 2 and 4 when FSO link is off, and the third term in regions 2 and 3 if FSO link is on.

Fig. 2.8 shows the variation of the average BER against the average SNR of the FSO link, for fixed values of γ_{th}^{RF} and $\bar{\gamma}_{RF}$. Again, there is very little difference between single FSO threshold and dual FSO threshold cases, in terms of BER performance. Some minor increase in the average BER is seen at high values of $\bar{\gamma}_{FSO}$, which may be understood with a similar argument as follows.

Specifically, with dual FSO threshold and high $\bar{\gamma}_{FSO}$, the FSO link is on for some extra time when SNR is between the lower and upper FSO thresholds, instead of it using a better-quality RF link. This results in some increase in the average BER. Slightly improved performance is also seen at very low values of $\bar{\gamma}_{FSO}$, which can be explained with the following argument. Now most of the operation in region 2 and 3 of Fig. 2.6 is preceded by operation in region 4 and 5, respectively. As such, the FSO link is mostly off in these regions, resulting in either shifting to a better quality RF link (region 2), or an outage being declared (region 3), both of which lead to an improved average BER.

2.3.3 Ergodic Capacity

Based on similar reasoning for BER analysis, the capacity of the hybrid system for dual FSO threshold case is given by

$$\begin{aligned} C^{(2)} =& C_{FSO}(\gamma_{th,u}^{FSO}) + P_{out}^{FSO}(\gamma_{th,l}^{FSO}, \gamma_{th,u}^{FSO}) \cdot C_{RF}(\gamma_{th}^{RF}) \\ &+ \left[C_{FSO}(\gamma_{th,l}^{FSO}) - C_{FSO}(\gamma_{th,u}^{FSO})\right] \cdot \frac{P_{hi}^{FSO}}{P_{hi}^{FSO} + P_{low}^{FSO}}, \end{aligned} \tag{2.39}$$

where $C_{FSO}(.)$ and $C_{RF}(.)$ are defined in Eqs. (2.24) and (2.25) respectively. Specifically, the first addition term in the above expression corresponds to the operation in region 1 of Fig. 2.6, the second term in region 2 and 4 when FSO link is off, and the third term in region 2 and 3 if FSO link is on.

Fig. 2.9 shows the variation of the ergodic capacity against the average SNR of the FSO link, for fixed values of γ_{th}^{RF} and $\bar{\gamma}_{RF}$. The capacity performance of dual FSO threshold case is essentially the same as that of single FSO threshold case. Minor deterioration at high values of $\bar{\gamma}_{FSO}$, and minor improvement at low values of $\bar{\gamma}_{FSO}$ are observed, similar to the average BER performance. Specifically, with high $\bar{\gamma}_{FSO}$, FSO link is on more often when the system operates in region 2 of Fig. 2.6 instead of shifting to a better quality RF link, which results in certain capacity reduction. Similarly, with low $\bar{\gamma}_{FSO}$, FSO link is mostly off, and the system switches to a better quality RF link when operating in region 2, which increases the capacity.

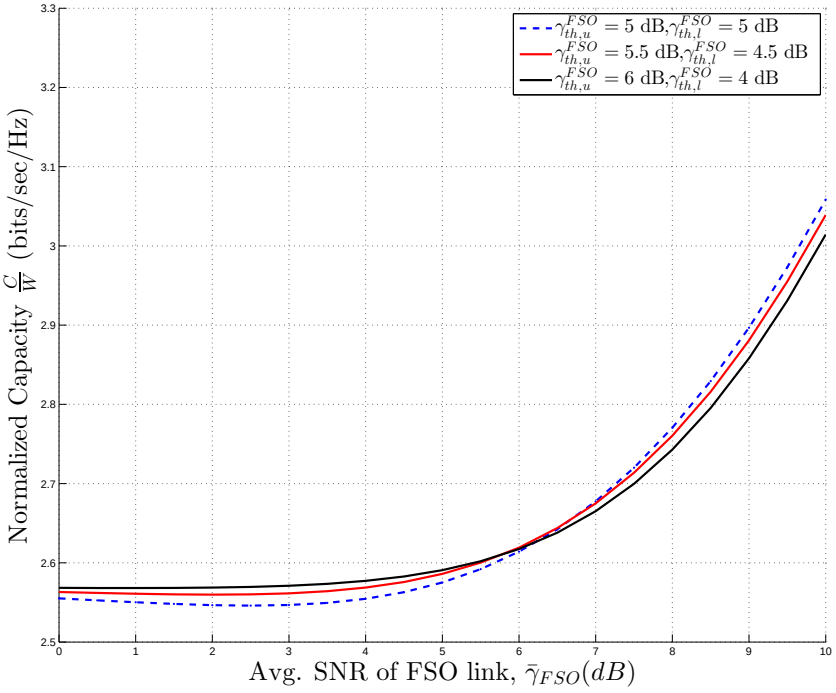

Figure 2.9: Ergodic capacity for dual FSO threshold case as a function of average SNR of the FSO link - $\bar{\gamma}_{RF} = 8$ dB , $\gamma_{th}^{RF} = 5$ dB , $m = 5$, $\sigma_x = 0.25$.

Chapter 3

Extended Delivery Time Analysis for Cognitive Packet Transmission with Work-preserving Strategy

In this chapter, we carry out a thorough statistical analysis on the EDT of secondary packet transmission with work-preserving strategy. In general, the transmission of a secondary packet involves an interleaved sequence of transmission and waiting time slots, both of which can have random time duration. We first derive the exact closed-form expression for the distribution function of EDT assuming a fixed packet transmission time. Both, the ideal scenario of continuous sensing, in which the SU will continuously sense for the channel availability, and the practical scenario of periodic sensing, in which the SU will sense the channel periodically, are considered. We also generalize the analysis to the case where the transmission time depends on the instantaneous channel quality, and as such, is random. The exact statistics for the EDT for secondary packet transmission can be directly used to predict the delay performance of some low-traffic intensity secondary applications.

We then apply these statistical results on EDT to the secondary queuing analysis. The queuing analysis for secondary transmission is a challenging problem even for Poisson arrival traffic. The main difficulty results from the fact that packets will experience two different types of service time depending on whether the packets see an empty queue or not upon arrival. In this chapter, we solve this problem by using the mean value technique with the M/G/1 queuing model. Both average queuing delay and average queue length are calculated in closed form. Simulation results are included to validate the obtained analytical results.

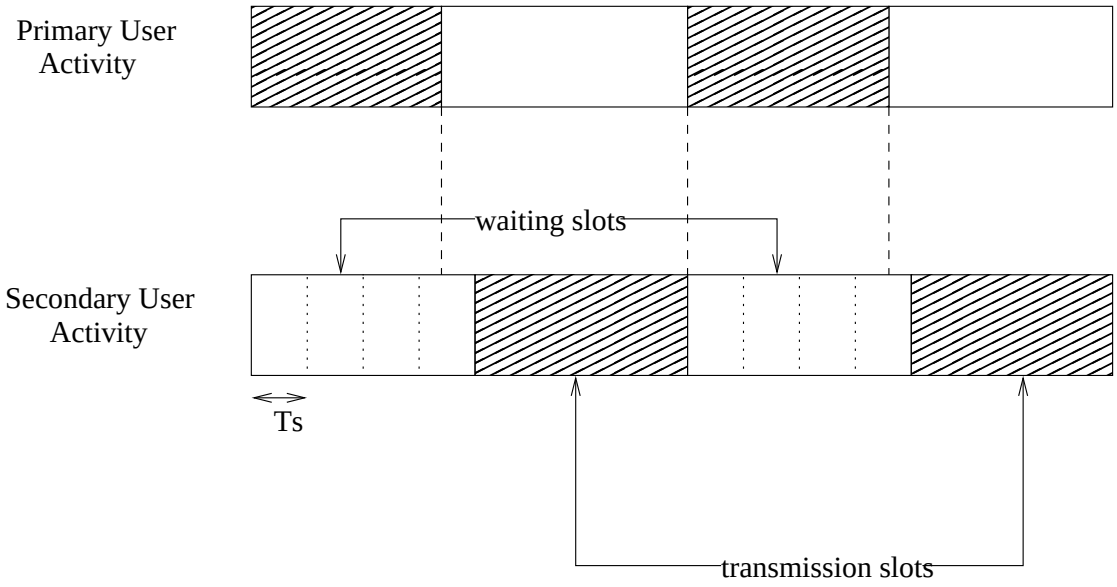

Figure 3.1: Illustration of PU and SU activities and SU sensing for periodic sensing case.

3.1 System Model and Problem Formulation

We consider a cognitive transmission scenario where the SU opportunistically accesses a channel of the primary system for data transmission. The occupancy of that channel by the PU evolves independently according to a homogeneous continuous-time Markov chain with an average busy period of λ and an average idle period of μ. Thus, the duration of busy and idle periods are exponentially distributed. The SU opportunistically accesses the channel in an interweave fashion. Specifically, the SU can use the channel only after PU stops transmission. As soon as the PU restarts transmission, the SU instantaneously stops its transmission, and thus no interference is caused to the PU.

The SU monitors PU activity through spectrum sensing. With continuous sensing, the SU continuously senses the channel for availability. Thus, the SU starts its transmission as soon as the channel becomes available. As soon as the PU reappears, SU stops its transmission. We also consider the case where the SU senses the channel periodically, with an interval of T_s. If the PU is sensed busy, the SU will wait for T_s time units and re-sense the channel. With periodic sensing, there is a small amount of time when the PU has stopped its transmission, but the SU has not yet acquired the channel, as illustrated in Fig. 3.1. During transmission, the SU continuously monitors PU activity i.e. even with periodic sensing, the SU reverts to continuous sensing for detecting the PU in order to return the channel back. As soon as the PU restarts, the SU stops its transmission. The continuous period of time during which the PU is off and the SU is

transmitting is referred to as a transmission slot. Similarly, the continuous period of time during which the PU is transmitting is referred to as a waiting slot. For periodic sensing case, the waiting slot also includes the time when the PU has stopped transmission, but the SU has not sensed the channel yet.

In this work, we analyze the packet delivery time of a secondary system, which includes an interweaved sequence of the transmission time and the waiting time. The resulting EDT for a packet is mathematically given by $T_{ED} = T_w + T_{tr}$, where T_w is the total waiting time for the SU and T_{tr} is the packet transmission time. Note that both T_w and T_{tr} are, in general, random variables, with T_w depending on T_{tr}, PU behaviour and sensing strategies, and T_{tr} depending on packet size and secondary channel condition when available. In what follows, we first derive the exact distribution of the EDT T_{ED} for both continuous sensing and periodic sensing cases, which are then applied to the secondary queuing analysis in section 3.3.

3.2 Extended Delivery Time Analysis

In this section, we investigate the EDT of a secondary system for a single packet arriving at a random point in time. We first consider a fast varying channel and/or a long packet, where the transmission time T_{tr} can be estimated as a constant, given by

$$T_{tr} \approx \frac{H}{W \int_0^\infty \log_2(1+\gamma) f_\gamma(\gamma) d\gamma}, \tag{3.1}$$

where H is the entropy of the packet, W is the available bandwidth and $f_\gamma(\gamma)$ is the PDF of the SNR of the fading channel. We then consider the case of short packets, where T_{tr} cannot be treated as a constant. For both continuous sensing and periodic sensing scenarios, we derive the exact distribution of T_{ED}. These analyses also characterize the delay of some low-rate secondary applications. For example, in wireless sensor networks for health care monitoring, forest fire detection, air pollution monitoring, disaster prevention, landslide detection etc., the transmitter needs to periodically transmit measurement data to the sink with a long duty cycle. The EDT essentially characterizes the delay of measurement data collection.

3.2.1 Continuous Sensing

The EDT for packet transmission by the SU consists of interweaved waiting slots and transmission slots. We first focus on the distribution of T_w. We assume,

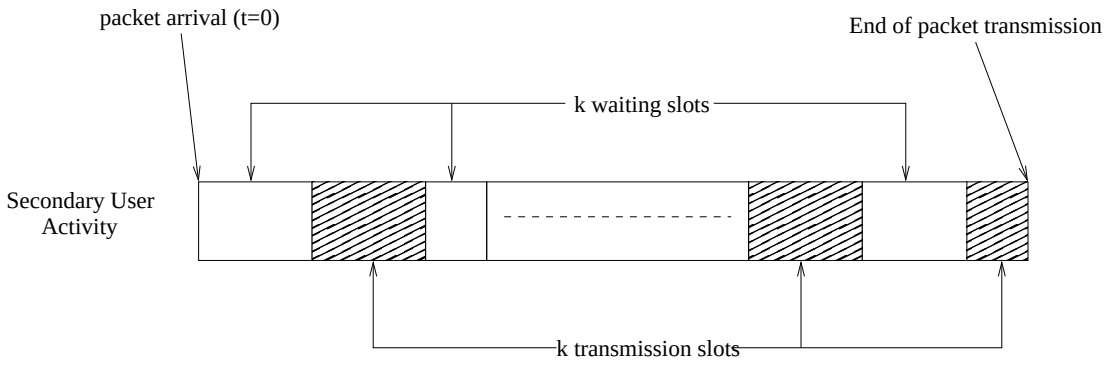

Figure 3.2: Illustration of secondary transmission when the PU is on at $t = 0$.

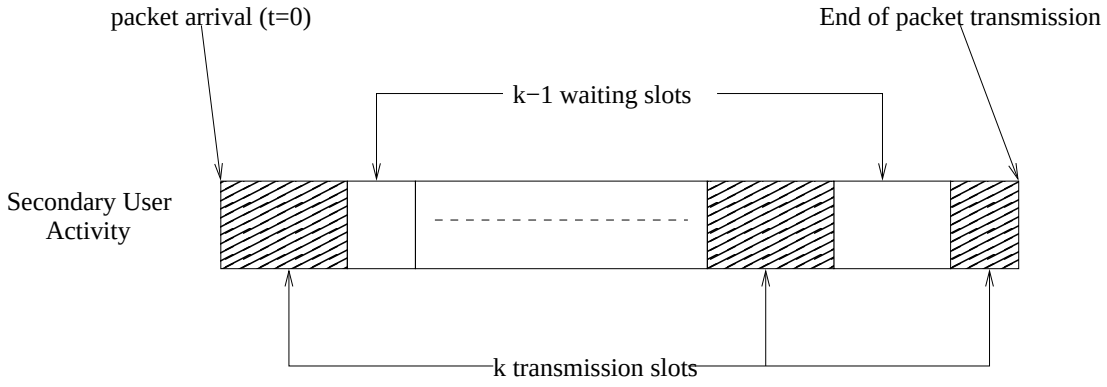

Figure 3.3: Illustration of secondary transmission when the PU is off at $t = 0$.

without loss of generality, that the packet arrives at $t = 0$. The distribution of T_w depends on whether the PU was on or off at that instance, as illustrated in Figs. 3.2 and 3.3. We denote the PDF of the waiting time of the SU for the case when PU is on at $t = 0$, and for the case when PU is off at $t = 0$, by $f_{T_w,p_{on}}(t)$ and $f_{T_w,p_{off}}(t)$, respectively. The PDF of the waiting time T_w for the SU is then given by

$$f_{T_w}(t) = \frac{\lambda}{\lambda+\mu} f_{T_w,p_{on}}(t) + \frac{\mu}{\lambda+\mu} f_{T_w,p_{off}}(t), \tag{3.2}$$

where $\frac{\lambda}{\lambda+\mu}$ and $\frac{\mu}{\lambda+\mu}$ are the stationery probabilities that the PU is on or off at $t = 0$, respectively. The two probability density functions $f_{T_w,p_{on}}(t)$ and $f_{T_w,p_{off}}(t)$ above are calculated independently as follows.

When the PU is on at $t = 0$, T_w includes k waiting slots if k transmission slots are needed for packet transmission. Let $\mathcal{P}_k$ represent the probability that the SU completes packet transmission in k transmission slots, and $f_{T_w,k}(t)$ represent the PDF of the total time duration of k SU waiting slots. Then the PDF of the total waiting time for the SU, for the case when PU is on at $t = 0$, is given by

$$f_{T_w,p_{on}}(t) = \sum_{k=1}^{\infty} \mathcal{P}_k \times f_{T_w,k}(t). \tag{3.3}$$

Note that $f_{T_w,k}(t)$ is the PDF of the sum of k independent and identically distributed exponential random variables with average λ. Therefore $f_{T_w,k}(t)$ is given by

$$f_{T_w,k}(t) = \frac{1}{\lambda^k} \frac{t^{k-1}}{(k-1)!} e^{\frac{-t}{\lambda}}. \tag{3.4}$$

$\mathcal{P}_k$ can be calculated as the probability that k SU transmission slots have a total time of more than T_{tr}, whereas $k-1$ transmission slots have a total time of less than T_{tr}. Since the total time for k transmission slots follows the Erlang distribution with PDF

$$f_{T_{tr},k}(t) = \frac{1}{\mu^k} \frac{t^{k-1}}{(k-1)!} e^{\frac{-t}{\mu}}, \tag{3.5}$$

we can show that

$$\mathcal{P}_k = \int_{T_{tr}}^{\infty} \frac{1}{\mu^k} \frac{t^{k-1}}{(k-1)!} e^{\frac{-t}{\mu}} dt - \int_{T_{tr}}^{\infty} \frac{1}{\mu^{k-1}} \frac{t^{k-2}}{(k-2)!} e^{\frac{-t}{\mu}} dt. \tag{3.6}$$

After using integration by parts on the first integral and cancelling the terms, $\mathcal{P}_k$ can be calculated as

$$\mathcal{P}_k = \frac{{T_{tr}}^{k-1} e^{\frac{-T_{tr}}{\mu}}}{\mu^{k-1}(k-1)!}. \tag{3.7}$$

After substituting Eqs. (3.4) and (3.7) into Eq. (3.3), we get

$$f_{T_w,p_{on}}(t) = \sum_{k=1}^{\infty} \frac{{T_{tr}}^{k-1} e^{\frac{-T_{tr}}{\mu}}}{\mu^{k-1}(k-1)!} \times \frac{1}{\lambda^k} \frac{t^{k-1}}{(k-1)!} e^{\frac{-t}{\lambda}}. \tag{3.8}$$

Finally, applying the definition of Bessel function, we arrive at the following closed-form expression for $f_{T_w,p_{on}}(t)$

$$f_{T_w,p_{on}}(t) = \frac{1}{\lambda} e^{\frac{-T_{tr}}{\mu}} I_0\left(2\sqrt{\frac{T_{tr}t}{\mu\lambda}}\right) e^{\frac{-t}{\lambda}}, \tag{3.9}$$

where $I_n(.)$ is the modified Bessel function of the first kind of order n.

Similarly, the PDF for T_w when PU is off at $t = 0$ can be obtained as

$$f_{T_w,p_{off}}(t) = \sum_{k=1}^{\infty} \mathcal{P}_k \times f_{T_w,k-1}(t) = e^{\frac{-T_{tr}}{\mu}}\delta(t) + \sum_{k=2}^{\infty} \frac{{T_{tr}}^{k-1} e^{\frac{-T_{tr}}{\mu}}}{\mu^{k-1}(k-1)!} \times \frac{1}{\lambda^{k-1}} \frac{t^{k-2}}{(k-2)!} e^{\frac{-t}{\lambda}}, \tag{3.10}$$

which simplifies to

$$f_{T_w,p_{off}}(t) = e^{\frac{-T_{tr}}{\mu}}\delta(t) + \sqrt{\frac{T_{tr}}{\mu\lambda t}} e^{\frac{-T_{tr}}{\mu}} I_1\left(2\sqrt{\frac{T_{tr}t}{\mu\lambda}}\right) e^{\frac{-t}{\lambda}}, \tag{3.11}$$

where $\delta(t)$ is the delta function. Note that the term $e^{\frac{-T_{tr}}{\mu}}\delta(t)$ corresponds to the the case that the number of waiting slots is equal to 0.

After substituting Eqs. (3.9) and (3.11) into (3.2), and noting $T_{ED} = T_w + T_{tr}$, the PDF for the EDT T_{ED} for continuous sensing case is given by

$$\begin{aligned} f_{T_{ED}}(t) = {} & \frac{\mu}{\lambda+\mu} e^{\frac{-T_{tr}}{\mu}} \delta(t - T_{tr}) + u(t - T_{tr}) \frac{1}{\lambda+\mu} e^{\frac{-t}{\lambda}} \\ & \times \left[I_0\left(2\sqrt{\frac{T_{tr}(t-T_{tr})}{\mu\lambda}}\right) + \sqrt{\frac{T_{tr}\mu}{\lambda(t-T_{tr})}} I_1\left(2\sqrt{\frac{T_{tr}(t-T_{tr})}{\mu\lambda}}\right) \right], \end{aligned} \tag{3.12}$$

where $u(.)$ is the step function.

Fig. 3.4 plots the analytical expression for the PDF of the EDT with continuous sensing, given in Eq. (3.12). The corresponding plot for the simulation results is also shown. The perfect match between analytical and simulation results verify our analytical approach.

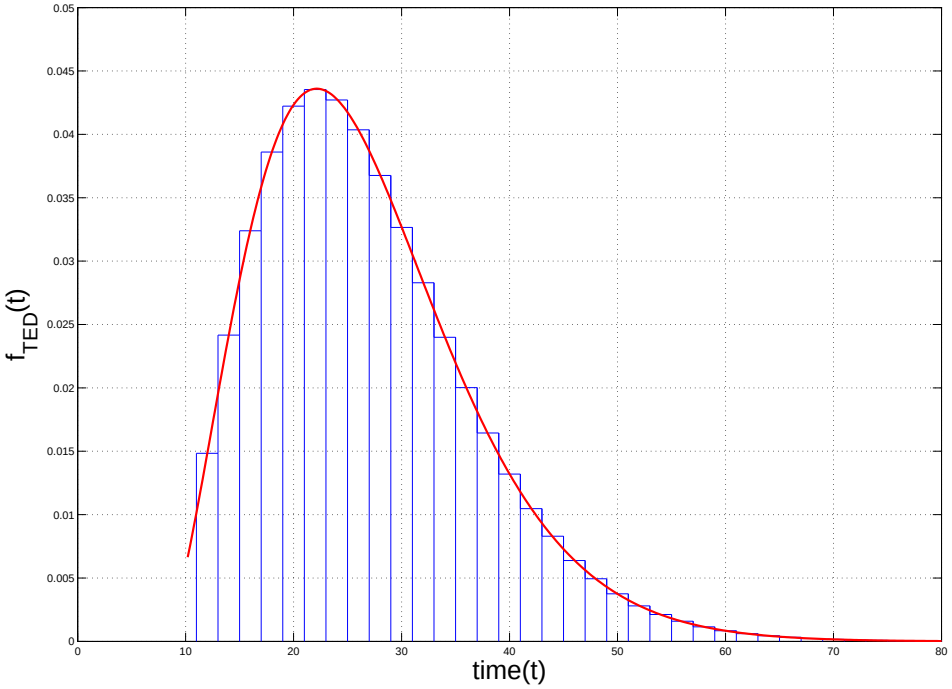

Figure 3.4: Simulation verification for the analytical PDF of T_{ED} with continuous sensing ($T_{tr} = 10$, $\lambda = 3$, and $\mu = 2$).

3.2.2 Periodic Sensing

In the case of periodic sensing, the waiting time T_w will be a multiple of T_s, which is a known constant quantity. Therefore T_w will have a discrete distribution. Similar to continuous sensing case, we can write the probability that the waiting time T_w is nT_s by considering the PU is on or off at $t = 0$ separately, as

$$\Pr[T_w = nT_s] = \frac{\lambda}{\lambda+\mu}\Pr[T_w, p_{on} = nT_s] + \frac{\mu}{\lambda+\mu}\Pr[T_w, p_{off} = nT_s], \qquad (3.13)$$

where $\Pr[T_w, p_{on} = nT_s]$ is the probability that the total waiting time for the SU is nT_s when PU is on at $t = 0$, and $\Pr[T_w, p_{off} = nT_s]$ the probability when PU is off at $t = 0$.

It can be shown based on the illustration in Fig. 3.2 that

$$\Pr[T_w, p_{on} = nT_s] = \sum_{k=1}^{\infty} \mathcal{P}_k \times \Pr[T_{w,k} = nT_s], \qquad (3.14)$$

where $\mathcal{P}_k$ is the probability that the SU completes its transmission in k slots, given in Eq. (3.7), and $\Pr[T_{w,k} = nT_s]$ is the probability that the SU waiting time in k

slots is nT_s, given by

$$\Pr[T_{w,k} = nT_s] = (1-\beta)^k(\beta)^{n-k}\binom{n-1}{k-1}, \tag{3.15}$$

where

$$\beta = \frac{\lambda}{\lambda+\mu} + \frac{\mu}{\lambda+\mu}e^{-(\frac{1}{\lambda}+\frac{1}{\mu})T_s}, \tag{3.16}$$

as shown in Appendix A.2. If we assume that T_s is very small, we can approximate β with $e^{\frac{-T_s}{\lambda}}$. After substituting Eqs. (3.7) and (3.15) into Eq. (3.14), and some manipulation, we can calculate $\Pr[T_w, p_{on} = nT_s]$ as

$$\Pr[T_w, p_{on} = nT_s] = (1-\beta)\beta^{n-1}e^{\frac{-T_{tr}}{\mu}} \times \sum_{0}^{n-1}\left[\frac{T_{tr}(1-\beta)}{\mu\beta}\right]^k \frac{1}{k!}\binom{n-1}{k}, \tag{3.17}$$

which simplifies to

$$\Pr[T_w, p_{on} = nT_s] = (1-\beta)\beta^{n-1}e^{\frac{-T_{tr}}{\mu}} \times {}_1F_1\left(1-n; 1; \frac{-T_{tr}(1-\beta)}{\mu\beta}\right), \tag{3.18}$$

where ${}_1F_1(.,.,.)$ is the generalized Hyper-geometric function. Similarly, $\Pr[T_w, p_{off} = nT_s]$ in Eq. (3.13) can be calculated as

$$\Pr[T_w, p_{off} = nT_s] = \sum_{k=1}^{\infty}\mathcal{P}_k \times \Pr[T_{w,k-1} = nT_s]. \tag{3.19}$$

After substituting Eqs. (3.7) and (3.15) into Eq. (3.19), and some manipulation, we get

$$\begin{aligned}\Pr[T_w, p_{off} = nT_s] = e^{-\frac{T_{tr}}{\mu}}\delta[n] + \left[\frac{T_{tr}(1-\beta)\beta^{n-1}}{\mu}\right]e^{\frac{-T_{tr}}{\mu}} \\ \times \sum_{k=0}^{n-1}\left[\frac{T_{tr}(1-\beta)}{\mu\beta}\right]^k \frac{1}{(k+1)!}\binom{n-1}{k},\end{aligned} \tag{3.20}$$

which eventually simplifies to

$$\begin{aligned}\Pr[T_w, p_{off} = nT_s] = e^{-\frac{T_{tr}}{\mu}}\delta[n] + \left[\frac{T_{tr}(1-\beta)\beta^{n-1}}{\mu}\right]e^{\frac{-T_{tr}}{\mu}} \\ \times {}_1F_1\left(1-n; 2; \frac{-T_{tr}(1-\beta)}{\mu\beta}\right)u[n-1].\end{aligned} \tag{3.21}$$

After substituting Eqs. (3.18) and (3.21) into Eq. (3.13), the probability mass

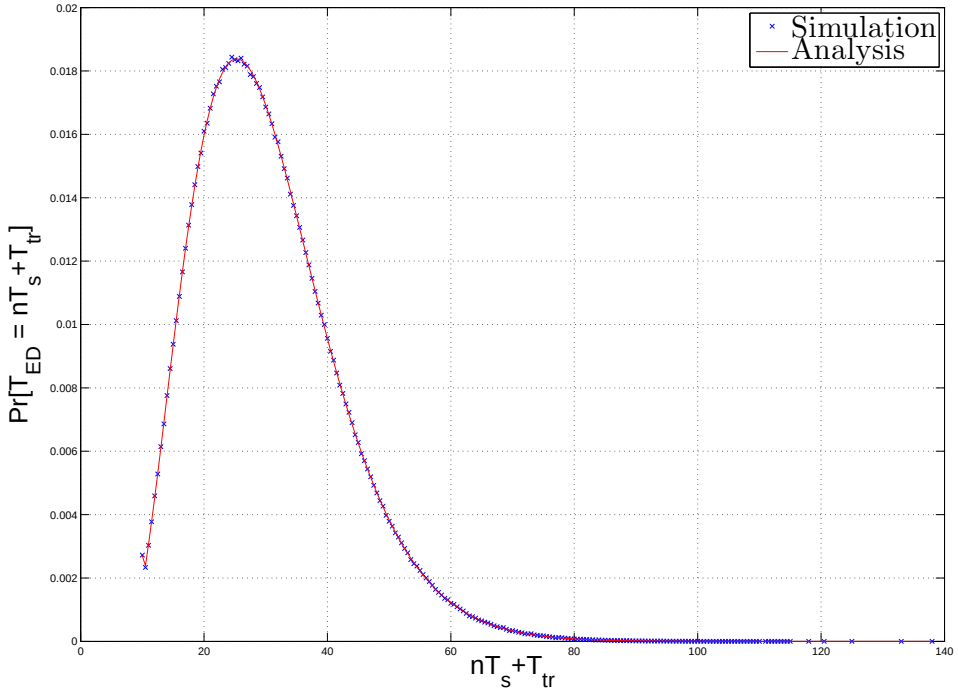

Figure 3.5: Simulation verification of the analytical PMF of T_{ED} with periodic sensing ($T_{tr} = 10$, $\lambda = 3$, $\mu = 2$, and $T_s = 0.5$).

function (PMF) of the EDT for periodic sensing case is given by

$$\Pr[T_{ED} = nT_s + T_{tr}] = \frac{\lambda}{\lambda+\mu}(1-\beta)\beta^{n-1}e^{\frac{-T_{tr}}{\mu}} \times {}_1F_1\left(1-n;1;\frac{-T_{tr}(1-\beta)}{\mu\beta}\right)u[n] + \frac{\mu}{\lambda+\mu}\left[\left(\frac{T_{tr}(1-\beta)\beta^{n-1}}{\mu}\right)e^{\frac{-T_{tr}}{\mu}}{}_1F_1\left(1-n;2;\frac{-T_{tr}(1-\beta)}{\mu\beta}\right)u[n-1] + e^{-\frac{T_{tr}}{\mu}}\delta[n]\right]. \tag{3.22}$$

Fig. 3.5 plots the PMF of delivery time T_{ED} for periodic sensing case, and the corresponding simulation result. The plots show that the analytical results conform to the simulation results. Fig. 3.6 shows the PMF envelope of the packet delivery time with periodic sensing for various values of sensing period T_s. As can be seen, the performance of periodic sensing improves with reduction in the sensing interval T_s. As T_s approaches 0, the performance of periodic sensing comes close to that of continuous sensing, as expected.

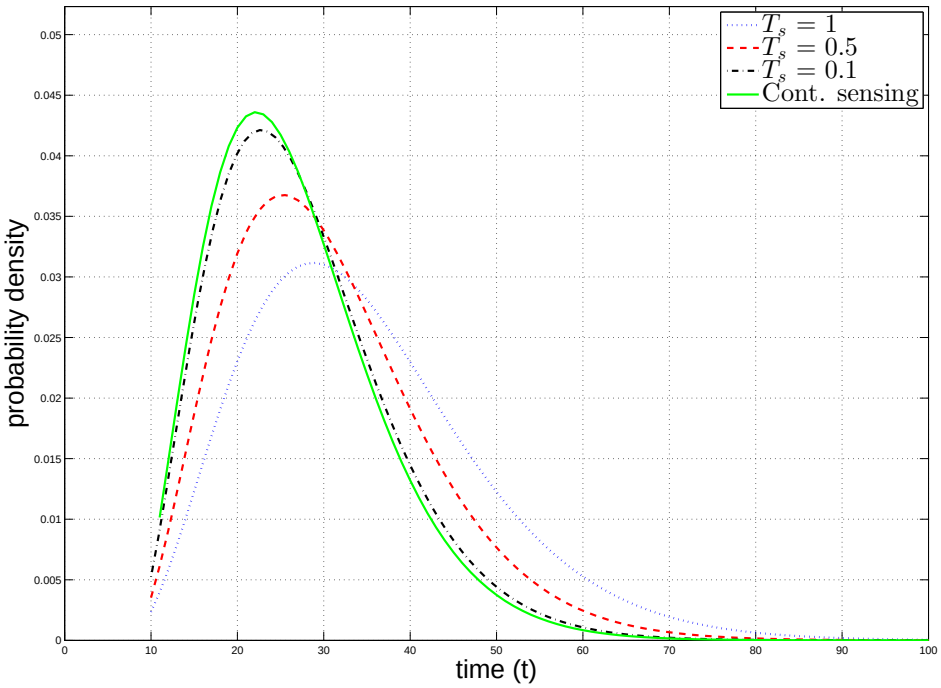

Figure 3.6: Distribution of the EDT with continuous and periodic sensing ($T_{tr} = 10$, $\lambda = 3$, and $\mu = 2$).

3.2.3 Short Packets

In the earlier subsections, the packet transmission time T_{tr} was considered to be a constant depending on the average SNR, which applies to long packets and/or fast fading scenario. Now we consider the transmission of short packets, where T_{tr} depends on the instantaneous SNR of the secondary channel.

Constant SNR during packet transmission

For a short enough packet, slow fading scenario, or a quasi-static channel, it can be assumed that the received SNR of the secondary channel γ will not change for the complete duration of the packet transmission. The transmission time T_{tr}, a random variable, will be a function of the received SNR γ, defined as

$$T_{tr} = \frac{H}{W \log_2(1+\gamma)}, \tag{3.23}$$

where H is the entropy of the data packet in bits. Assuming a Rayleigh fading model for the secondary channel with an SNR PDF given by

$$f_\gamma(\gamma) = \frac{1}{\bar{\gamma}} e^{\frac{\gamma}{\bar{\gamma}}}, \tag{3.24}$$

the PDF of the transmission time T_{tr} can be derived as [49]

$$f_{T_{tr}}(T) = \frac{H}{\bar{\gamma} T^2} e^{\left[\frac{1}{\bar{\gamma}} + \frac{H}{T} - e^{\frac{H}{T}}_{\bar{\gamma}}\right]}, \tag{3.25}$$

where $\bar{\gamma}$ is the average link SNR. The exact distribution of the EDT of a single packet for the continuous sensing case can then be calculated as

$$f^{v,c}_{T_{ED}}(t) = \int_0^t f_{T_{ED}}(t|T_{tr}) \cdot f_{T_{tr}}(T_{tr}) dT_{tr}, \tag{3.26}$$

where $f_{T_{ED}}(.|T_{tr})$ is the conditional PDF of the EDT of the SU for a given T_{tr}, as given in Eq. (3.12). For the discrete sensing case, the exact distribution of EDT will be given by

$$f^{v,p}_{T_{ED}}(t) = \sum_{n=0}^{\lfloor \frac{t}{T_s} \rfloor} \Pr[T_{ED} = nT_s + T_{tr} | T_{tr} = t - nT_s] \times f_{T_{tr}}(t - nT_s), \tag{3.27}$$

where $\Pr[T_{ED} = nT_s + T_{tr} | T_{tr} = t - nT_s]$ is the probability that the EDT of a packet for given data transmission time T_{tr} is $nT_s + T_{tr}$, as defined in Eq. (3.22). More

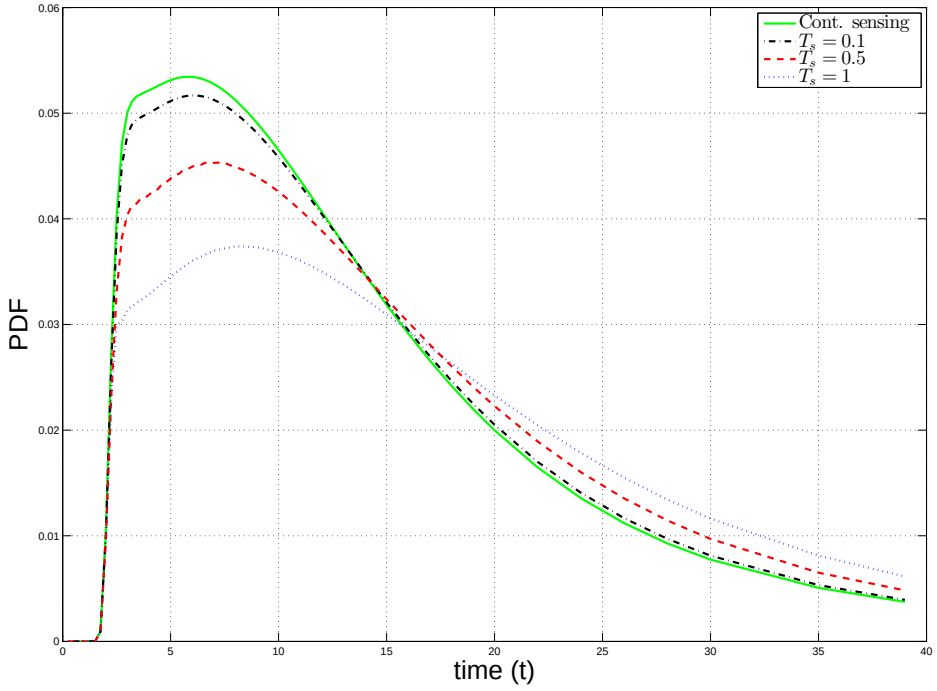

Figure 3.7: PDF of EDT for short packets ($H = 100$, $W = 10$, $\bar{\gamma} = 8$ dB $\lambda = 3$, and $\mu = 2$).

specifically, each summation term in the above equation refers to the probability that the SU waiting time is nT_s and the physical packet transmission time is $t - nT_s$.

Fig. 3.7 shows the numerically computed PDFs of the EDT for short packets for continuous sensing case and periodic sensing cases with $T_s = 0.1$, $T_s = 0.5$, and $T_s = 1$. As the periodic sensing interval approaches 0, the corresponding PDF curve comes closer to the PDF curve for continuous sensing.

One shot transmission

For a very short packet, where the packet transmission will complete in only one secondary transmission slot, the packet needs to wait for at most one slot. Using the PDF given Eq. (3.4) with $k = 1$, the PDF of the EDT for such packets with continuous sensing can be calculated as

$$f_{T_{ED}}^{o,c}(t) = \frac{\lambda}{\lambda+\mu}\int_0^t \frac{1}{\lambda} e^{\frac{-(t-T_{tr})}{\lambda}} f_{T_{tr}}(T_{tr})dT_{tr} + \frac{\mu}{\lambda+\mu} f_{T_{tr}}(t). \tag{3.28}$$

Similarly, for periodic sensing case, using $\Pr[T_{w,k} = nT_s]$ from Eq. (3.15) with $k = 1$, the probability distribution function of the EDT for such packets is given

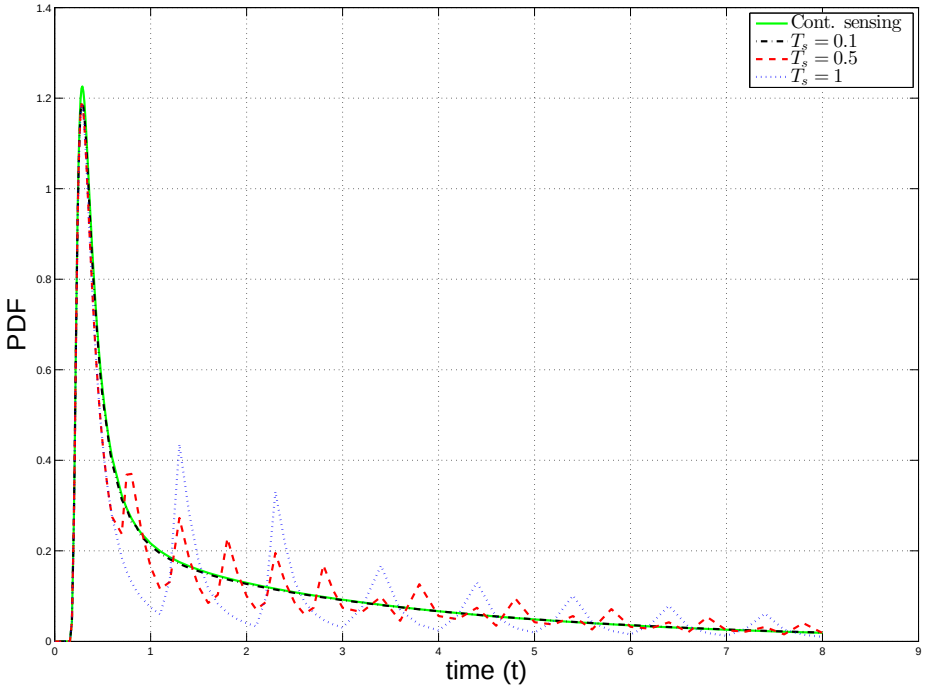

Figure 3.8: PDF of EDT for one shot transmission ($H = 10$, $W = 10$, $\bar{\gamma} = 8$ dB $\lambda = 3$, and $\mu = 2$).

by

$$f_{T_{ED}}^{o,p}(t) = \frac{\mu}{\lambda+\mu} f_{T_{tr}}(t) + \frac{\lambda}{\lambda+\mu} \sum_{n=1}^{\lfloor \frac{t}{T_s} \rfloor} (1-\beta)(\beta)^{n-1}.f_{T_{tr}}(t - n.T_s). \tag{3.29}$$

Fig. 3.8 displays the numerically computed PDFs of the EDT for very short packets for continuous sensing and periodic sensing cases. The first peak in all the curves correspond to the case that the incoming packet finds the PU to be off, and hence gets transmitted immediately. The oscillations seen in the curves for $T_s = 0.5$ and $T_s = 1$ can be attributed to sharp-peaked nature of the PDF of the transmission time T_{tr}, where each peak in the above curve corresponds to a different value of n in Eq. (3.29).

3.3 Application to Secondary Queuing Analysis

In this section, we consider the transmission delay for the secondary system in a queuing set-up. In particular, the secondary traffic intensity is high and, as such, a first-in-first-out queue is introduced to hold packets until being transmitted. We

assume that equal-sized packet arrival follows a Poisson process with intensity $\frac{1}{\psi}$, i.e. the average time duration between packet arrivals is ψ. For the sake of simplicity, the packets are assumed to be of the same long length, such that their transmission time T_{tr} is a fixed constant in the following analysis. As such, the secondary packet transmission can be modelled as a general M/G/1 queue (with a Markovian arrival and general service time), where the service time is closely related to the EDT we studied in the previous section. The service time of a packet is defined as the time it takes from the instant when the packet becomes available for transmission, either by arrival in case of an empty queue or by becoming the first packet in the queue due to completion of the previous packet's transmission, until the instant when it gets completely transmitted.

Note also from the EDT analysis, the waiting time of a packet depends on whether the PU is on or off when the packet is available for transmission. As such, different secondary packets will experience two types of service time characteristics. Specifically, some packets might see that there are one or more packets waiting in the queue or being transmitted upon arrival. Such packets will have to wait in the queue until transmission completion of previous packets. Once all the previous packets are transmitted, the new arriving packet will find the PU to be off. We term such packets as type 1 packets. On the other hand, some packets will arrive when the queue is empty, and will immediately become available for transmission. Such packets might find the PU to be on or off. We will call this type of packets, type 2 packets. To facilitate subsequent queuing analysis, we now calculate the first and second moments of the service time for these two types of packets.

3.3.1 Service Time Moments

Type 1 packets

The average service time of type 1 packets is equal to the EDT of packets that find the PU off at the start of their transmission. Specifically, the first moment of the service time of type 1 packets with continuous sensing, $E[ST_{type1}] \triangleq E[ST_{p_{off}}]^{(c)}$, can be calculated as

$$E[ST_{Type1}] = T_{tr} + \lambda \left(\frac{T_{tr}}{\mu}\right), \tag{3.30}$$

and the second moment, $E[ST^2_{type1}] \triangleq E[ST^2_{p_{off}}]^{(c)}$, as

$$E[ST^2_{Type1}] = \lambda^2 \left[\left(\frac{T_{tr}}{\mu}\right)^2 + 2\frac{T_{tr}}{\mu}\right] + 2\frac{\lambda {T_{tr}}^2}{\mu} + {T_{tr}}^2, \tag{3.31}$$

as shown in Appendix A.3.

With periodic sensing, the first and second moment of service time of type 1 packets can be calculated as

$$E[ST_{type1}] \triangleq E[ST_{p_{off}}]^{(p)} = T_{tr}\left(1 + \frac{T_s}{\mu(1-\beta)}\right), \tag{3.32}$$

and

$$E[ST^2_{type1}] \triangleq E[ST^2_{p_{off}}]^{(p)} = \frac{{T_s}^2}{(1-\beta)^2}\left[\left(\frac{T_{tr}}{\mu}\right)^2 + 2\frac{T_{tr}}{\mu}\right] - \frac{{T_s}^2}{1-\beta}\left(\frac{T_{tr}}{\mu}\right) + \frac{T_s}{1-\beta}\frac{2{T_{tr}}^2}{\mu} + {T_{tr}}^2, \tag{3.33}$$

respectively, as shown in Appendix A.5.

Type 2 packets

Type 2 packets may find the PU on or off at the start of their service upon arrival. Therefore, the service time of type 2 packets is the weighted average of the EDTs of packets that find the PU on at the start of their transmission, and those that find PU off. Mathematically speaking, $E[ST_{Type2}]$ and $E[ST^2_{Type2}]$ can be calculated as

$$E[ST_{Type2}] = P_{on,2} \cdot E[ST_{p_{on}}] + (1 - P_{on,2}) \cdot E[ST_{p_{off}}], \tag{3.34}$$

and

$$E[ST^2_{Type2}] = P_{on,2} \cdot E[ST^2_{p_{on}}] + (1 - P_{on,2}) \cdot E[ST^2_{p_{off}}], \tag{3.35}$$

where $P_{on,2}$ denotes the probability that a type 2 packet finds PU on upon arrival, $E[ST_{p_{on}}]$ and $E[ST^2_{p_{on}}]$ are the first and second moments of the EDT of a packet that finds PU on at $t = 0$, respectively, and $E[ST_{p_{off}}]$ and $E[ST^2_{p_{off}}]$ are the moments for PU off case. In particular, $E[ST_{p_{on}}]$ and $E[ST^2_{p_{on}}]$ have been calculated for continuous sensing case in Appendix A.4, and for periodic sensing case in Appendix A.6.

The following argument will lead to the derivation of an expression for $P_{on,2}$. Whenever the transmission of the last packet in the queue is completed, due to the memoryless property of exponential distribution, the time it takes for the next packet to arrive will follow an exponential distribution with average ψ. At the start of that time interval, it is known that the PU is off. The probability that the PU is on, $P_{p_{on}}(t)$, conditioned on the time elapsed since the completion of last

packet transmission, t, is given by [50]

$$P_{p_{on}}(t) = \Pr[\text{PU on at } t_0 + t \mid \text{PU off at } t_0] = \frac{\lambda}{\lambda + \mu}\left[1 - e^{-(\frac{1}{\lambda}+\frac{1}{\mu})t}\right]. \quad (3.36)$$

Removing the conditioning on t, the probability for the PU being on when a type 2 packet arrives, $P_{on,2}$, is obtained as

$$P_{on,2} = E[P_{p_{on}}(t)] = \int_0^\infty P_{p_{on}}(t) \cdot \frac{1}{\psi} e^{-\frac{t}{\psi}} dt. \quad (3.37)$$

It can be shown that the above simplifies to

$$P_{on,2} = \frac{\lambda\psi}{\lambda\psi + \lambda\mu + \mu\psi}. \quad (3.38)$$

Substituting the moments $E[ST_{p_{on}}]$, $E[ST^2_{p_{on}}]$, $E[ST_{p_{off}}]$, and $E[ST^2_{p_{off}}]$ for continuous and periodic sensing cases, and $P_{on,2}$ into Eqs. (3.34) and (3.35), we can obtain the moments of type 2 packet service time. As an example, the first moment of the service time for type 2 packets with continuous sensing is given, after substituting Eqs. (3.30), (3.38), and (A.23) into Eq. (3.34), by

$$E[ST_{Type2}] = \frac{\lambda^2\psi}{\lambda\psi + \lambda\mu + \mu\psi} + \left(1 + \frac{\lambda}{\mu}\right) T_{tr}. \quad (3.39)$$

The other moments can be similarly obtained.

3.3.2 Queuing Analysis

In this subsection, we derive the expression for the expected delay for a packet in the queue. For clarity, we focus on continuous sensing in the following. The expression for periodic sensing can be similarly obtained. The average total delay is given by

$$E[D] = E[ST] + E[Q], \quad (3.40)$$

where $E[ST]$ is the average service time of an arbitrary packet, and $E[Q]$ is the average wait time in the queue. $E[ST]$ is a weighted average of $E[ST_{Type1}]$ and $E[ST_{Type2}]$, as defined in Eqs. (3.30) and (3.34), respectively, given by

$$E[ST] = (1 - p_0) \cdot E[ST_{type1}] + p_0 \cdot E[ST_{type2}], \quad (3.41)$$

where p_0 is the probability of the queue being empty at any given time instance and $1 - p_0$ is the utilization factor of the queue, which is, in turn, related to $E[ST]$

as

$$1 - p_0 = \frac{E[ST]}{\psi}. \tag{3.42}$$

Simultaneously solving Eqs. (3.41) and (3.42), we can obtain $E[ST]$ and p_0 as

$$E[ST] = \frac{\psi E[ST_{type2}]}{\psi + E[ST_{type2}] - E[ST_{type1}]}, \tag{3.43}$$

and

$$p_0 = \frac{\psi - E[ST_{type1}]}{\psi + E[ST_{type2}] - E[ST_{type1}]}, \tag{3.44}$$

respectively.

The average delay in the queue, $E[D]$, can be calculated using the mean value technique [51] as

$$E[Q] = E[N_Q] \cdot E[ST_{type1}] + (1 - p_0) \cdot E[R], \tag{3.45}$$

where $E[N_Q]$ is the average number of packets waiting in the queue, not including the current packet in service, $E[ST_{type1}]$ is the average service time of a packet in the queue (type 1 packet), and $E[R]$ is the mean residual time of the packet currently being served. Specifically, the first addition term in corresponds to the average total service time of the packets currently waiting in the queue, if any, and the second term to the waiting time for the currently served packet, if any. Given that a packet is being served at a given instance, the probabilities that the packet is a type 1 packet or type 2 packet, are equal to $\frac{(1-p_0)E[ST_{type1}]}{(1-p_0)E[ST_{type1}]+p_0E[ST_{type2}]}$ and $\frac{p_0E[ST_{type2}]}{(1-p_0)E[ST_{type1}]+p_0E[ST_{type2}]}$, respectively. Therefore, mean residual service time, $E[R]$ can be calculated as

$$\begin{aligned} E[R] = & \frac{(1 - p_0)E[ST_{type1}]}{(1 - p_0)E[ST_{type1}] + p_0E[ST_{type2}]} \cdot E[R_1] \\ & + \frac{p_0E[ST_{type2}]}{(1 - p_0)E[ST_{type1}] + p_0E[ST_{type2}]} \cdot E[R_2], \end{aligned} \tag{3.46}$$

where $E[R_1]$ and $E[R_2]$ are the mean residual times for type 1 and type 2 packets, respectively, defined by [52]

$$E[R_1] = \frac{E[ST_{type1}^2]}{2E[ST_{type1}]}, \tag{3.47}$$

and

$$E[R_2] = \frac{E[ST_{type2}^2]}{2E[ST_{type2}]}. \tag{3.48}$$

Recalling the Little's law stating that

$$E[N_Q] = \frac{E[Q]}{\psi}, \tag{3.49}$$

$E[Q]$ can be obtained after much simplification as

$$E[Q] = \frac{E[ST^2]}{2(\psi - E[ST_{type1}])}, \tag{3.50}$$

where $E[ST^2]$ is the second moment of the average service time of all packets, defined by

$$E[ST^2] = \frac{(\psi - E[ST_{type1}]) \cdot E[ST_{type2}^2] + E[ST_{type2}] \cdot E[ST_{type1}^2]}{\psi + E[ST_{type2}] - E[ST_{type1}]}. \tag{3.51}$$

The average number of packets waiting in the queue, not including the packet currently in transmission, is given by

$$E[N_Q] = \frac{E[ST^2]}{2\psi(\psi - E[ST_{type1}])}. \tag{3.52}$$

Finally, the average total delay for secondary packets can be simply expressed as

$$E[D] = \frac{\psi E[ST_{type2}]}{\psi + E[ST_{type2}] - E[ST_{type1}]} + \frac{E[ST^2]}{2(\psi - E[ST_{type1}])}. \tag{3.53}$$

Fig. 3.9 shows the variation of average total delay against the arrival rate of data packet with continuous sensing. The graph is based on the assumption that the average delay between packet arrival is greater than the average service time of the SU, as otherwise the queue will become unstable. For comparison purposes, we have included the average queuing delay obtained by modeling the secondary queue using the standard expression for average queuing delay given by $E[D] = E[ST] + \frac{E[ST^2]}{2(\psi - E[ST])}$, where the service time moments were simply given by Eqs. (3.41) and (3.51). The simulation results clearly show our analytical approach is more accurate.

Fig. 3.10 shows the variation of average delay including the queuing delay against the arrival rate of data packet. As the periodic sensing interval becomes small, the periodic sensing curves converge to the continuous sensing curve.

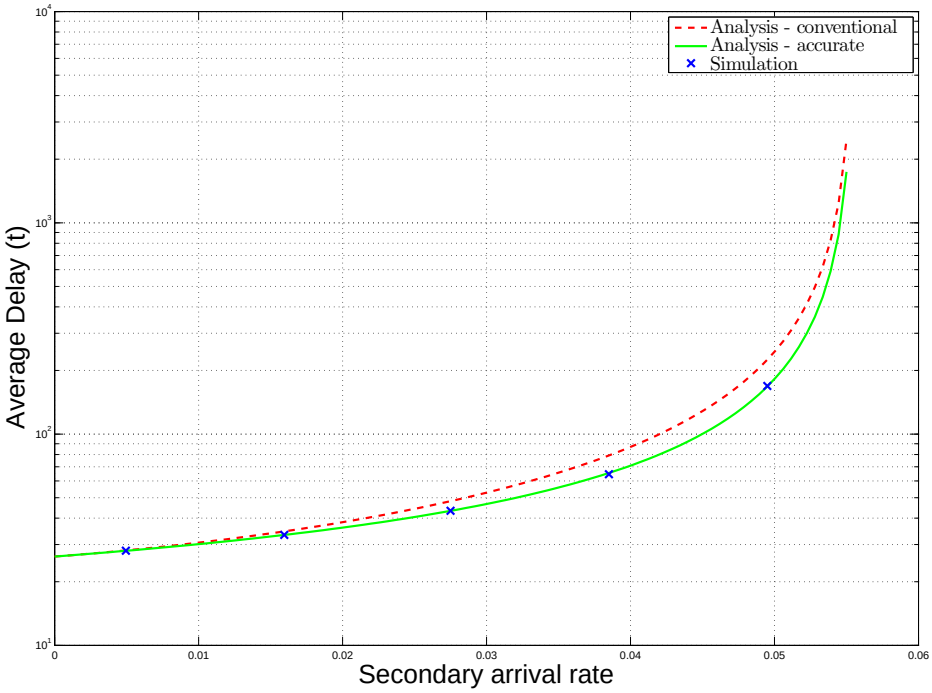

Figure 3.9: Simulation verification for the analytical average queuing delay with continuous sensing ($T_{tr} = 3$, $\lambda = 10$, and $\mu = 2$)

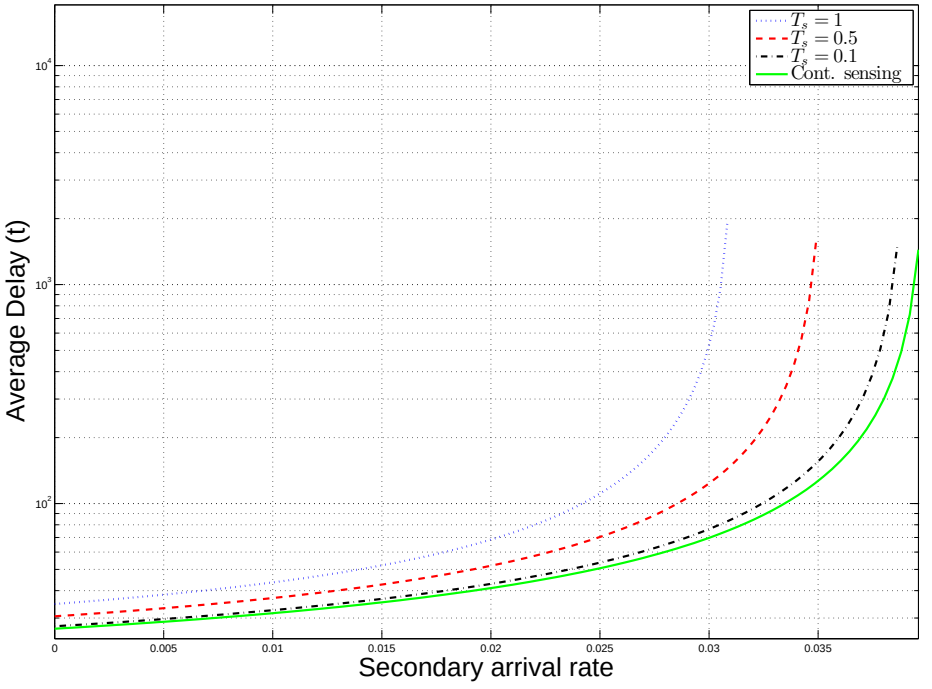

Figure 3.10: Average queuing delay ($T_{tr} = 10$, $\lambda = 3$, and $\mu = 2$).

Chapter 4

Extended Delivery Time Analysis for Cognitive Packet Transmission with Non-work-preserving Strategy

In the previous chapter, we discussed the scenario of cognitive radio system with work-preserving strategy, where the secondary transmission can continue from the point where it was interrupted, without wasting the previous transmission. Typically, work-preserving packet transmission requires packets to be coded with certain rateless codes such as fountain codes, which may not be available in the secondary system.

In this chapter, we analyze the EDT or secondary packet transmission with non-work-preserving strategy, where the secondary transmitter needs to transmit the whole packet if the packet transmission was interrupted by PU activities. In general, the transmission of a secondary packet involves an interweaved sequence of wasted transmission slots and waiting time slots, both of which can have random time duration, followed by the final successful transmission slot. In this chapter, we first derive the exact expressions for the distribution function of EDT assuming a fixed packet transmission time. The generalization to random packet transmission time can be addressed in a similar manner as for non-work-preserving strategy. We consider three spectrum sensing scenarios – i) ideal continuous sensing, in which the SU will continuously sense the channel for availability, ii) perfect periodic sensing, in which the SU will sense the channel periodically, and iii) imperfect periodic sensing, in which the SU will sense the channel periodically and there is a chance of sensing a free channel to be busy. For each scenario, we derive the

exact statistics of the EDT for secondary packet transmission in terms of moment generating function (MGF) and PDF, which can be directly used to predict the delay performance of some low-traffic intensity secondary applications. To the best of our knowledge, the complete statistics of the EDT for non-work-conserving strategy has not been investigated in literature. We further apply these results to the secondary queuing analysis. Specifically, we investigate the queuing delay performance for the secondary system with periodic sensing in an M/G/1 setup. The queuing analysis for the other two sensing scenarios can be similarly addressed. The performance tradeoff involved in different sensing scenarios are investigated through selected numerical examples.

4.1 System Model and Problem Formulation

We consider a cognitive transmission scenario very similar to that considered in Chapter 3, but with non-work-preserving strategy. In addition to continuous sensing and perfect periodic sensing scenarios, we also consider imperfect periodic sensing scenario, where there is a non-zero probability of missed detection, i.e. sensing a free channel to be busy in a certain sensing attempt. We assume that the chance of sensing a busy channel to be free is negligible, which can be achieved by adjusting the sensing thresholds properly. During transmission, the SU continuously monitors PU activity. As soon as the PU restarts, the SU discontinues its transmission. The continuous period of time during which the PU is off and the SU is transmitting is referred to as a transmission slot. Similarly, the continuous period of time during which the PU is transmitting is referred to as a waiting slot. In what follows, we first derive the distribution of the EDT T_{ED} for continuous sensing, perfect periodic sensing, and imperfect periodic sensing cases, which are then applied to the secondary queuing analysis in section 4.3.

4.2 Extended Delivery Time Analysis

In this section, we investigate the EDT of secondary system for a single packet arriving at a random point in time. These analyses also characterize the delay of some low-traffic-intensity secondary applications. For example, in wireless sensor networks for health care monitoring, forest fire detection, air pollution monitoring, disaster prevention, landslide detection etc., the transmitter needs to periodically transmit measurement data to the sink with a relatively long duty cycle. The EDT essentially characterizes the delay of measurement data collection.

4.2.1 Continuous Sensing

The EDT for packet transmission by the SU consists of interweaved waiting slots and wasted transmission slots, followed by the final successful transmission slot of duration T_{tr}. We assume, without loss of generality, that the packet arrives at $t = 0$. The distribution of T_w depends on whether the PU was on or off at that instance. We denote the PDF of the waiting time of the SU for the case when PU is on at $t = 0$, and for the case when PU is off at $t = 0$, by $f^{(c)}_{T_w,p_{on}}(t)$ and $f^{(c)}_{T_w,p_{off}}(t)$, respectively. The PDF of the EDT T_{ED} for the SU is then given by

$$f^{(c)}_{T_{ED}}(t) = \frac{\lambda}{\lambda+\mu} f^{(c)}_{T_w,p_{on}}(t - T_{tr}) + \frac{\mu}{\lambda+\mu} f^{(c)}_{T_w,p_{off}}(t - T_{tr}), \tag{4.1}$$

where $\frac{\lambda}{\lambda+\mu}$ and $\frac{\mu}{\lambda+\mu}$ are the stationery probabilities that the PU is on or off at $t = 0$, respectively. The two probability density functions $f_{T_w,p_{on}}(t)$ and $f_{T_w,p_{off}}(t)$ above are calculated independently as follows.

Let $\mathcal{P}_k$ be the probability that the SU was successful in sending the packet in the k^{th} transmission slot. This means that each of the first $(k-1)$ slots had a time duration of less than T_{tr}, while the k^{th} transmission slot had a duration more than T_{tr}. Thus, $\mathcal{P}_k$ can be calculated, while noting that the duration of secondary transmission slots is exponentially distributed with mean μ, as

$$\mathcal{P}_k = e^{-\frac{T_{tr}}{\mu}} \cdot \left(1 - e^{-\frac{T_{tr}}{\mu}}\right)^{k-1}. \tag{4.2}$$

For the case when PU is off at $t = 0$, if a certain packet is transmitted completely in the k^{th} transmission slot, then the total wait time for that packet includes $(k-1)$ secondary waiting slots and $(k-1)$ wasted transmission slots. Note that the duration of each of these $(k-1)$ waiting slots, denoted by the random variable T_{wait}, which is equal to PU on time in a single waiting slot, follows an exponential distribution for the continuous sensing case, with PDF given by

$$f^{(c)}_{T_{wait}}(t) = \frac{1}{\lambda} e^{\frac{-t}{\lambda}} u(t), \tag{4.3}$$

while the duration of each of the previous $(k-1)$ wasted secondary transmission slots, denoted by the random variable T_{waste}, follows a truncated exponential distribution, with PDF given by

$$f_{T_{waste}}(t) = \frac{1}{1 - e^{-\frac{T_{tr}}{\mu}}} \frac{1}{\mu} e^{\frac{-t}{\mu}} \cdot (u(t) - u(t - T_{tr})), \tag{4.4}$$

where $u(t)$ is the unit step function. The MGF of $T_{w,p_{off}}$ for the continuous sensing case, $\mathcal{M}^{(c)}_{T_w,p_{off}}(s)$ can be calculated as

$$\mathcal{M}^{(c)}_{T_w,p_{off}}(s) = \sum_{k=1}^{\infty} \mathcal{P}_k \times \left(\mathcal{M}^{(c)}_{T_{wait}}(s)\right)^{k-1} \times \left(\mathcal{M}_{T_{waste}}(s)\right)^{k-1}, \tag{4.5}$$

where $\mathcal{M}^{(c)}_{T_{wait}}(s)$ is the MGF of T_{wait} for the continuous sensing case, given by

$$\mathcal{M}^{(c)}_{T_{wait}}(s) = \frac{1}{1-\lambda s}, \tag{4.6}$$

and $\mathcal{M}_{T_{waste}}(s)$ is the MGF of T_{waste}, given by

$$\mathcal{M}_{T_{waste}}(s) = \frac{1-e^{T_{tr}(s-\frac{1}{\mu})}}{(1-\mu s)(1-e^{-\frac{T_{tr}}{\mu}})}. \tag{4.7}$$

After substituting Eqs. (4.2), (4.6), and (4.7) into Eq. (4.5), and applying the definition of binomial expansion on $(e^{T_{tr}(s-\frac{1}{\mu})}-1)^{k-1}$, Eq. (4.5) becomes

$$\mathcal{M}^{(c)}_{T_w,p_{off}}(s) = e^{-\frac{T_{tr}}{\mu}} \sum_{k=1}^{\infty} \frac{1}{(\lambda s-1)^{k-1}(\mu s-1)^{k-1}} \sum_{i=0}^{k-1} (-1)^i \binom{k-1}{i} \cdot e^{iT_{tr}(s-\frac{1}{\mu})}. \tag{4.8}$$

Changing the sequence of the two summations, and applying the definition of negative binomial distribution, we get

$$\mathcal{M}^{(c)}_{T_w,p_{off}}(s) = e^{-\frac{T_{tr}}{\mu}} + e^{-\frac{T_{tr}}{\mu}} \left[1-e^{T_{tr}(s-\frac{1}{\mu})}\right] \sum_{i=0}^{\infty} (-1)^i e^{iT_{tr}(s-\frac{1}{\mu})} \frac{1}{[s(\lambda\mu s-\lambda-\mu)]^{i+1}}. \tag{4.9}$$

Using the following general formula for partial fractions

$$\frac{1}{[x(x-a)]^n} = \sum_{j=0}^{n-1} (-1)^n \binom{2n-j-2}{n-1} \frac{1}{a^{2n-j-1}} \left[\frac{1}{x^{j+1}} + \frac{(-1)^{j+1}}{(x-a)^{j+1}}\right], \tag{4.10}$$

the proof of which is given in appendix A.7, we get

$$\begin{aligned}\mathcal{M}^{(c)}_{T_w,p_{off}}(s) = {} & e^{-\frac{T_{tr}}{\mu}} - e^{-\frac{T_{tr}}{\mu}} \left[1-e^{T_{tr}(s-\frac{1}{\mu})}\right] \\ & \times \sum_{i=0}^{\infty} \frac{e^{iT_{tr}(s-\frac{1}{\mu})}}{(\lambda\mu)^{i+1}} \sum_{j=0}^{i} \binom{2i-j}{i} \frac{1}{\alpha^{2i-j+1}} \left[\frac{1}{s^{j+1}} + \frac{(-1)^{j+1}}{(s-\alpha)^{j+1}}\right],\end{aligned} \tag{4.11}$$

where $\alpha = \frac{1}{\lambda} + \frac{1}{\mu}$. Taking the inverse MGF, and applying the definition of generalized hypergeometric function, we obtain the PDF of $T_{w,p_{off}}$ for continuous sensing

case, as

$$f^{(c)}_{T_w,p_{off}}(t) = e^{-\frac{T_{tr}}{\mu}}\delta(t) + \frac{e^{-\frac{T_{tr}}{\mu}}}{\lambda+\mu}(1-e^{-\alpha t})u(t) - \frac{e^{-\frac{2T_{tr}}{\mu}}}{\lambda+\mu}(1-e^{-\alpha(t-T_{tr})})u(t-T_{tr}) + \sum_{i=1}^{\infty}\frac{(\lambda\mu)^i}{(\lambda+\mu)^{2i+1}}\binom{2i}{i}\Big[{}_1F_1\left(-i;-2i;-\alpha(t-iT_{tr})\right)e^{-(i+1)\frac{T_{tr}}{\mu}}u(t-iT_{tr}) - {}_1F_1\left(-i;-2i;-\alpha(t-(i+1)T_{tr})\right)e^{-(i+2)\frac{T_{tr}}{\mu}}u(t-(i+1)T_{tr}) - {}_1F_1\left(-i;-2i;\alpha(t-iT_{tr})\right)e^{-\alpha t}e^{-(i+1)\frac{T_{tr}}{\mu}}u(t-iT_{tr}) + {}_1F_1\left(-i;-2i;\alpha(t-(i+1)T_{tr})\right)e^{-\alpha t}e^{-(i+2)\frac{T_{tr}}{\mu}}u(t-(i+1)T_{tr})\Big], \tag{4.12}$$

where ${}_1F_1(.,.,.)$ is the generalized Hyper-geometric function. Note that the impulse corresponds to the case that the packet is transmitted without waiting.

For the case when PU is on at $t = 0$, the MGF of $T_{w,p_{on}}$ for the continuous sensing case $\mathcal{M}^{(c)}_{T_w,p_{on}}(s)$ can be similarly calculated as

$$\mathcal{M}^{(c)}_{T_w,p_{on}}(s) = \sum_{k=1}^{\infty}\mathcal{P}_k \times \left(\mathcal{M}^{(c)}_{T_{wait}}(s)\right)^k \times \left(\mathcal{M}_{T_{waste}}(s)\right)^{k-1}. \tag{4.13}$$

Using similar manipulations used for $T_{w,p_{off}}$, it is easy to arrive at

$$\mathcal{M}^{(c)}_{T_w,p_{on}}(s) = -e^{-\frac{T_{tr}}{\mu}}\sum_{i=0}^{\infty}(-1)^i e^{iT_{tr}(s-\frac{1}{\mu})}\left[\frac{\mu s-1}{[s(\lambda\mu s-\lambda-\mu)]^{i+1}}\right]. \tag{4.14}$$

Substituting Eq. (4.10) into Eq. (4.14), and carrying out some manipulation, we get

$$\mathcal{M}^{(c)}_{T_w,p_{on}}(s) = e^{-\frac{T_{tr}}{\mu}}\sum_{i=0}^{\infty}\frac{e^{iT_{tr}(s-\frac{1}{\mu})}}{(\lambda\mu)^{i+1}}\sum_{j=0}^{i}\binom{2i-j}{i}\frac{\mu s-1}{\alpha^{2i-j+1}}\left[\frac{1}{s^{j+1}}+\frac{(-1)^{j+1}}{(s-\alpha)^{j+1}}\right]. \tag{4.15}$$

Performing some further manipulations, taking inverse MGF, and applying the

definition of generalized hypergeometric function, we obtain the PDF of $T_{w,p_{on}}$ as

$$
\begin{aligned}
f^{(c)}_{T_w,p_{on}}(t) &= \frac{e^{-\frac{T_{tr}}{\mu}}}{\lambda+\mu}(1+\frac{\mu}{\lambda}e^{-\alpha t})u(t) \\
&+\sum_{i=1}^{\infty}\frac{(\lambda\mu)^i}{(\lambda+\mu)^{2i+1}}\left[\binom{2i}{i}{}_1F_1\left(-i;-2i;-\alpha(t-iT_{tr})\right)\cdot e^{-(i+1)\frac{T_{tr}}{\mu}}\cdot u(t-iT_{tr})\right. \\
&-\binom{2i}{i}\frac{\mu}{\lambda}e^{-\alpha(t-iT_{tr})}{}_1F_1\left(-i;-2i;\alpha(t-iT_{tr})\right)\cdot e^{-(i+1)\frac{T_{tr}}{\mu}}\cdot u(t-iT_{tr}) \\
&-\binom{2i-1}{i}\left(1+\frac{\mu}{\lambda}\right){}_1F_1\left(1-i;1-2i;-\alpha(t-iT_{tr})\right)\cdot e^{-(i+1)\frac{T_{tr}}{\mu}}\cdot u(t-iT_{tr}) \\
&\left.+\binom{2i-1}{i}\left(1+\frac{\mu}{\lambda}\right)e^{-\alpha(t-iT_{tr})}{}_1F_1\left(1-i;1-2i;\alpha(t-iT_{tr})\right)\cdot e^{-(i+1)\frac{T_{tr}}{\mu}}\cdot u(t-iT_{tr})\right].
\end{aligned}
\tag{4.16}
$$

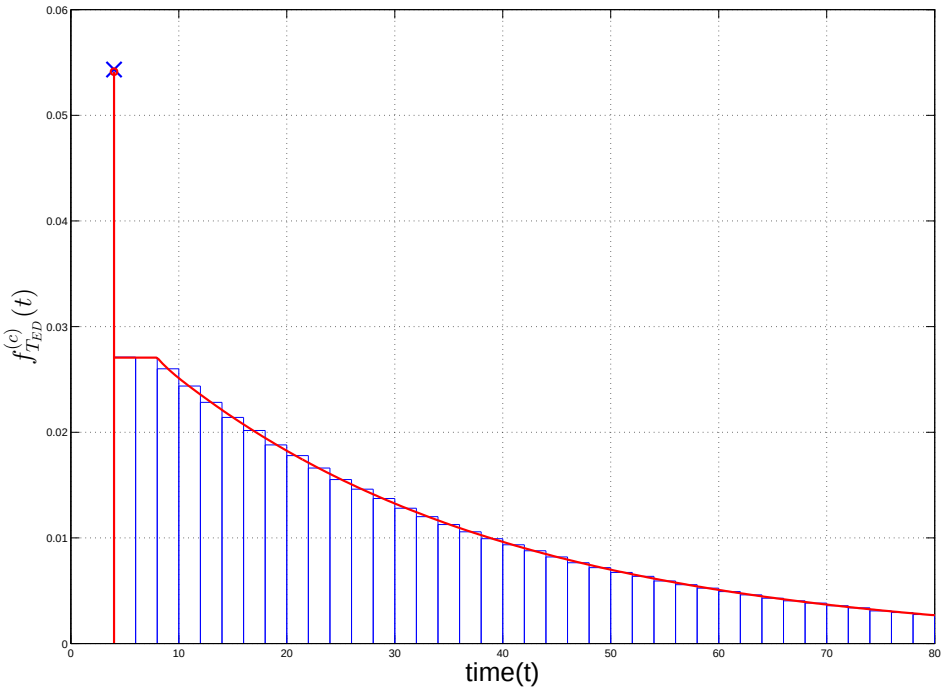

Figure 4.1: Simulation verification for the analytical PDF of T_{ED} with continuous sensing ($T_{tr}=4$, $\lambda=3$, and $\mu=2$).

Fig. 4.1 plots the analytical expression for the PDF of the EDT with continuous sensing as given in Eq. (4.1). The corresponding plot for the simulation results is also shown. The perfect match between analytical and simulation results verify our analytical approach.

4.2.2 Perfect Periodic Sensing

For the perfect periodic sensing case, the PDF of the EDT T_{ED} for the SU packet transmission is given by

$$f_{T_{ED}}^{(p)}(t) = \frac{\lambda}{\lambda+\mu} f_{T_w,p_{on}}^{(p)}(t-T_{tr}) + \frac{\mu}{\lambda+\mu} f_{T_w,p_{off}}^{(p)}(t-T_{tr}), \tag{4.17}$$

where $f_{T_w,p_{on}}^{(p)}(t)$ and $f_{T_w,p_{off}}^{(p)}(t)$ denote the PDFs of the waiting time of the SU with perfect periodic sensing, for the case when PU is on at $t=0$, and for the case when PU is off at $t=0$, respectively. We again derive the PDF of waiting time through MGF approach. The MGF of $T_{w,p_{off}}$ for the perfect periodic sensing case, $\mathcal{M}_{T_w,p_{off}}^{(p)}(s)$, can be calculated as

$$\mathcal{M}_{T_w,p_{off}}^{(p)}(s) = \sum_{k=1}^{\infty} \mathcal{P}_k \times \left(\mathcal{M}_{T_{wait}}^{(p)}(s)\right)^{k-1} \times \left(\mathcal{M}_{T_{waste}}(s)\right)^{k-1}, \tag{4.18}$$

where $\mathcal{P}_k$ is the probability that the SU was successful in sending the packet in the k^{th} transmission slot, given in Eq. (4.2), $\mathcal{M}_{T_{waste}}(s)$ is the MGF of the time duration of a wasted transmission slot T_{waste}, which is, noting that the PDF of T_{waste} remains the same as given in Eq. (4.4) due to the memoryless property of exponential distribution, given in Eq. (4.7), and $\mathcal{M}_{T_{wait}}^{(p)}(s)$ denotes the MGF of the wait time in a single waiting slot. With periodic sensing, T_{wait} consists of multiple T_s, and follows a geometric distribution. The MGF can be obtained as

$$\mathcal{M}_{T_{wait}}^{(p)}(s) = \sum_{n=1}^{\infty} (1-\beta)\beta^{n-1} e^{nsT_s}, \tag{4.19}$$

where β denotes the probability that the primary user is on at a given sensing instant provided that it was on at the previous sensing instant T_s time units earlier, given by Eq. (3.16). Note that β is a constant again due to the memoryless property of exponential distribution. Substituting Eqs. (4.2), (4.7), and (4.19) into Eq. (4.18), while noting $(\mathcal{M}_{T_{wait}}^{(p)}(s))^k = \sum_{n=k}^{\infty}(1-\beta)^k\beta^{n-k}\binom{n-1}{k-1}e^{nsT_s}$, we get

$$\mathcal{M}_{T_w,p_{off}}^{(p)}(s) = e^{-\frac{T_{tr}}{\mu}} + e^{-\frac{T_{tr}}{\mu}} \sum_{k=2}^{\infty}\sum_{n=k-1}^{\infty} (1-\beta)^{k-1}\beta^{n-k+1}\binom{n-1}{k-2} e^{nsT_s} \frac{[e^{T_{tr}(s-\frac{1}{\mu})}-1]^{k-1}}{(\mu s-1)^{k-1}}. \tag{4.20}$$

After performing some manipulation, using the definition of generalized hypergeometric function, and taking the inverse MGF, we obtain

$$f^{(p)}_{T_w,p_{off}}(t) = e^{-\frac{T_{tr}}{\mu}}\delta(t) + \sum_{n=1}^{\infty}\left[\frac{(1-\beta)\beta^{n-1}}{\mu}e^{-\frac{(t-nT_s)}{\mu}}e^{-\frac{T_{tr}}{\mu}}{}_1F_1\left(1-n;1;-\frac{1-\beta}{\beta}\frac{t-nT_s}{\mu}\right)\right.$$
$$+\sum_{i=1}^{n}\left[(-1)^i e^{-(i+1)\frac{T_{tr}}{\mu}}\binom{n-1}{i-1}\frac{1}{(i-1)!}\frac{(t-iT_{tr}-nT_s)^{i-1}}{\mu^i}(1-\beta)^i\beta^{n-i}e^{\frac{-(t-nT_s-iT_{tr})}{\mu}}\right.$$
$$\left.\left.\times{}_2F_2\left(i+1,i-n;i,i;-\frac{1-\beta}{\beta}\frac{(t-nT_s-iT_{tr})}{\mu}\right)\right]\right]. \tag{4.21}$$

Note that the impulse corresponds to the case that the packet is transmitted without waiting.

For the case when PU is on at $t=0$, the MGF of $T_{w,p_{on}}$ for the perfect periodic sensing case, $\mathcal{M}^{(p)}_{T_w,p_{on}}(s)$ can be calculated as

$$\mathcal{M}^{(p)}_{T_w,p_{on}}(s) = \sum_{k=1}^{\infty}\mathcal{P}_k \times \left(\mathcal{M}^{(p)}_{T_{wait}}(s)\right)^k \times \left(\mathcal{M}_{T_{waste}}(s)\right)^{k-1}. \tag{4.22}$$

Substituting Eqs. (4.2), (4.7), and (4.19) into Eq. (4.22), and performing similar manipulation as for PU off case, we can arrive at

$$\mathcal{M}^{(p)}_{T_w,p_{on}}(s) = e^{-\frac{T_{tr}}{\mu}}\sum_{n=1}^{\infty}e^{nsT_s}\beta^n\sum_{i=0}^{n-1}(-1)^i e^{iT_{tr}(s-\frac{1}{\mu})}$$
$$\times\sum_{k=i+1}^{n}\binom{k-1}{i}\left(\frac{1-\beta}{\beta}\right)^k\binom{n-1}{k-1}\frac{(-1)^{k-1}}{(\mu s-1)^{k-1}}, \tag{4.23}$$

which, after performing some manipulation, using the definition of hypergeometric function, and taking the inverse MGF, becomes

$$f^{(p)}_{T_w,p_{on}}(t) = e^{-\frac{T_{tr}}{\mu}}\sum_{n=1}^{\infty}(1-\beta)\beta^{n-1}\delta(t-nT_s)$$
$$+e^{-\frac{T_{tr}}{\mu}}\sum_{n=2}^{\infty}(n-1)\frac{(1-\beta)^2\beta^{n-2}}{\mu}e^{-\frac{t-nT_s}{\mu}}{}_1F_1\left(2-n;2;-\frac{1-\beta}{\beta}\cdot\frac{t-nT_s}{\mu}\right)$$
$$+\sum_{n=1}^{\infty}\sum_{i=1}^{n-1}(-1)^i e^{-(i+1)\frac{T_{tr}}{\mu}}\binom{n-1}{i}(1-\beta)^{i+1}\beta^{n-i-1}\frac{t^{i-1}e^{-\frac{t-nT_s-iT_{tr}}{\mu}}}{(i-1)!\mu^i}$$
$$\times{}_1F_1\left(i+1-n;i;-\frac{1-\beta}{\beta}\cdot\frac{t-nT_s-iT_{tr}}{\mu}\right). \tag{4.24}$$

Note that the sequence of impulses corresponds to the case that the packet is transmitted in the first transmission attempt on acquiring the channel after a

random number of sensing intervals/attempts.

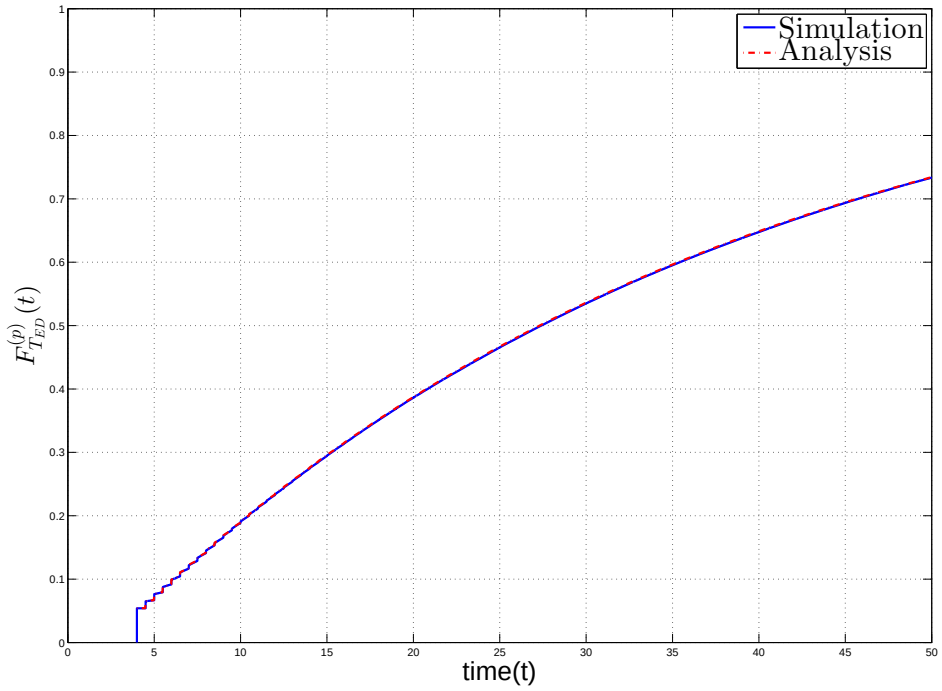

Figure 4.2: Simulation verification for the analytical CDF of T_{ED} with periodic sensing ($T_{tr} = 4$, $\lambda = 3$, $\mu = 2$, and $T_s = 0.5$).

Fig. 4.2 plots the CDF of the EDT with periodic sensing, $F_{T_{ED}}^{(p)}(t)$, obtained by numerical integration of the analytical PDF expression given by Eq. (4.17). The corresponding plot for the simulation results is also shown. The perfect match between analytical and simulation results verify our analytical approach.

4.2.3 Imperfect Periodic Sensing

In the previous section, we assumed that the periodic sensing is perfect, i.e. the SU can always correctly sense whether the channel is free or not. A more practical scenario is with imperfect sensing i.e. the secondary user may not always be able to correctly sense whether the channel is free or not. Specifically, we assume that a busy channel is never sensed as free to protect the PU, while a free channel may be erroneously sensed as busy with a probability p_e. We further assume for mathematical tractability that the probability of the primary user turning back on before a successful sensing of idle channel by the secondary user is negligible. Thus, each waiting period of the secondary user can be considered as a sum of two geometric random variables, one catering for the delay until the primary user turns

off, and the other accounting for the delay due to missed detection. Denoting the PDFs of the waiting time of the SU with imperfect periodic sensing, for the case when PU is on at $t = 0$, and for the case when PU is off at $t = 0$, by $f^{(im)}_{T_w,p_{on}}(t)$ and $f^{(im)}_{T_w,p_{off}}(t)$, respectively, the PDF of the EDT T_{ED} for the SU is given by

$$f^{(im)}_{T_{ED}}(t) = \frac{\lambda}{\lambda+\mu} f^{(im)}_{T_w,p_{on}}(t - T_{tr}) + \frac{\mu}{\lambda+\mu} f^{(im)}_{T_w,p_{off}}(t - T_{tr}). \tag{4.25}$$

For the case when PU is off at $t = 0$, the MGF of $T_{w,p_{off}}$ for the imperfect periodic sensing case, $\mathcal{M}^{(im)}_{T_w,p_{off}}(s)$ can be defined as

$$\mathcal{M}^{(im)}_{T_w,p_{off}}(s) = \sum_{k=1}^{\infty} \mathcal{P}_k \times \left(\mathcal{M}^{(p)}_{T_{wait}}(s)\right)^{k-1} \times \left(\mathcal{M}_{T_{mis}}(s)\right)^k \times \left(\mathcal{M}_{T_{waste}}(s)\right)^{k-1}, \tag{4.26}$$

where $\left(\mathcal{M}_{T_{mis}}(s)\right)^k$ is the MGF of the extra waiting time due to sensing errors in k slots, defined by

$$\left(\mathcal{M}_{T_{mis}}(s)\right)^k = \sum_{m=0}^{\infty} (1-p_e)^k p_e^m \binom{m+k-1}{k-1} e^{msT_s}. \tag{4.27}$$

After substituting Eqs. (4.2), (4.7), (4.19), and (4.27) into Eq. (4.26), we arrive at

$$\begin{aligned}\mathcal{M}^{(im)}_{T_w,p_{off}}(s) &= e^{-\frac{T_{tr}}{\mu}} \sum_{k=1}^{\infty} \sum_{n=k-1}^{\infty} (1-\beta)^{k-1} \beta^{n-k+1} \binom{n-1}{k-2} e^{nsT_s} \\ &\times \sum_{m=0}^{\infty} (1-p_e)^k p_e^m \binom{m+k-1}{k-1} e^{msT_s} \frac{1}{(\mu s - 1)^{k-1}} \sum_{i=0}^{k-1} (-1)^{k-i-1} \binom{k-1}{i} \cdot e^{iT_{tr}(s-\frac{1}{\mu})},\end{aligned} \tag{4.28}$$

which, on taking the inverse MGF, becomes

$$\begin{aligned}f^{(im)}_{T_w,p_{off}}(t) = &\sum_{n=1}^{\infty} \sum_{k=2}^{n+1} \sum_{m=0}^{\infty} \sum_{i=0}^{k-1} (1-\beta)^{k-1} \beta^{n-k+1} (1-p_e)^k p_e^m \binom{n-1}{k-2} \binom{m+k-1}{k-1} \\ &\times \binom{k-1}{i} (-1)^i e^{-(i+1)\frac{T_{tr}}{\mu}} \frac{(t - nT_s - mT_s - iT_{tr})^{k-2}}{\Gamma[k-1]\mu^{k-1}} e^{-\frac{(t-nT_s-mT_s-iT_{tr})}{\mu}} \\ &+ \sum_{m=0}^{\infty} (1-p_e) p_e^m e^{-\frac{T_{tr}}{\mu}} \delta[t - mT_s].\end{aligned} \tag{4.29}$$

Similarly, for the case when PU is on at $t = 0$, the MGF of $T_{w,p_{on}}$ for the

imperfect periodic sensing case, $\mathcal{M}^{(im)}_{T_w,p_{on}}(s)$ can be defined as

$$\mathcal{M}^{(im)}_{T_w,p_{on}}(s) = \sum_{k=1}^{\infty} \mathcal{P}_k \times \left(\mathcal{M}^{(p)}_{T_{wait}}(s)\right)^k \times \left(\mathcal{M}_{T_{mis}}(s)\right)^k \times \left(\mathcal{M}_{T_{waste}}(s)\right)^{k-1}, \quad (4.30)$$

which, after substituting Eqs. (4.2), (4.7), (4.19), and (4.27), becomes

$$\begin{aligned}\mathcal{M}^{(im)}_{T_w,p_{on}}(s) = {} & e^{-\frac{T_{tr}}{\mu}} \sum_{k=1}^{\infty}\sum_{n=k}^{\infty}(1-\beta)^k\beta^{n-k}\binom{n-1}{k-1}e^{nsT_s} \\ & \sum_{m=0}^{\infty}(1-p_e)^k p_e^m \binom{m+k-1}{k-1} e^{msT_s} \frac{1}{(\mu s-1)^{k-1}} \sum_{i=0}^{k-1}(-1)^{k-i-1}\binom{k-1}{i} \cdot e^{iT_{tr}(s-\frac{1}{\mu})}.\end{aligned} \quad (4.31)$$

Finally, taking the inverse MGF, we get

$$\begin{aligned}f^{(im)}_{T_w,p_{on}}(t) = {} & \sum_{n=1}^{\infty}\sum_{k=2}^{n}\sum_{m=0}^{\infty}\sum_{i=0}^{k-1}(1-\beta)^k\beta^{n-k}(1-p_e)^k p_e^m \binom{n-1}{k-1}\binom{m+k-1}{k-1}\binom{k-1}{i} \\ & \times (-1)^i \cdot e^{-(i+1)\frac{T_{tr}}{\mu}} \frac{(t-nT_s-mT_s-iT_{tr})^{k-2}}{\Gamma[k-1]\mu^{k-1}} e^{-\frac{(t-nT_s-mT_s-iT_{tr})}{\mu}} \\ & + \sum_{n=1}^{\infty}\sum_{m=0}^{\infty}(1-\beta)\beta^{n-1}(1-p_e)p_e^m e^{-\frac{T_{tr}}{\mu}}\delta[t-nT_s-mT_s].\end{aligned} \quad (4.32)$$

Fig. 4.3 plots the CDF of the EDT with imperfect periodic sensing, $F^{(im)}_{T_{ED}}(t)$, obtained by numerical integration of the analytical PDF expression given in Eq. (4.25). The corresponding plot for the simulation results is also shown. As can be seen, the analytical results are fairly accurate for small values of p_e. The analytical results are slightly different from the simulation results as we ignored the probability that the PU returns before a successful sensing of the idle channel. The plots of the analytical and simulation results for $p_e = 0$ match perfectly, which corresponds to the perfect periodic sensing case.

4.3 Application to Secondary Queuing Analysis

In this section, we consider the average transmission delay for the secondary system in a queuing set-up as an application of the analytical results in previous section. In particular, the secondary traffic intensity is high and, as such, a first-in-first-out queue is introduced to hold packets until transmission. We assume that equal-sized packet arrival follows a Poisson process with intensity $\frac{1}{\psi}$, i.e. the average time duration between packet arrivals is ψ. For the sake of simplicity, the packets are

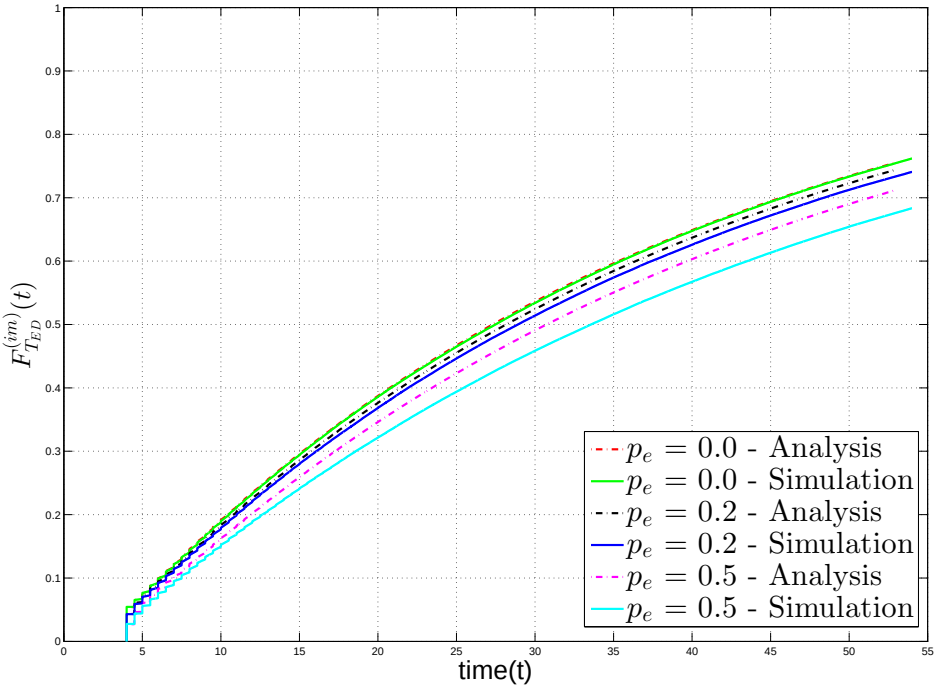

Figure 4.3: Simulation verification for the analytical CDF of T_{ED} with imperfect periodic sensing ($T_{tr} = 4$, $\lambda = 3$, $\mu = 2$, and $T_s = 0.5$).

assumed to be of the same length, such that their transmission time T_{tr} be a fixed constant in the following analysis. As such, the secondary packet transmission can be modelled as a general M/G/1 queue, where the service time is closely related to the EDT studied in the previous section. [1]

Note also from the EDT analysis, the waiting time of a packet depends on whether the PU is on or off when the packet is available for transmission. As such, different secondary packets will experience two types of service time characteristics. Specifically, some packets might see upon arrival that there are one or more packets waiting in the queue or being transmitted. Such packets will have to wait in the queue until transmission completion of previous packets. Once all the previous packets are transmitted, the new arriving packet will find the PU to be off. We term such packets as type 1 packets. On the other hand, some packets will arrive when the queue is empty, and will immediately become available for transmission. Such packets might find the PU to be on or off. We will call this type of packets, type 2 packets. To facilitate subsequent queuing analysis, we now calculate the first and second moments of the service time for these two types

[1] The analytical results can also be applied to more complicated queuing models and traffic models, with some further manipulation. They are out of scope of this work.

of packets. We focus on the perfect periodic sensing case in the following while noting the analysis for the remaining two sensing scenarios can be similarly solved.

4.3.1 Service Time Moments

First moments

We first consider the first moment of the service time for packets seeing PU off, denoted by $ST_{p_{off}}$. Noting that $ST_{p_{off}} = T_{w,p_{off}} + T_{tr}$, due to the memoryless property of our scenario with non-work-preserving strategy, we can calculate its mean $E[ST_{p_{off}}]$ by following the conditional expectations approach as

$$E[ST_{p_{off}}] = e^{-\frac{T_{tr}}{\mu}} \cdot T_{tr} + (1 - e^{-\frac{T_{tr}}{\mu}}) \cdot E[(T_{waste} + T_{wait} + ST_{p_{off}})]. \tag{4.33}$$

Here the first addition term corresponds to the case that the complete packet is successfully transmitted in the first transmission slot, and the second addition term refers to the case when the complete packet is not successfully transmitted. For periodic sensing, it can be shown, from Eqs. (4.7) and (4.19), that $E[T_{wait}] = \frac{T_s}{1-\beta}$ and $E[T_{waste}] = \mu - T_{tr}\frac{e^{-\frac{T_{tr}}{\mu}}}{1-e^{-\frac{T_{tr}}{\mu}}}$. The first moment can be calculated from Eq. (4.33) as

$$E[ST_{p_{off}}] = \frac{1 - e^{-\frac{T_{tr}}{\mu}}}{e^{-\frac{T_{tr}}{\mu}}} \left(\mu + \frac{T_s}{1-\beta}\right). \tag{4.34}$$

Since the case with PU on at $t = 0$ is precisely the same as the case of PU off at $t = 0$ preceded by a waiting slot, we can define $E[ST_{p_{on}}]$, the first moment of the service time for packets seeing PU on as

$$E[ST_{p_{on}}] = E[ST_{p_{off}}] + \frac{T_s}{1-\beta} = \frac{1 - e^{-\frac{T_{tr}}{\mu}}}{e^{-\frac{T_{tr}}{\mu}}} \cdot \mu + \frac{1}{e^{-\frac{T_{tr}}{\mu}}} \cdot \frac{T_s}{1-\beta}. \tag{4.35}$$

Second moments

Using a similar technique for calculating the first moment, we can write

$$E[ST_{p_{off}}^2] = e^{-\frac{T_{tr}}{\mu}} \cdot T_{tr}^2 + (1 - e^{-\frac{T_{tr}}{\mu}}) \cdot E[(T_{waste} + T_{wait} + ST_{p_{off}})^2]. \tag{4.36}$$

It can be shown from Eqs. (4.7) and (4.19) that $E[T_{wait}^2] = T_s^2\frac{1+\beta}{(1-\beta)^2}$ and $E[T_{waste}^2] = 2\mu^2 + \frac{e^{-\frac{T_{tr}}{\mu}}}{1-e^{-\frac{T_{tr}}{\mu}}}(-T_{tr}^2 - 2\mu T_{tr})$. Expanding the terms inside $E[.]$, the above equation

can be written as

$$E[ST^2_{p_{off}}] = e^{-\frac{T_{tr}}{\mu}} \cdot T^2_{tr} + (1 - e^{-\frac{T_{tr}}{\mu}}) \cdot \left[T^2_s \frac{1+\beta}{(1-\beta)^2} + 2\mu^2 + \frac{e^{-\frac{T_{tr}}{\mu}}}{1 - e^{-\frac{T_{tr}}{\mu}}}(-T^2_{tr} - 2\mu T_{tr}) \right.$$
$$+E[ST^2_{p_{off}}] + 2\frac{T_s}{1-\beta}\left(\mu - T_{tr}\frac{e^{-\frac{T_{tr}}{\mu}}}{1 - e^{-\frac{T_{tr}}{\mu}}}\right) + 2\frac{T_s}{1-\beta} \cdot \frac{1 - e^{-\frac{T_{tr}}{\mu}}}{e^{-\frac{T_{tr}}{\mu}}}\left(\mu + \frac{T_s}{1-\beta}\right)$$
$$\left. +2\left(\mu - T_{tr}\frac{e^{-\frac{T_{tr}}{\mu}}}{1 - e^{-\frac{T_{tr}}{\mu}}}\right) \cdot \frac{1 - e^{-\frac{T_{tr}}{\mu}}}{e^{-\frac{T_{tr}}{\mu}}}\left(\mu + \frac{T_s}{1-\beta}\right)\right]. \tag{4.37}$$

Simplifying the above, we obtain

$$E[ST^2_{p_{off}}] = \frac{1}{e^{-\frac{T_{tr}}{\mu}}}\left[-2T_{tr}\frac{T_s}{1-\beta} - 2\mu T_{tr}\right] + \left(\frac{1 - e^{-\frac{T_{tr}}{\mu}}}{e^{-\frac{T_{tr}}{\mu}}}\right)\frac{1}{e^{-\frac{T_{tr}}{\mu}}}\left[2\mu\frac{T_s}{1-\beta} + 2\mu^2\right]$$
$$+ \left(\frac{1 - e^{-\frac{T_{tr}}{\mu}}}{e^{-\frac{T_{tr}}{\mu}}}\right) T^2_s \frac{1+\beta}{(1-\beta)^2} + \left(\frac{1 - e^{-\frac{T_{tr}}{\mu}}}{e^{-\frac{T_{tr}}{\mu}}}\right)^2 \left[2\frac{T^2_s}{(1-\beta)^2} + 2\mu\frac{T_s}{1-\beta}\right]. \tag{4.38}$$

Similarly, the second moment of the service time for packets seeing PU on, $E[ST^2_{p_{on}}]$ can be defined as

$$E[ST^2_{p_{on}}] = E[(T_{wait} + ST_{p_{off}})^2], \tag{4.39}$$

which, after substitution of the relevant terms and simplification, becomes

$$E[ST^2_{p_{on}}] = \frac{1}{e^{-\frac{T_{tr}}{\mu}}}\left[-2T_{tr}\frac{T_s}{1-\beta} - 2\mu T_{tr} + T^2_s\frac{1+\beta}{(1-\beta)^2}\right]$$
$$+ \left(\frac{1 - e^{-\frac{T_{tr}}{\mu}}}{e^{-\frac{T_{tr}}{\mu}}}\right)\frac{1}{e^{-\frac{T_{tr}}{\mu}}}\left[2\mu\frac{T_s}{1-\beta} + 2\mu^2 + 2\frac{T^2_s}{(1-\beta)^2} + 2\mu\frac{T_s}{1-\beta}\right]. \tag{4.40}$$

4.3.2 Queuing Analysis

The moments of the service time for type 1 packets are same as the moments of those packets which find PU off, i.e.

$$E[ST_{type1}] = E[ST_{p_{off}}], \tag{4.41}$$

and

$$E[ST^2_{type1}] = E[ST^2_{p_{off}}], \tag{4.42}$$

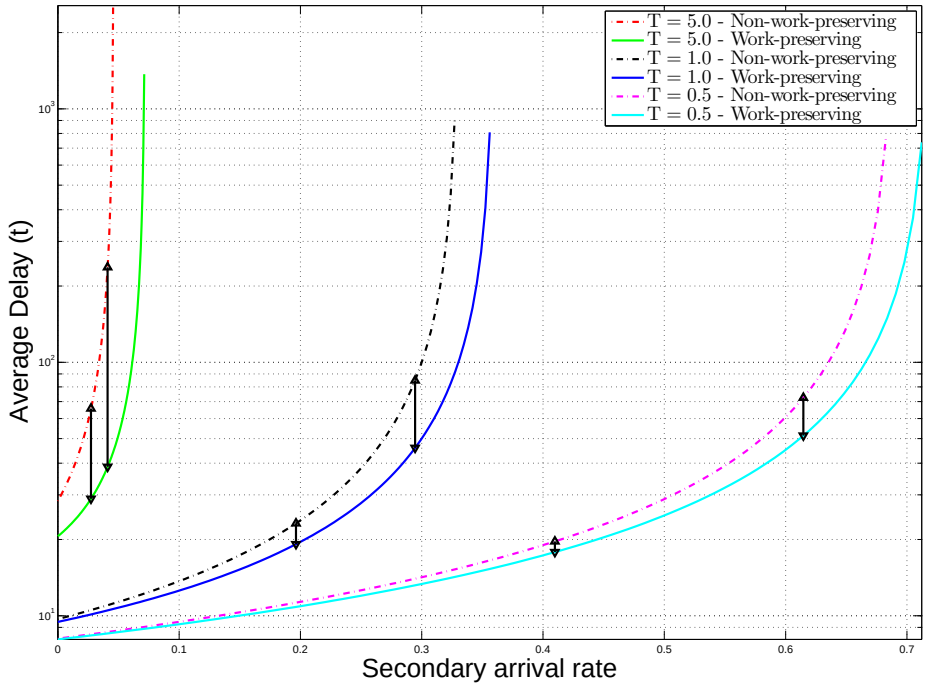

Figure 4.4: Average queuing delay with perfect periodic sensing ($T_s = 0.5$, $\lambda = 10$ and $\mu = 6$)

where $E[ST_{p_{off}}]$ and $E[ST^2_{p_{off}}]$ are defined in Eqs. (4.34) and (4.38), respectively. As per the analysis given in the previous chapter, the moments of the service time for type 2 packets are given by

$$E[ST_{type2}] = P_{on,2} \cdot E[ST_{p_{on}}] + (1 - P_{on,2}) \cdot E[ST_{p_{off}}], \tag{4.43}$$

and

$$E[ST^2_{type2}] = P_{on,2} \cdot E[ST^2_{p_{on}}] + (1 - P_{on,2}) \cdot E[ST^2_{p_{off}}], \tag{4.44}$$

where $P_{on,2}$ denotes the probability that a type 2 packet finds PU on upon arrival, given in Eq. (3.38), and $E[ST_{p_{on}}]$ and $E[ST^2_{p_{on}}]$ are defined in Eqs. (4.35) and (4.40), respectively.

The average total delay for secondary packets is defined in Eq. (3.53), and the average number of packets waiting in the queue, not including the packet currently being transmitted, in Eq. (3.52).

Fig. 4.4 shows the average delay including the queuing delay against the rate of arrival of data packets, for various values of T_{tr}, both for work-preserving and non-work-preserving strategies. It can be seen that as expected, work-preserving strategy always performs better than non-work-preserving strategy. Also, the per-

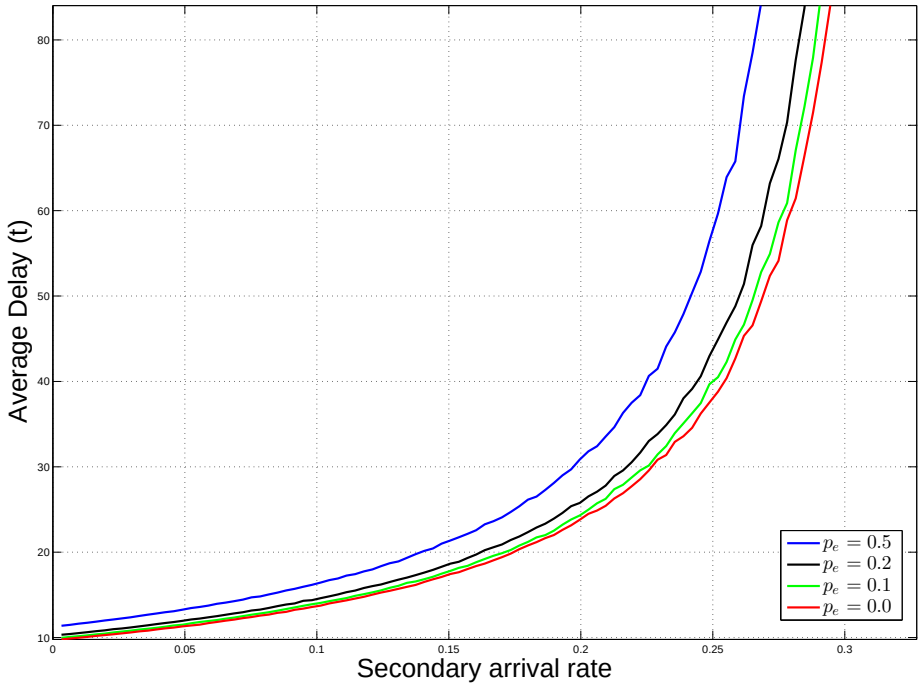

Figure 4.5: Average queuing delay with imperfect periodic sensing ($T_s = 0.5$, $\lambda = 10$, $\mu = 6$, and $T = 1$)

formance difference between the two strategies reduces as the packet transmission time T_{tr} decreases, as shown by the vertical lines in the figure.

Fig. 4.5 shows the simulation results for average delay including the queuing delay against the rate of arrival of data packets, for various values of p_e, for imperfect periodic sensing scenario. It can be seen that as expected, increasing p_e increases the queuing delay.

Chapter 5

Conclusion

5.1 Summary

RF spectrum scarcity problem is a major problem faced by the wireless communication industry today. This work studied two proposed solutions for the RF spectrum scarcity problem.

We analyzed the performance of a switching based hybrid FSO/RF scheme. Both single FSO threshold and dual FSO threshold cases were considered. For both cases, we evaluated their outage probability, average BER for the non-outage period of time, and ergodic capacity over practical fading channels. The expressions for the above metrics for the hybrid schemes were obtained in terms of the corresponding expressions for FSO and RF links. Exact expressions were obtained for the outage probability and BER for both FSO and RF links and capacity of the RF link. Approximate expression were obtained for the capacity of the FSO link. Numerical results show that considerable performance improvement can be obtained when using a hybrid scheme. Dual FSO threshold achieves a similar level of performance as single FSO threshold, while increasing the life time of the FSO communication link.

We also studied the extended delivery time of a data packet appearing at the secondary user in an interweave cognitive setup with work-preserving strategy. Exact analytical results for the probability distribution of the EDT for a fixed-size data packet were obtained for both continuous sensing and periodic sensing. These results were then applied to analyze the expected delay of a packet at SU in a queuing setup. Simulation results were presented to verify the analytical results.

We further studied the extended delivery time of a data packet appearing at the secondary user in an interweave cognitive setup assuming non-work-preserving strategy. Exact analytical results for the probability distribution of the EDT for

a fixed-size data packet were obtained for continuous sensing, perfect periodic sensing, and imperfect periodic sensing. These results were then applied to analyze the expected delay of a packet at SU in a queuing setup. Simulation results were presented to verify the analytical results. These analytical results will facilitate the design and optimization of secondary systems for diverse target applications.

5.2 Future Directions

The current research related to FSO/RF system can be modified to analyze the same performance metrics assuming the more general Gamma-Gamma fading model for the FSO link. Though the Gamma-Gamma model is more complicated, but valid for wider range of turbulence effects. Other than that, some new systems may also be analyzed. One of them might be a hybrid FSO/RF system in which data is multiplexed on the FSO and RF channels when the SNRs of both of them are above a certain threshold. When at least one of the SNRs falls below the threshold, the system would adopt a diversity scheme by transmitting the same data on both the links, and choose the link with the better SNR, or use maximal ratio combining (MRC). The bit error rate and the ergodic capacity can be analyzed for this system.

For the cognitive radio systems, several extensions to the presented result in the thesis can be considered. Accurate analysis can be carried out for packets with variable size or variable transmission time. In the thesis, the activity on the target channel were assumed to be Markovian. We may consider a non-Markovian model where either one of the on and off times, or both of them are not exponentially distributed. Further, these analyses can be extended to cover the cases of multiple primary channels and/or multiple secondary users. For each of the proposed modifications, both work-preserving and non-work-preserving strategies may be considered.

Appendix A

A.1 Derivation of Average Electrical SNR for FSO Link

In this appendix, we derive an expression for the average electrical SNR for the FSO link, $\bar{\gamma}_{FSO}$. The turbulence fading coefficient for the FSO link h is a log-normal random variable with unit average. Specifically $h = e^{2X}$ where X is a normal random variable defined by

$$X \sim N(-\sigma_x^2, \sigma_x^2). \tag{A.1}$$

After applying the relation in Eq. (2.3), $\bar{\gamma}_{FSO}$ is calculated as

$$\bar{\gamma}_{FSO} = E[\gamma_{FSO}] = \frac{\alpha^2 g^2 E_s}{\sigma_n^2} E[h^2] = \frac{\alpha^2 g^2 E_s}{\sigma_n^2} E[e^{4X}]. \tag{A.2}$$

Direct calculation of the expectation is possible, but tedious. We present in the following an alternative approach by defining a new random variable $Y = 2X - 2\sigma_x^2$. It is not difficult to see that Y is also a normal random variable with mean $\mu_y = -4\sigma_x^2$ and variance $\sigma_y^2 = 4\sigma_x^2$. It follows that $E[e^{2Y}] = 1$. Therefore, we can calculate the average electrical SNR for FSO link as

$$\bar{\gamma}_{FSO} = \frac{\alpha^2 g^2 E_s}{\sigma_n^2} E[e^{4\sigma_x^2} e^{2Y}] = \frac{\alpha^2 g^2 E_s}{\sigma_n^2} e^{4\sigma_x^2}. \tag{A.3}$$

A.2 Derivation of Probability Distribution of SU Waiting Time in k slots

In this appendix, we derive the expression for the probability that the total SU waiting time over k waiting slots is equal to nT_s for the periodic sensing case,

$\Pr[T_{w,k} = nT_s]$. $\Pr[T_{w,k} = nT_s]$ can be equivalently calculated as the probability that it takes n sensing instances to find exactly k times that the PU is off. Applying the result of negative binomial distribution, we can calculate $\Pr[T_{w,k} = nT_s]$ as

$$\Pr[T_{w,k} = nT_s] = (1-\beta)^k(\beta)^{n-k}\binom{n-1}{k-1}, \tag{A.4}$$

where β is the probability that primary user is on at the sensing instant, which, due to the memoryless property of exponential distribution, is a constant. Since the SU only senses every T_s time period, there is chance that the PU turns off and then back on between two sensing instants. To account for such possibilities, we can model PU activity with a continuous-time Markov process, where the transition rates are given by $\frac{1}{\lambda}$ and $\frac{1}{\mu}$. Given that the PU was on at a given time instant, the probability that the PU is still on after time T_s is given by [50]

$$\beta = \frac{\lambda}{\lambda+\mu} + \frac{\mu}{\lambda+\mu}e^{-(\frac{1}{\lambda}+\frac{1}{\mu})T_s}. \tag{A.5}$$

The above definition is valid for any value of $T_s > 0$. If we assume that T_s is small, and the chance of the PU turning back on again before the SU senses a free channel is negligible, we can approximately use $\beta = e^{\frac{-T_s}{\lambda}}$.

A.3 Calculation of Moments of EDT for Work-preserving strategy with Continuous Sensing - PU off at $t = 0$ case

In this appendix, we present the calculation for the first and second moments of the EDT of packets that find PU off at the start of their service for the continuous sensing case, $E[ST_{p_{off}}]^{(c)}$ and $E[ST^2_{p_{off}}]^{(c)}$.

The first moment of the EDT for the case when PU is off at $t = 0$, $E[ST_{p_{off}}]^{(c)}$, is defined as

$$E[ST_{p_{off}}]^{(c)} = \int_{T_{tr}}^{\infty} t f_{T_w,p_{off}}(t - T_{tr})dt \tag{A.6}$$

With a change of variable $s = t - T_{tr}$, we get

$$E[ST_{p_{off}}]^{(c)} = \int_{0}^{\infty} (s + T_{tr}) f_{T_w,p_{off}}(s)ds \tag{A.7}$$

After substituting Eq. (3.10) and using $\int_0^\infty f_{T_w,p_{off}}(s)ds = 1$, we arrive at

$$E[ST_{p_{off}}]^{(c)} = T_{tr} + \int_0^\infty s \sum_{k=2}^{\infty} \frac{{T_{tr}}^{k-1} e^{\frac{-T_{tr}}{\mu}}}{\mu^{k-1}(k-1)!} \times \frac{1}{\lambda^{k-1}} \frac{s^{k-2}}{(k-2)!} e^{\frac{-s}{\lambda}} ds \tag{A.8}$$

which, after some manipulation, becomes

$$E[ST_{p_{off}}]^{(c)} = T_{tr} + e^{\frac{-T_{tr}}{\mu}} \lambda \sum_{k=2}^{\infty} \frac{{T_{tr}}^{k-1}}{\mu^{k-1}(k-1)!(k-2)!} \tag{A.9}$$

$$\times \int_0^\infty \frac{s^{k-1} e^{\frac{-s}{\lambda}}}{\lambda^k} ds \tag{A.10}$$

Applying the definition of the standard gamma function, the above expression becomes

$$E[ST_{p_{off}}]^{(c)} = T_{tr} + e^{\frac{-T_{tr}}{\mu}} \lambda \sum_{k=2}^{\infty} \frac{{T_{tr}}^{k-1}}{\mu^{k-1}(k-2)!} \tag{A.11}$$

With a change in summation variable, and after some manipulation, we get

$$E[ST_{p_{off}}]^{(c)} = T_{tr} + e^{\frac{-T_{tr}}{\mu}} \lambda \left(\frac{T_{tr}}{\mu}\right) e^{\frac{T_{tr}}{\mu}} = T_{tr} + \lambda \left(\frac{T_{tr}}{\mu}\right) \tag{A.12}$$

The second moment, $E[ST^2_{p_{off}}]^{(c)}$, is defined as

$$E[ST^2_{p_{off}}]^{(c)} = \int_{T_{tr}}^\infty t^2 f_{T_w,p_{off}}(t - T_{tr}) dt \tag{A.13}$$

With a change of variable $s = t - T_{tr}$, and using $\int_0^\infty f_{T_w,p_{off}}(s)ds = 1$ we get

$$E[ST^2_{p_{off}}]^{(c)} = {T_{tr}}^2 + 2T_{tr}(E[ST_{p_{off}}]^{(c)} - T_{tr}) + \int_0^\infty s^2 f_{T_w,p_{off}}(s) ds \tag{A.14}$$

Following similar derivation steps as for $E[ST_{p_{off}}]^{(c)}$, we get

$$E[ST^2_{p_{off}}]^{(c)} = {T_{tr}}^2 + 2T_{tr}(E[ST_{p_{off}}]^{(c)} - T_{tr}) + e^{\frac{-T_{tr}}{\mu}} \lambda^2 \sum_{k=0}^{\infty} \left(\frac{T_{tr}}{\mu}\right)^{k+1} \frac{k+2}{k!} \tag{A.15}$$

Further dividing the term inside the integral into two parts, and a further change

in summation variable we get

$$E[ST_{p_{off}}^2]^{(c)} = {T_{tr}}^2 + 2T_{tr}(E[ST_{p_{off}}]^{(c)} - T_{tr}) + e^{\frac{-T_{tr}}{\mu}}\lambda^2 \sum_{k=0}^{\infty} \left(\frac{T_{tr}}{\mu}\right)^{k+2} \frac{1}{k!} + 2e^{\frac{-T_{tr}}{\mu}}\lambda^2 \sum_{k=0}^{\infty} \left(\frac{T_{tr}}{\mu}\right)^{k+1} \frac{1}{k!} \tag{A.16}$$

Replacing the summation by the natural exponent, using the definition of $E[ST_{p_{off}}]^{(c)}$, and simplifying, we get

$$E[ST_{p_{off}}^2]^{(c)} = \lambda^2 \left[\left(\frac{T_{tr}}{\mu}\right)^2 + 2\frac{T_{tr}}{\mu}\right] + 2\frac{\lambda {T_{tr}}^2}{\mu} + {T_{tr}}^2 \tag{A.17}$$

A.4 Calculation of Moments of EDT for Work-preserving strategy with Continuous Sensing - PU on at $t = 0$ case

In this appendix, we present the calculation for the first and second moments of the EDT of packets that find PU on at the start of their service for the continuous sensing case, $E[ST_{p_{on}}]^{(c)}$ and $E[ST_{p_{on}}^2]^{(c)}$.

The first moment of the EDT for the case when PU is on at $t = 0$, $E[ST_{p_{on}}]^{(c)}$, is defined as

$$E[ST_{p_{on}}]^{(c)} = \int_{T_{tr}}^{\infty} t f_{T_w, p_{on}}(t - T_{tr}) dt. \tag{A.18}$$

With a change of variable $s = t - T_{tr}$ we get

$$E[ST_{p_{on}}]^{(c)} = \int_{0}^{\infty} (s + T_{tr}) f_{T_w, p_{on}}(s) ds. \tag{A.19}$$

After substituting Eq. (3.8) and some manipulation, we arrive at

$$E[ST_{p_{on}}]^{(c)} = T_{tr} + e^{\frac{-T_{tr}}{\mu}}\lambda \sum_{k=1}^{\infty} \frac{{T_{tr}}^{k-1}}{\mu^{k-1}(k-1)!(k-1)!} \times \int_{0}^{\infty} \frac{s^k e^{\frac{-s}{\lambda}}}{\lambda^{k+1}} ds. \tag{A.20}$$

Applying the definition of the standard Gamma function, the above expression becomes

$$E[ST_{p_{on}}]^{(c)} = T_{tr} + e^{\frac{-T_{tr}}{\mu}}\lambda \sum_{k=1}^{\infty} \frac{{T_{tr}}^{k-1} k}{\mu^{k-1}(k-1)!}. \tag{A.21}$$

With a change in summation variable, and after some manipulation, we get

$$E[ST_{p_{on}}]^{(c)} = T_{tr} + e^{\frac{-T_{tr}}{\mu}}\lambda\left[\sum_{k=1}^{\infty}\frac{{T_{tr}}^k}{\mu^k(k-1)!} + \sum_{k=0}^{\infty}\frac{{T_{tr}}^k}{\mu^k, k!}\right], \tag{A.22}$$

which finally simplifies to

$$E[ST_{p_{on}}]^{(c)} = T_{tr} + e^{\frac{-T_{tr}}{\mu}}\lambda\left(\frac{T_{tr}}{\mu}\right)e^{\frac{T_{tr}}{\mu}} + e^{\frac{-T_{tr}}{\mu}}\lambda e^{\frac{T_{tr}}{\mu}} = T_{tr} + \lambda\left(1 + \frac{T_{tr}}{\mu}\right).$$

The second moment, $E[ST^2_{p_{on}}]^{(c)}$ is defined as

$$E[ST^2_{p_{on}}]^{(c)} = \int_{T_{tr}}^{\infty} t^2 f_{T_w,p_{on}}(t - T_{tr})dt. \tag{A.23}$$

With a change of variable $s = t - T_{tr}$, we get

$$E[ST^2_{p_{on}}]^{(c)} = {T_{tr}}^2 + 2T_{tr}(E[ST_{p_{on}}]^{(c)} - T_{tr}) + \int_0^{\infty} s^2 f_{T_w,p_{on}}(s)ds. \tag{A.24}$$

Following the similar derivation steps for $E[ST_{p_{on}}]^{(c)}$, we get

$$\begin{aligned} E[ST^2_{p_{on}}]^{(c)} &= {T_{tr}}^2 + 2T_{tr}(E[ST_{p_{on}}]^{(c)} - T_{tr}) + e^{\frac{-T_{tr}}{\mu}}\lambda^2\sum_{k=0}^{\infty}\left(\frac{T_{tr}}{\mu}\right)^{k+2}\frac{1}{k!} \\ &+ 4e^{\frac{-T_{tr}}{\mu}}\lambda^2\sum_{k=0}^{\infty}\left(\frac{T_{tr}}{\mu}\right)^{k+1}\frac{1}{k!} + 2e^{\frac{-T_{tr}}{\mu}}\lambda^2\sum_{k=0}^{\infty}\left(\frac{T_{tr}}{\mu}\right)^{k}\frac{1}{k!}. \end{aligned} \tag{A.25}$$

Replacing the summation by the natural exponent, we arrive at the following closed-form expression

$$E[ST^2_{p_{on}}]^{(c)} = \lambda^2\left[\left(\frac{T_{tr}}{\mu}\right)^2 + 4\frac{T_{tr}}{\mu} + 2\right] + 2\lambda T_{tr}\left[1 + \frac{T_{tr}}{\mu}\right] + {T_{tr}}^2. \tag{A.26}$$

A.5 Calculation of Moments of EDT for Work-preserving strategy with Periodic Sensing - PU off at $t = 0$ case

In this appendix, we derive expressions for the first and second moments of the EDT of packets that find PU off at the start of their service for the periodic sensing case, $E[ST_{p_{off}}]^{(p)}$ and $E[ST^2_{p_{off}}]^{(p)}$.

$$E[ST_{p_{off}}]^{(p)} = E[nT_s + T_{tr}] = T_s E[n] + T_{tr} \tag{A.27}$$

where

$$E[n] = \sum_{n=1}^{\infty} nPr[T_w, p_{off} = nT_s]. \tag{A.28}$$

After substituting Eq. (3.19), we get

$$E[n] = \sum\nolimits_{n=0}^{\infty} \left[n\left(\frac{T_{tr}(1-\beta)\beta^{n-1}}{\mu}\right) e^{\frac{-T_{tr}}{\mu}} \times \sum_{k=0}^{n-1} \left(\frac{T_{tr}(1-\beta)}{\mu\beta}\right)^k \frac{1}{(k+1)!} \binom{n-1}{k} \right] \tag{A.29}$$

Performing some manipulation, we obtain

$$\begin{aligned} E[n] = e^{\frac{-T_{tr}}{\mu}} \sum_{k=0}^{\infty} \Bigg[& \frac{1}{1-\beta}\left(\frac{T_{tr}}{\mu}\right)^{k+1} \frac{1}{k!} \\ & \times \sum_{n=k+1}^{\infty} (1-\beta)^{k+2} \beta^{n-k-1} \frac{n!}{(n-1-k)!(k+1)!} \Bigg] \end{aligned} \tag{A.30}$$

Noting that the second summation equals 1, the above expression can be written as

$$E[n] = \frac{1}{1-\beta}\left(\frac{T_{tr}}{\mu}\right) \tag{A.31}$$

Thus we have

$$E[ST_{p_{off}}]^{(p)} = T_{tr}\left(1 + \frac{T_s}{\mu(1-\beta)}\right) \tag{A.32}$$

The second moment is computed as

$$E[ST_{p_{off}}^2]^{(p)} = E[(nT_s + T_{tr})^2] = {T_s}^2 E[n^2] + 2T_s T_{tr} E[n] + {T_{tr}}^2, \tag{A.33}$$

where $E[n]$ is as defined in equation (A.31), and

$$\begin{aligned} E[n^2] = \sum\nolimits_{n=1}^{\infty} \Bigg[& n^2\left(\frac{T_{tr}(1-\beta)\beta^{n-1}}{\mu}\right) e^{\frac{-T_{tr}}{\mu}} \\ & \times \sum_{k=0}^{n-1} \left(\frac{T_{tr}(1-\beta)}{\mu\beta}\right)^k \frac{1}{(k+1)!} \binom{n-1}{k} \Bigg]. \end{aligned} \tag{A.34}$$

Changing the sequence of the two summations, and using $n^2(n-1)! = (n+1)! - n!$,

we arrive at

$$E[n^2] = \sum_{k=0}^{\infty} \left[\left(\frac{T_{tr}(1-\beta)}{\mu\beta} \right)^{k+1} e^{\frac{-T_{tr}}{\mu}} \frac{1}{(k+1)!} \times \left[\sum_{n=k+1}^{\infty} \beta^n \frac{(n+1)!}{(n-1-k)!k!} - \sum_{n=k+1}^{\infty} \beta^n \frac{n!}{(n-1-k)!k!} \right] \right]. \tag{A.35}$$

Using similar manipulations as done for $E[n]$, we obtain

$$E[n^2] = \sum_{k=0}^{\infty} \left[\left(\frac{T_{tr}(1-\beta)}{\mu\beta} \right)^{k+1} e^{\frac{-T_{tr}}{\mu}} \times \left[\frac{(k+1)(k+2)}{(1-\beta)^2(k+1)!} - \frac{(k+1)}{(1-\beta)(k+1)!} \right] \right]. \tag{A.36}$$

Further manipulating the factorial terms, we get

$$E[n^2] = e^{\frac{-T_{tr}}{\mu}} \left[\sum_{k=1}^{\infty} \frac{1}{(1-\beta)^2} \frac{1}{(k-1)!} \left(\frac{T_{tr}}{\mu} \right)^{k+1} + 2 \sum_{k=0}^{\infty} \frac{1}{(1-\beta)^2} \frac{1}{k!} \left(\frac{T_{tr}}{\mu} \right)^{k+1} - \sum_{k=0}^{\infty} \frac{1}{(1-\beta)} \frac{1}{k!} \left(\frac{T_{tr}}{\mu} \right)^{k+1} \right], \tag{A.37}$$

which simplifies to

$$E[n^2] = \frac{1}{(1-\beta)^2} \left[\left(\frac{T_{tr}}{\mu} \right)^2 + 2\frac{T_{tr}}{\mu} \right] - \frac{1}{(1-\beta)} \left(\frac{T_{tr}}{\mu} \right). \tag{A.38}$$

Thus the expression for second moment is given by

$$E[ST_{p_{off}}^2]^{(p)} = \frac{{T_s}^2}{(1-\beta)^2} \left[\left(\frac{T_{tr}}{\mu} \right)^2 + 2\frac{T_{tr}}{\mu} \right] - \frac{{T_s}^2}{1-\beta} \left(\frac{T_{tr}}{\mu} \right) + \frac{T_s}{1-\beta} \frac{2{T_{tr}}^2}{\mu} + {T_{tr}}^2. \tag{A.39}$$

A.6 Calculation of Moments of EDT for Work-preserving strategy with Periodic Sensing - PU on at $t = 0$ case

In this appendix, we derive expressions for the first and second moments of the EDT of packets that find PU on at the start of their service for the periodic sensing case, $E[ST_{p_{on}}]^{(p)}$ and $E[ST_{p_{on}}^2]^{(p)}$.

When PU is on at $t = 0$, the first moment of the EDT, $E[ST_{p_{on}}]^{(p)}$, is defined as

$$E[ST_{p_{on}}]^{(p)} = E[nT_s + T_{tr}] = T_s E[n] + T_{tr}, \tag{A.40}$$

where

$$E[n] = \sum_{n=1}^{\infty} nPr[T_w, p_{on} = nT_s]. \tag{A.41}$$

After substituting Eq. (3.17) and some manipulation, we obtain

$$E[n] = e^{\frac{-T_{tr}}{\mu}} \frac{1}{(1-\beta)} \sum_{k=0}^{\infty} \left[\left(\frac{T_{tr}}{\mu} \right)^k \frac{k+1}{k!} \times \sum_{n=k+1}^{\infty} (1-\beta)^{k+2} \beta^{n-k-1} \frac{n!}{(n-1-k)!(k+1)!} \right]. \tag{A.42}$$

Noting that the second summation is equal to 1, the above expression can be written as

$$E[n] = e^{\frac{-T_{tr}}{\mu}} \frac{1}{(1-\beta)} \sum_{k=0}^{\infty} \left[\left(\frac{T_{tr}}{\mu} \right)^k \frac{k+1}{k!} \right], \tag{A.43}$$

which simplifies to

$$E[n] = \frac{1}{1-\beta} \left(1 + \frac{T_{tr}}{\mu} \right). \tag{A.44}$$

Thus, $E[ST_{p_{on}}]^{(p)}$ can be finally expressed as

$$E[ST_{p_{on}}]^{(p)} = T_{tr} + \frac{T_s}{1-\beta} \left(1 + \frac{T_{tr}}{\mu} \right) \tag{A.45}$$

The second moment, $E[ST^2_{p_{on}}]^{(p)}$, is computed as

$$E[ST^2_{p_{on}}]^{(p)} = E[(nT_s + T_{tr})^2] = {T_s}^2 E[n^2] + 2T_s T_{tr} E[n] + {T_{tr}}^2, \tag{A.46}$$

where $E[n]$ is given in Eq. (A.44), and

$$E[n^2] = \sum_{n=1}^{\infty} \left[n^2 (1-\beta)\beta^{n-1} e^{\frac{-T_{tr}}{\mu}} \times \sum_{k=0}^{n-1} \left(\frac{T_{tr}(1-\beta)}{\mu\beta} \right)^k \frac{1}{k!} \binom{n-1}{k} \right]. \tag{A.47}$$

Changing the sequence of the two summations and applying $n^2(n-1)! = (n +$

$1)! - n!$, we obtain

$$E[n^2] = \sum_{k=0}^{\infty} \left[(1-\beta) \left(\frac{T_{tr}(1-\beta)}{\mu\beta} \right)^k e^{\frac{-T_{tr}}{\mu}} \frac{1}{k!} \times \left(\sum_{n=k+1}^{\infty} \beta^{n-1} \frac{(n+1)!}{(n-1-k)!k!} - \sum_{n=k+1}^{\infty} \beta^{n-1} \frac{n!}{(n-1-k)!k!} \right) \right]. \tag{A.48}$$

Using the similar manipulations for the calculation of $E[n]$, we obtain

$$E[n^2] = \sum_{k=0}^{\infty} \left[\left(\frac{T_{tr}}{\mu} \right)^k e^{\frac{-T_{tr}}{\mu}} \times \left(\frac{(k+1)(k+2)}{(1-\beta)^2 k!} - \frac{(k+1)}{(1-\beta)k!} \right) \right]. \tag{A.49}$$

With further manipulation on the factorial terms, we arrive at

$$\begin{aligned} E[n^2] =& \frac{e^{\frac{-T_{tr}}{\mu}}}{(1-\beta)^2} \left[\sum_{k=2}^{\infty} \frac{1}{(k-2)!} \left(\frac{T_{tr}}{\mu} \right)^k + 4 \sum_{k=1}^{\infty} \frac{1}{(k-1)!} \left(\frac{T_{tr}}{\mu} \right)^k + 2 \sum_{k=0}^{\infty} \frac{1}{k!} \left(\frac{T_{tr}}{\mu} \right)^k \right] \\ & - \frac{e^{\frac{-T_{tr}}{\mu}}}{(1-\beta)} \left[\sum_{k=1}^{\infty} \frac{1}{(k-1)!} \left(\frac{T_{tr}}{\mu} \right)^k + \sum_{k=0}^{\infty} \frac{1}{k!} \left(\frac{T_{tr}}{\mu} \right)^k \right], \end{aligned} \tag{A.50}$$

which finally simplifies to

$$E[n^2] = \frac{1}{(1-\beta)^2} \left[\left(\frac{T_{tr}}{\mu} \right)^2 + 4\frac{T_{tr}}{\mu} + 2 \right] - \frac{1}{(1-\beta)} \left[\frac{T_{tr}}{\mu} + 1 \right]. \tag{A.51}$$

Thus the second moment, $E[ST_{p_{on}}^2]^{(p)}$, can be calculated in the following closed-form expression

$$E[ST_{p_{on}}^2]^{(p)} = \frac{{T_s}^2}{(1-\beta)^2} \left[\left(\frac{T_{tr}}{\mu} \right)^2 + 4\frac{T_{tr}}{\mu} + 2 \right] + \frac{T_s}{1-\beta}(2T_{tr} - T_s) \cdot \left[1 + \frac{T_{tr}}{\mu} \right] + {T_{tr}}^2. \tag{A.52}$$

A.7 Proof of Identity involving Partial Fractions used in the derivation of MGF for non-work-preserving strategy

In this appendix, we prove by induction, Eq. (4.10). The base case, with $n = 0$, is obvious, as

$$\frac{1}{x(x-a)} = \frac{1}{a}\left[-\frac{1}{x} + \frac{1}{x-a}\right]. \tag{A.53}$$

Assuming that the equation is true for $n = k$, we can write

$$\begin{aligned}\frac{1}{[x(x-a)]^{k+1}} &= \frac{1}{[x(x-a)]^{k}} \times \frac{1}{x(x-a)} \\ &= \sum_{j=0}^{k-1}(-1)^k \binom{2k-j-2}{k-1} \frac{1}{a^{2k-j-1}}\left[\frac{1}{x^{j+2}(x-a)} + \frac{(-1)^{j+1}}{(x-a)^{j+2}x}\right].\end{aligned} \tag{A.54}$$

To prove the induction hypothesis, we will use the following two relationships,

$$\frac{1}{x^k(x-a)} = \frac{1}{a^k(x-a)} + \sum_{i=1}^{k} \frac{-1}{a^{k+1-i}x^i}, \tag{A.55}$$

and

$$\frac{1}{x(x-a)^k} = \frac{(-1)^k}{a^k x} + \sum_{i=1}^{k} \frac{(-1)^{k-i}}{a^{k+1-i}(x-a)^i}. \tag{A.56}$$

Eq. (A.55) can be proved using the following argument,

$$\begin{aligned}\frac{1}{a^k(x-a)} + \sum_{i=1}^{k} \frac{-1}{a^{k+1-i}x^i} &= \frac{1}{a^k(x-a)}\left[\frac{x^k}{a^k} - \sum_{i=1}^{k}\frac{x^{k-i}(x-a)}{a^{k+1-i}}\right] \\ &= \frac{1}{a^k(x-a)}\left[\frac{x^k}{a^k} - \sum_{i=1}^{k}\frac{x^{k+1-i}}{a^{k+1-i}} + \sum_{i=1}^{k}\frac{x^{k-i}}{a^{k-i}}\right] = \frac{1}{x^k(x-a)}.\end{aligned} \tag{A.57}$$

Eq. (A.56) can also be proved using a similar argument. Substituting Eqs. (A.55) and (A.56) into Eq. (A.54), we obtain

$$\frac{1}{[x(x-a)]^{k+1}} = \sum_{j=0}^{k-1}(-1)^k\binom{2k-j-2}{k-1}\frac{1}{a^{2k-j-1}}\left[\sum_{i=1}^{j+2}\frac{-1}{a^{j+3-i}x^i} + \frac{1}{a^{j+2}(x-a)} + \sum_{i=1}^{j+2}\frac{(-1)^{i+1}}{a^{j+3-i}(x-a)^i} + \frac{-1}{a^{j+2}x}\right]. \tag{A.58}$$

Performing some further manipulation on Eq. (A.54), and using the identity

$$\sum_{k=0}^{n}\binom{m+k-1}{k} = \binom{n+m}{n}, \tag{A.59}$$

it can be shown that

$$\frac{1}{[x(x-a)]^{k+1}} = \sum_{i=0}^{k}(-1)^{k+1}\binom{2k-i}{k}\frac{1}{a^{2k-i+1}}\left[\frac{1}{x^{i+1}} + \frac{(-1)^{i+1}}{(x-a)^{i+1}}\right], \tag{A.60}$$

which proves the induction hypothesis.

Bibliography

[1] "Introduction to wireless communications," in *Design and Performance of 3G Wireless Networks and Wireless Lans*, pp. 1–12, Springer US, 2006.

[2] A. Goldsmith, S. Jafar, I. Maric, and S. Srinivasa, "Breaking spectrum gridlock with cognitive radios: An information theoretic perspective," *Proc. of the IEEE*, vol. 97, pp. 894–914, May 2009.

[3] S. Haykin, "Cognitive radio: brain-empowered wireless communications," *IEEE J. Sel. Areas Commun.*, vol. 23, pp. 201–220, Feb 2005.

[4] J. Mitola and J. Maguire, G.Q., "Cognitive radio: making software radios more personal," *IEEE Pers. Commun.*, vol. 6, pp. 13–18, Aug 1999.

[5] R. Thomas, L. DaSilva, and A. MacKenzie, "Cognitive networks," in *1st IEEE Int. Symp. on New Frontiers in Dynamic Spectrum Access Netw., 2005. DySPAN 2005. 2005*, pp. 352–360, Nov 2005.

[6] I. F. Akyildiz, W.-Y. Lee, M. C. Vuran, and S. Mohanty, "Next generation/dynamic spectrum access/cognitive radio wireless networks: A survey," *Comput. Netw. J.*, vol. 50, no. 13, pp. 2127 – 2159, 2006.

[7] M. Islam, C. Koh, S. W. Oh, X. Qing, Y. Lai, C. Wang, Y.-C. Liang, B. Toh, F. Chin, G. Tan, and W. Toh, "Spectrum survey in Singapore: Occupancy measurements and analyses," in *Proc. 3rd Int. Conf. Cognitive Radio Oriented Wireless Netw. and Commun., 2008. CrownCom 2008.*, pp. 1–7, May 2008.

[8] B. Hamdaoui, "Adaptive spectrum assessment for opportunistic access in cognitive radio networks," *IEEE Trans. Wireless Commun.*, vol. 8, pp. 922–930, Feb 2009.

[9] Q. Zhao, S. Geirhofer, L. Tong, and B. Sadler, "Opportunistic spectrum access via periodic channel sensing," *IEEE Trans. Signal Process.*, vol. 56, pp. 785–796, Feb 2008.

[10] Q. Zhao, L. Tong, A. Swami, and Y. Chen, "Decentralized cognitive MAC for opportunistic spectrum access in ad hoc networks: A pomdp framework," *IEEE J. Sel. Areas Commun.*, vol. 25, pp. 589–600, April 2007.

[11] K. Huang and Z. Wang, *Millimeter Wave Communication Systems*. IEEE Series on Digital & Mobile Communication, Wiley, 2011.

[12] F. Giannetti, M. Luise, and R. Reggiannini, "Mobile and personal communications in the 60 GHz band: a survey," *Wireless Pers. Commun.*, vol. 10, pp. 207–243, July 1999.

[13] L. C. Andrews, R. L. Phillips, and C. Y. Hopen, *Laser Beam Scintillation with Applications*. SPIE Publications, 2001.

[14] F. Nadeem, V. Kvicera, M. Awan, E. Leitgeb, S. Muhammad, and G. Kandus, "Weather effects on hybrid FSO/RF communication link," *IEEE J. Sel. Areas Commun.*, vol. 27, pp. 1687–1697, December 2009.

[15] H. Wu and M. Kavehrad, "Availability evaluation of ground-to-air hybrid FSO/RF links," *Int. J. Wireless Inf. Netw.*, vol. 14, pp. 33–45, March 2007.

[16] S. Vangala and H. Pishro-Nik, "A highly reliable FSO/RF communication system using efficient codes," in *Proc. IEEE Global Telecommun. Conf., 2007. GLOBECOM '07*, pp. 2232–2236, Nov 2007.

[17] A. Abdulhussein, A. Oka, T. T. Nguyen, and L. Lampe, "Rateless coding for hybrid free-space optical and radio-frequency communication," *IEEE Trans. Wireless Commun.*, vol. 9, pp. 907–913, March 2010.

[18] B. He and R. Schober, "Bit-interleaved coded modulation for hybrid RF/FSO systems," *IEEE Trans. Commun.*, vol. 57, pp. 3753–3763, December 2009.

[19] W. Zhang, S. Hranilovic, and C. Shi, "Soft-switching hybrid FSO/RF links using short-length raptor codes: design and implementation," *IEEE J. Sel. Areas Commun.*, vol. 27, pp. 1698–1708, December 2009.

[20] N. Letzepis, K. Nguyen, A. Guillen i Fabregas, and W. Cowley, "Outage analysis of the hybrid free-space optical and radio-frequency channel," *IEEE J. Sel. Areas Commun.*, vol. 27, pp. 1709–1719, December 2009.

[21] N. Chatzidiamantis, G. Karagiannidis, E. Kriezis, and M. Matthaiou, "Diversity combining in hybrid RF/FSO systems with PSK modulation," in *Proc. IEEE Int. Conf. Commun. (ICC), 2011*, pp. 1–6, June 2011.

[22] A. Kamboj, R. Mallik, M. Agrawal, and R. Schober, "Diversity combining in FSO systems in presence of non-Gaussian noise," in *Proc. Int. Conf. Signal Process. and Commun. (SPCOM), 2012*, pp. 1–5, July 2012.

[23] F. Borgonovo, M. Cesana, and L. Fratta, "Throughput and delay bounds for cognitive transmissions," in *Advances in Ad Hoc Networking* (P. Cuenca, C. Guerrero, R. Puigjaner, and B. Serra, eds.), vol. 265 of *IFIP International Federation for Information Processing*, pp. 179–190, Springer US, 2008.

[24] F. Khan, K. Tourki, M.-S. Alouini, and K. Qaraqe, "Delay performance of a broadcast spectrum sharing network in Nakagami-m fading," *IEEE Trans. Veh. Technol.*, vol. 63, pp. 1350–1364, March 2014.

[25] L. Sibomana, H.-J. Zepernick, H. Tran, and C. Kabiri, "Packet transmission time for cognitive radio networks considering interference from primary user," in *9th Int. Wireless Commun. and Mobile Computing Conf. (IWCMC), 2013*, pp. 791–796, July 2013.

[26] L. Musavian and S. Aissa, "Effective capacity of delay-constrained cognitive radio in nakagami fading channels," *IEEE Trans. Wireless Commun.*, vol. 9, pp. 1054–1062, March 2010.

[27] H. Tran, T. Duong, and H.-J. Zepernick, "Delay performance of cognitive radio networks for point-to-point and point-to-multipoint communications," *EURASIP J. on Wireless Commun. and Networking*, vol. 2012, no. 1, pp. 1–15, 2012.

[28] A. Farraj, S. Miller, and K. Qaraqe, "Queue performance measures for cognitive radios in spectrum sharing systems," in *IEEE GLOBECOM Workshops (GC Wkshps), 2011*, pp. 997–1001, Dec 2011.

[29] C. Jiang, Y. Chen, K. Liu, and Y. Ren, "Renewal-theoretical dynamic spectrum access in cognitive radio network with unknown primary behavior," *IEEE J. Sel. Areas Commun.*, vol. 31, pp. 406–416, March 2013.

[30] F. Gaaloul, H.-C. Yang, R. Radaydeh, and M.-S. Alouini, "Switch based opportunistic spectrum access for general primary user traffic model," *IEEE Wireless Commun. Lett.*, vol. 1, pp. 424–427, October 2012.

[31] Z. Liang and D. Zhao, "Quality of service performance of a cognitive radio sensor network," in *Proc. IEEE Int. Conf. Commun. (ICC), 2010*, pp. 1–5, May 2010.

[32] X. Li, J. Wang, H. Li, and S. Li, "Delay analysis and optimal access strategy in multichannel dynamic spectrum access system," in *Proc. Int. Conf. Computing, Netw. and Commun. (ICNC), 2012*, pp. 376–380, Jan 2012.

[33] S. Kandeepan, C. Saradhi, M. Filo, and R. Piesiewicz, "Delay analysis of cooperative communication with opportunistic relay access," in *Proc. IEEE 73rd Veh. Technol. Conf. (VTC Spring), 2011*, pp. 1–5, May 2011.

[34] H. Li and Z. Han, "Queuing analysis of dynamic spectrum access subject to interruptions from primary users," in *5th Int. Conf. Cognitive Radio Oriented Wireless Netw. Commun. (CROWNCOM), 2010 Proc.*, pp. 1–5, June 2010.

[35] C.-W. Wang and L.-C. Wang, "Analysis of reactive spectrum handoff in cognitive radio networks," *IEEE J. Sel. Areas Commun.*, vol. 30, pp. 2016–2028, November 2012.

[36] D. J. C. MacKay, "Fountain codes," *IEE Proc.-Commun.*, vol. 152, pp. 1062–1068, Dec 2005.

[37] J. Castura and Y. Mao, "Rateless coding over fading channels," *IEEE Commun. Lett.*, vol. 10, pp. 46–48, Jan 2006.

[38] M. Khalighi and M. Uysal, "Survey on free space optical communication: A communication theory perspective," *IEEE Commun. Surveys Tutorials*, vol. PP, no. 99, pp. 1–1, 2014.

[39] H. Moradi, M. Falahpour, H. Refai, P. LoPresti, and M. Atiquzzaman, "On the capacity of hybrid FSO/RF links," in *Proc. IEEE Global Telecommun. Conf. (GLOBECOM 2010), 2010*, pp. 1–5, Dec 2010.

[40] J. Li, J. Q. Liu, and D. Taylor, "Optical communication using subcarrier PSK intensity modulation through atmospheric turbulence channels," *IEEE Trans. Commun.*, vol. 55, pp. 1598–1606, Aug 2007.

[41] W. Huang, J. Takayanagi, T. Sakanaka, and M. Nakagawa, "Atmospheric optical communication system using subcarrier PSK modulation," in *Proc. IEEE Int. Conf. on Commun., 1993. ICC '93 Geneva. Tech. Program, Conf. Record*, vol. 3, pp. 1597–1601 vol.3, May 1993.

[42] H. Moradi, M. Falahpour, H. H. Refai, P. G. LoPresti, and M. Atiquzzaman, "Toward an optimal combined FSO/RF system via an adaptive bit rate control," in *Proc. SPIE Photonics West*, vol. 7587, pp. 75870X–75870X–10, 2010.

[43] S. Navidpour, M. Uysal, and M. Kavehrad, "Ber performance of free-space optical transmission with spatial diversity," *IEEE Trans. Wireless Commun.*, vol. 6, pp. 2813–2819, August 2007.

[44] H. Moradi, M. Falahpour, H. Refai, P. LoPresti, and M. Atiquzzaman, "BER analysis of optical wireless signals through lognormal fading channels with perfect CSI," in *Proc. IEEE 17th Int. Conf. on Telecommun. (ICT), 2010*, pp. 493–497, April 2010.

[45] S. Wilson, M. Brandt-Pearce, Q. Cao, and M. Baedke, "Optical repetition MIMO transmission with multipulse PPM," *IEEE J. Sel. Areas Commun.*, vol. 23, pp. 1901–1910, Sept 2005.

[46] S. Haas, *Capacity of and Coding for Multiple-aperture Wireless Optical Communications*. PhD dissertation, Massachusetts Institute of Technology, 2003.

[47] J. Proakis, *Digital Communications*. New York: Mc Graw Hill, 4th ed., 2000.

[48] J. Hossain, P. Vitthaladevuni, M.-S. Alouini, V. Bhargava, and A. Goldsmith, "Adaptive hierarchical modulation for simultaneous voice and multiclass data transmission over fading channels," *IEEE Trans. Veh. Technol.*, vol. 55, pp. 1181–1194, July 2006.

[49] A. Molisch, N. Mehta, J. S. Yedidia, and J. Zhang, "Performance of fountain codes in collaborative relay networks," *IEEE Trans. Wireless Commun.*, vol. 6, pp. 4108–4119, November 2007.

[50] E. Cinlar, *Introduction to stochastic processes*. Englewood Cliffs, NJ: Prentice-Hall, 1975.

[51] R. Boucherie and N. van Dijk, *Queueing Networks: A Fundamental Approach*. International Series in Operations Research & Management Science, Springer, 2010.

[52] I. Adan and J. Resing, *Queueing Theory*. Eindhoven University of Technology. Department of Mathematics and Computing Science, 2001.